

# Survey of spin liquid physics and/or materials

Gang Chen  
HKU

This topic is hard to be systematic.

# Theoretical classification

1. Topological spin liquid: intrinsic topological order, fully gapped.
2. Critical spin liquid: usually refers to QSLs with strongly coupled gapless gauge and gapless matter, e.g. 2d  $U(1)$  Dirac QSL, 2d  $U(1)$  spinon fermi surface QSL
3. Somewhat in between:  
3d  $U(1)$  QSL, 2d  $Z_2$  QSL with gapless fermionic matter may fit better to topological spin liquid.

With symmetries, more and finer QSLs can emerge.



# Experimental diagnosis

## 1. Thermodynamics:

$C_v$ ,  $\chi$ , NMR knight shift,  $\mu$ SR, neutron, etc

## 2. Spectroscopic measurements:

NMR- $T_1$ , inelastic neutron, etc

## 3. Charge physics, phonon sector (acoustic attenuation), thermal transports, etc

## Remark:

1. 需要把各种实验提供的信息综合起来，并不能孤立地看单一的实验。
2. 普适性和具体性重叠：当我们谈论特定phase时，关注的更多的是phase的普适性质。然而具体到某个系统时，就要考虑有些具体的实现，而具体实现又能带来一些新的特殊性。
3. 现象学和微观学结合：
  - a) 从某些现象归纳，来期望另外的现象
  - b) 从微观上推导模型解决，这个难度大，但相对solid

## Smoking guns measurements?

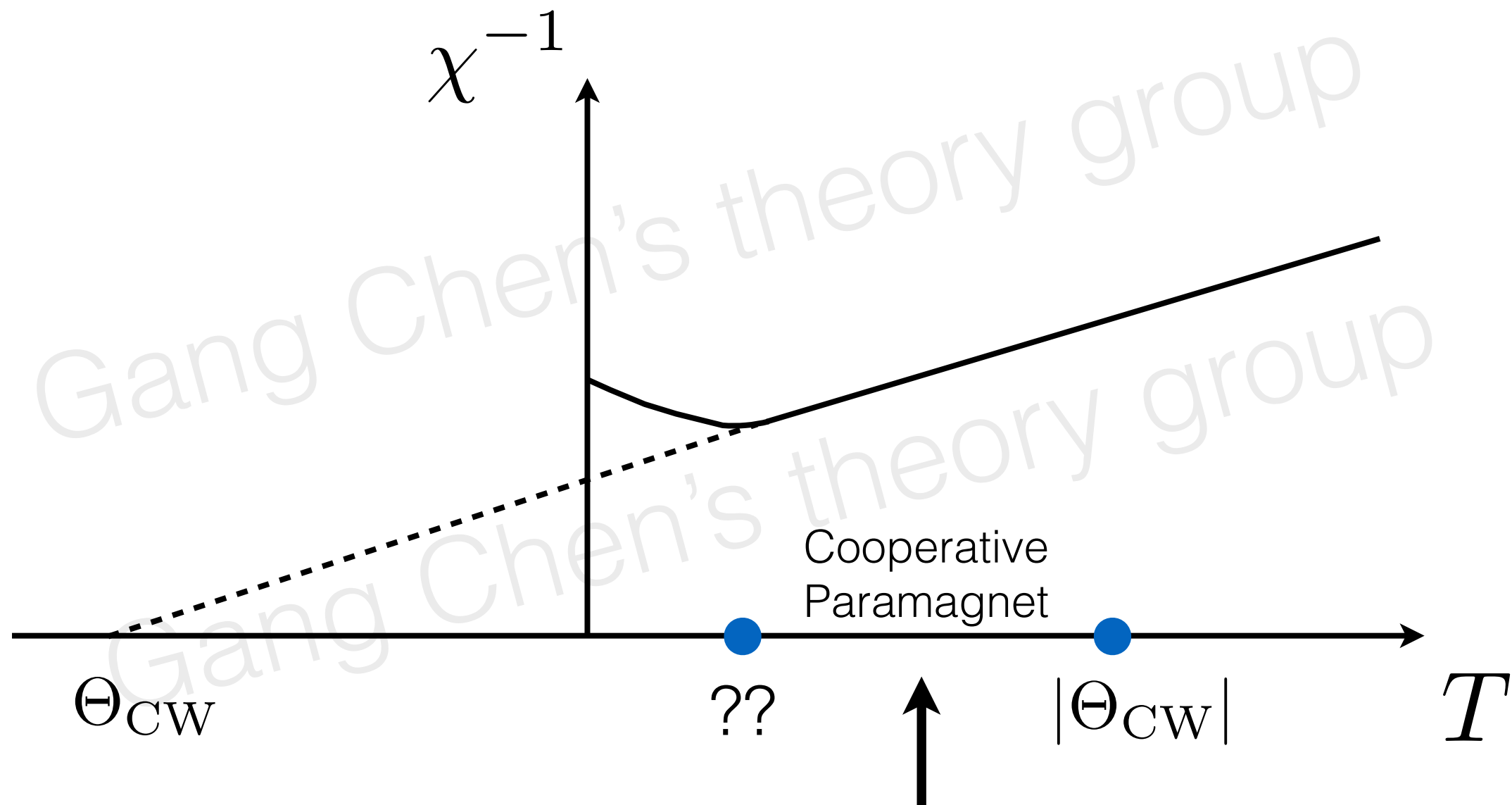
Smoking gun experiments are system specific, phase specific, degrees of freedom specific....

Some striking examples:

Pyrochlore spin ice U(1) QSL:  $C_v \sim T^3$ , prefactor is 1000 large of phonon's.

Gapped Kitaev spin liquid:  $kxy/T = \text{half quantization}$

澄清: spin liquid vs cooperative paramagnet



Classical spin liquid refers to this regime  
where the spin correlation is important.

## Some candidate spin liquid materials

- 2D triangular and Kagome lattice  
organics:  $\kappa$ -(BEDT-TTF) $_2$ Cu $_2$ (CN) $_3$ , EtMe $_3$ Sb[Pd(dmit) $_2$ ] $_2$ ,  $\kappa$ -H $_3$ (Cat-EDT-TTF) $_2$   
herbertsmithite (ZnCu $_3$ (OH) $_6$ Cl $_2$ ), Ba $_3$ NiSb $_2$ O $_9$ , Ba $_3$ CuSb $_2$ O $_9$ , LiZn $_2$ Mo $_3$ O $_8$ , ZnCu $_3$ (OH) $_6$ Cl $_2$   
volborthite (Cu $_3$ V $_2$ O $_7$ (OH) $_2$ ), BaCu $_3$ V $_2$ O $_3$ (OH) $_2$ , [NH $_4$ ] $_2$ [C $_7$ H $_{14}$ N][V $_7$ O $_6$ F $_{18}$ ], Na $_2$ IrO $_3$ , CsCu $_2$ Cl $_4$ ,  
CsCu $_2$ Br $_4$ , NiGa $_2$ S $_4$ , He-3 layers on graphite, YbMgGaO $_4$ , NaYbS $_2$ , etc
- 3D pyrochlore, hyperkagome, FCC lattice, diamond lattice, etc  
Na $_4$ Ir $_3$ O $_8$ , IrO $_2$ , Ba $_2$ YMoO $_6$ , Yb $_2$ Ti $_2$ O $_7$ , Pr $_2$ Zr $_2$ O $_7$ , Pr $_2$ Sn $_2$ O $_7$ , Tb $_2$ Ti $_2$ O $_7$ , Nd $_2$ Zr $_2$ O $_7$ , FeSc $_2$ S $_4$ , etc
- Kitaev honeycomb materials: RuCl $_3$ , etc
- Ultracold atom and molecules on optical lattices: temperature is too high now.

**Some candidate materials have already been ruled out.**

**Not being a QSL does not necessarily mean the physics is not interesting !**

# Some physical mechanisms (not uniquely defined)

或许可以提供寻找spin liquid一些线索吧

The more you work in this field, the more you feel that there is no (simple) general rule of thumb.

1. Weak Mott insulators: a couple organics,  $\text{Na}_4\text{Ir}_3\text{O}_8$ , etc
2. Cluster localization/Mott:  $1\text{T-TaS}_2$ ,  $\text{Li}_2\text{ZnMo}_3\text{O}_8$
3. Strong frustration: geometric frustration (not necessarily), small spin (not necessarily either), many many examples
4. Spin-orbital entanglement, orbital presence,  $\text{SU}(N)$  systems, etc

A characteristic (not always): Mott insulators with odd filling even with SOC.  
Counter examples: Kitaev QSL, Pyrochlore  $\text{U}(1)$  QSL

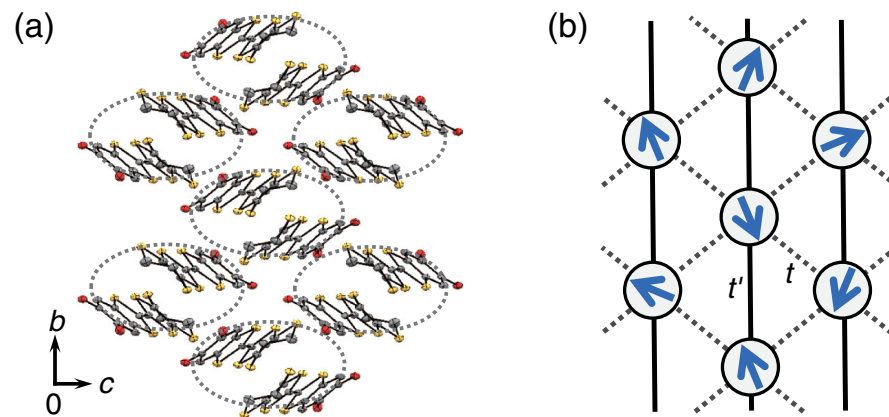
下边的报告内容按照quantum spin liquid的物理机制来组织，并部分address下边的问题

1. 自由度是什么 (degrees of freedom) ?
2. 自由度之间可能的相互作用 (interaction)
3. 相关的现象(relevant phenomena)
4. 什么的机制、解释、期望 (mechanism, explanation) 。

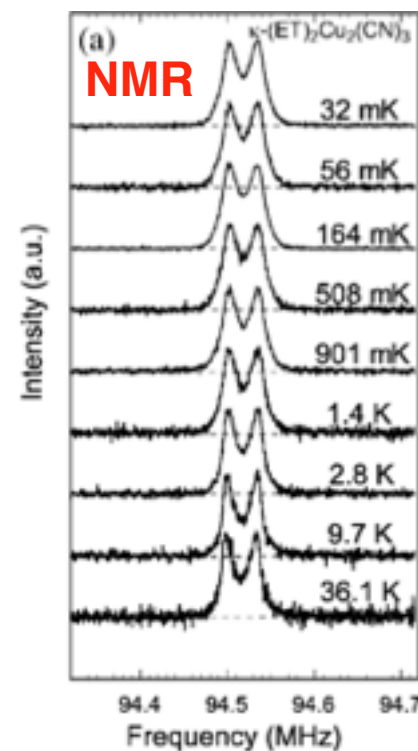
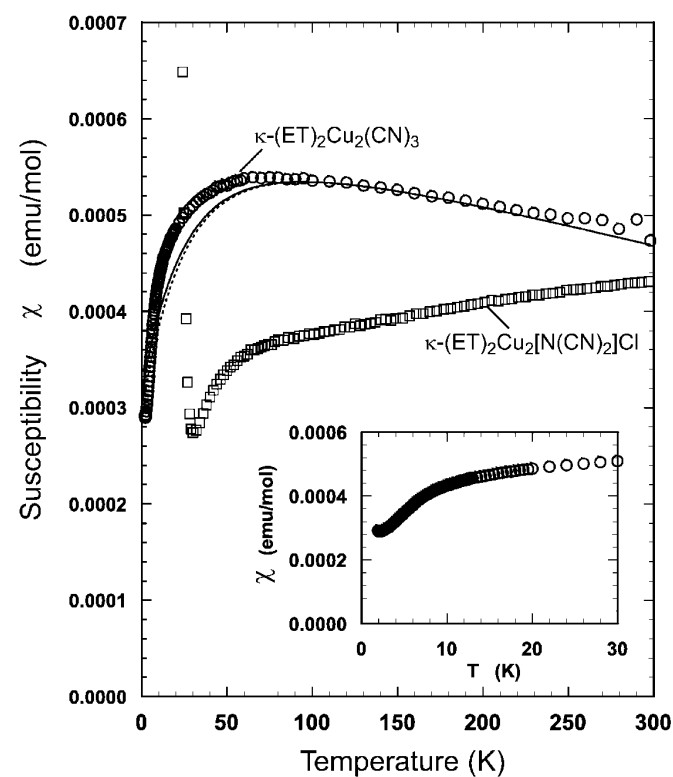
# Weak Mott insulator: organics



Kanoda



$\kappa$ -(BEDT-TTF)<sub>2</sub>Cu<sub>2</sub>(CN)<sub>3</sub>,  
EtMe<sub>3</sub>Sb[Pd(dmit)<sub>2</sub>]<sub>2</sub>,  
 $\kappa$ -H<sub>3</sub>(Cat-EDT-TTF)<sub>2</sub> **a new one!**



- \* No magnetic order down to 32mK
- \* Constant spin susceptibility at zero temperature

Other experiments: transport,  
heat capacity, optical absorption, etc,  
Unfortunately, **no neutron scattering** so far.

# Proximity to Mott transition

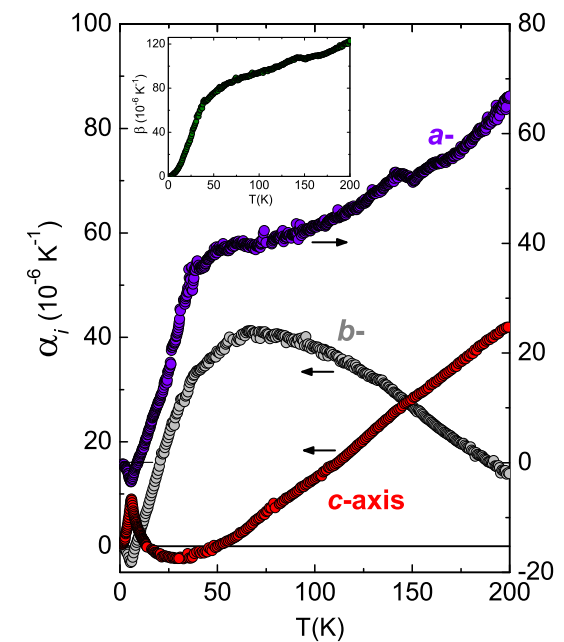
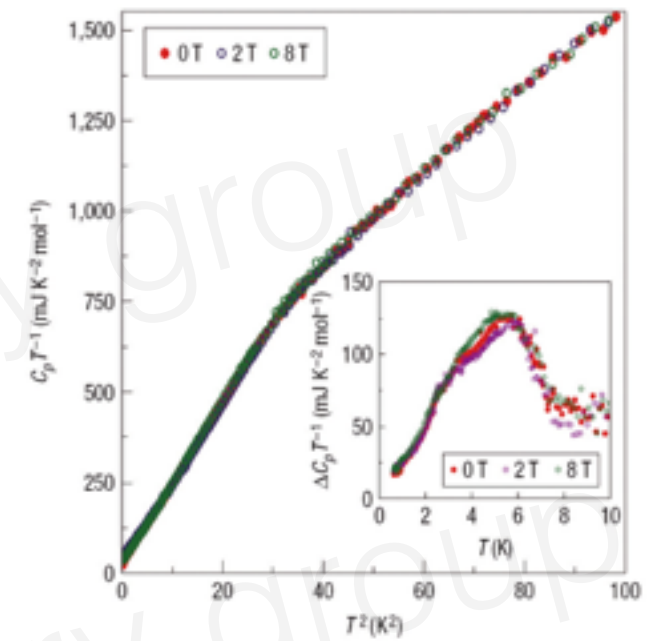
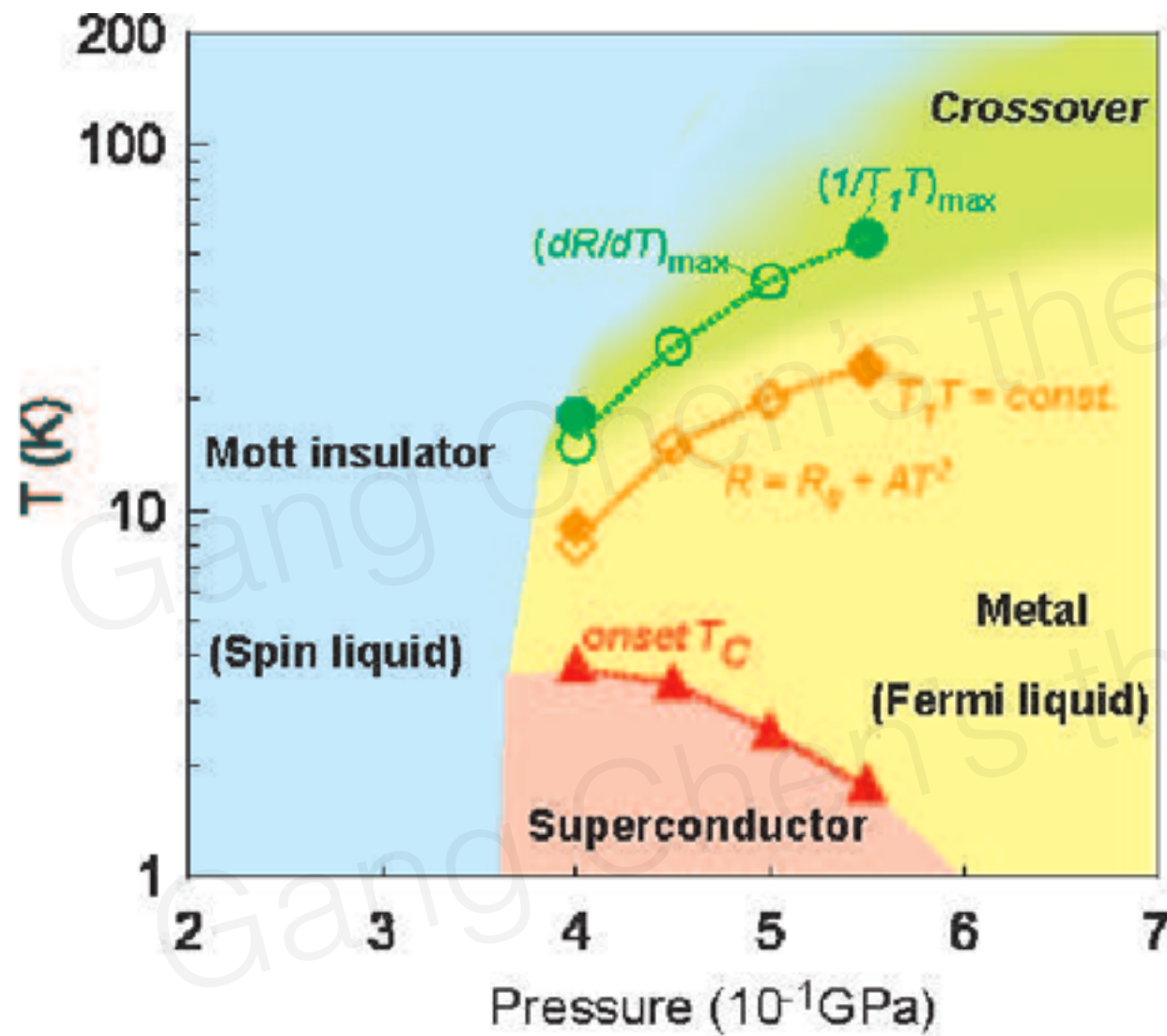
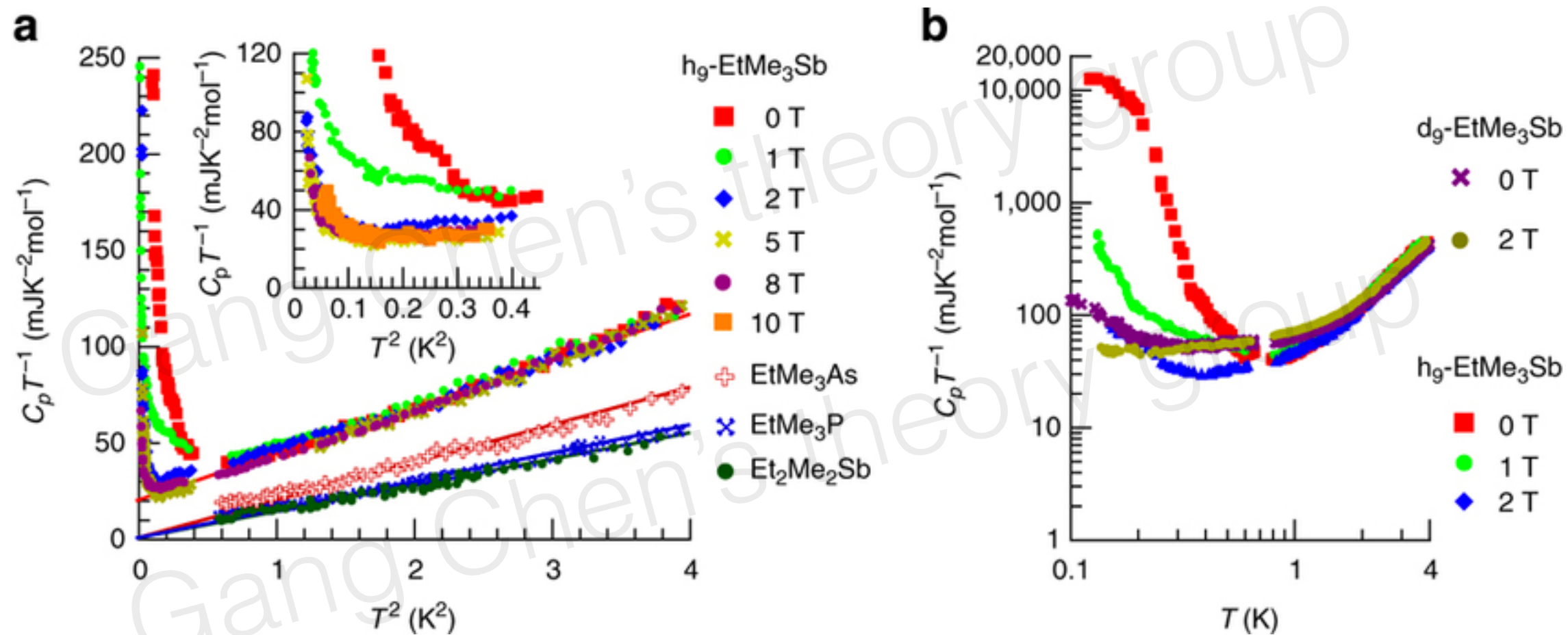


FIG. 1: (Color online) Uniaxial expansivities  $\alpha_i$  of  $\kappa$ -(BEDT-TTF) $_2$ Cu $_2$ (CN) $_3$  along the in-plane  $i = b$  and  $c$  axes (left scale) and along the out-of-plane  $i = a$  axis (right scale). Inset shows the volume expansion coefficient  $\beta$ .



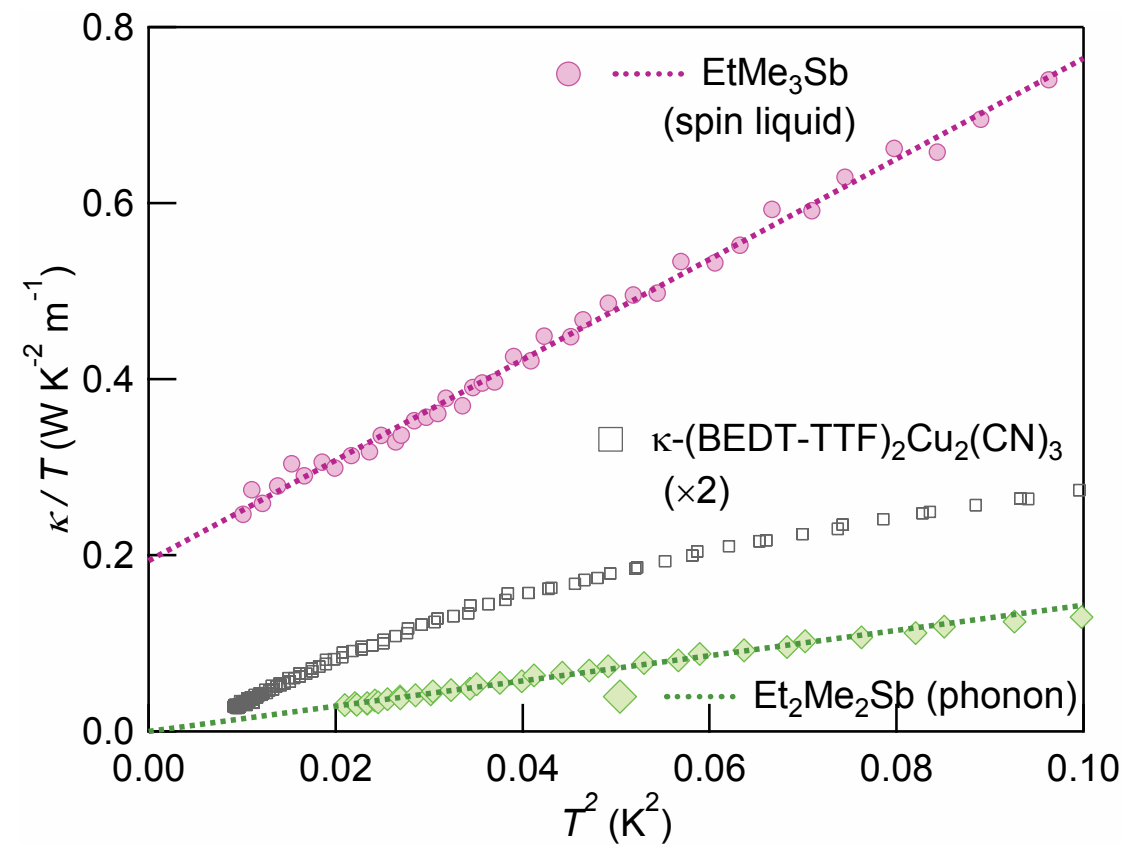
# dmit organics



# Thermal transport $\kappa_{xx}$ ??

## Thermal-transport studies of Two-dimensional Quantum Spin Liquids

Minoru Yamashita, Takasada Shibauchi, and Yuji Matsuda



Shiyan will talk about this in a couple days.

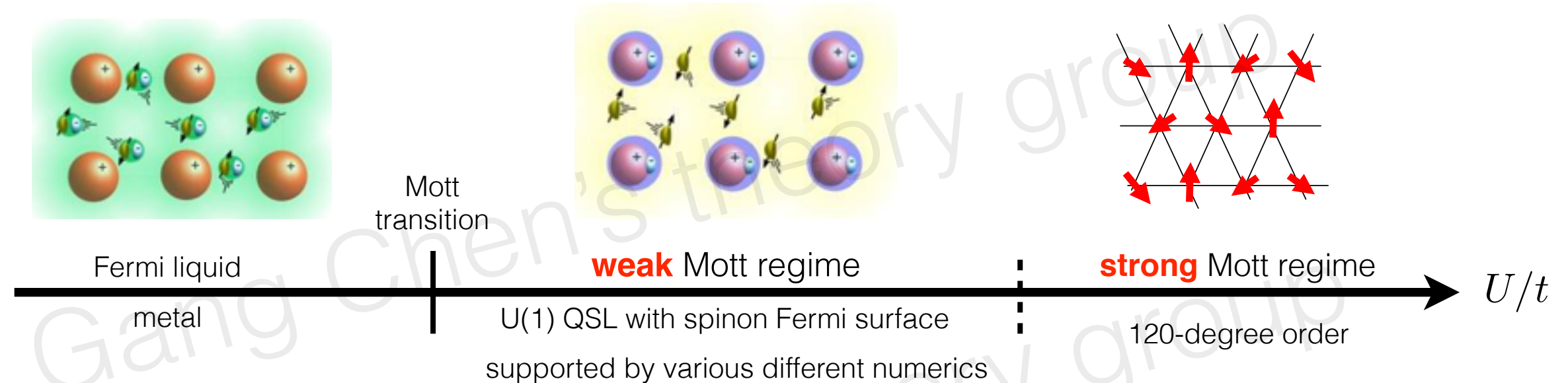
- Theoretical understanding: expected phase diagram

$$H = -t \sum_{\langle ij \rangle, \sigma} c_{i\sigma}^\dagger c_{j\sigma} + h.c. + U \sum_i n_{i\uparrow} n_{i\downarrow}$$



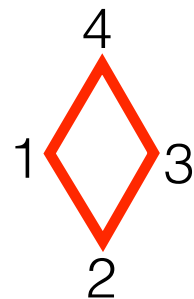
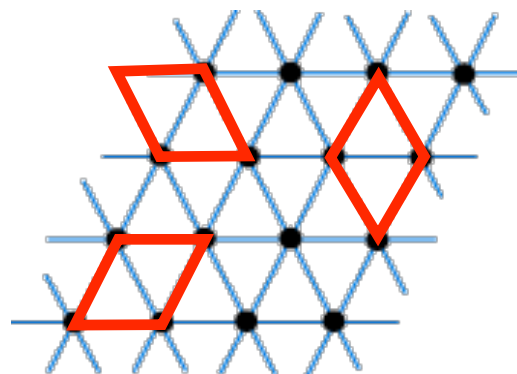
Sung-Sik Lee T Senthil P Lee

### Senthil's cartoon



- Physical mechanism** for weak Mott insulator spin liquids: perturbation in  $t/U$

$$H_{\text{pert}} = \sum_{ij} J_{ij} \mathbf{S}_i \cdot \mathbf{S}_j + K \sum_{1234} (P_{1234} + P_{1234}^{-1}) + \dots$$



4-site ring exchange

$$(\mathbf{S}_1 \cdot \mathbf{S}_2)(\mathbf{S}_3 \cdot \mathbf{S}_4) + (\mathbf{S}_1 \cdot \mathbf{S}_4)(\mathbf{S}_2 \cdot \mathbf{S}_3) - (\mathbf{S}_1 \cdot \mathbf{S}_3)(\mathbf{S}_2 \cdot \mathbf{S}_4)$$



Motrunich

# On top of this state

1. Amperean pairing:  $U1 \rightarrow Z2$  crossover (PA Lee, SS Lee)
2. Spin-lattice coupling:  $2k_F$  Kohn anomaly (Senthil, Mross)
3. Quantum oscillation (Motrunich)
4. Thermal Hall transport  $\kappa_{xy}$  (Nagaosa, PA Lee, Katsura)
5. Whether this state can exist in theory? How to describe it? (SS Lee, Max, Mross, Senthil, Hong Liu, etc)

“strong-coupled gapless system with infinite critical fermion modes”

# About triangular lattice Hubbard model

A recent numerics (DMRG) from Berkeley claims a chiral spin liquid.

Prof Donna Sheng may be a good person to consult.

**Observation of a chiral spin liquid phase of the Hubbard model on the triangular lattice: a density matrix renormalization group study**

Aaron Szasz,<sup>1,2,\*</sup> Johannes Motruk,<sup>1,2</sup> Michael P. Zaletel,<sup>3,1</sup> and Joel E. Moore<sup>1,2</sup>

<sup>1</sup>*Department of Physics, University of California, Berkeley, California 94720, USA*

<sup>2</sup>*Materials Sciences Division, Lawrence Berkeley National Laboratory, Berkeley, California 94720, USA*

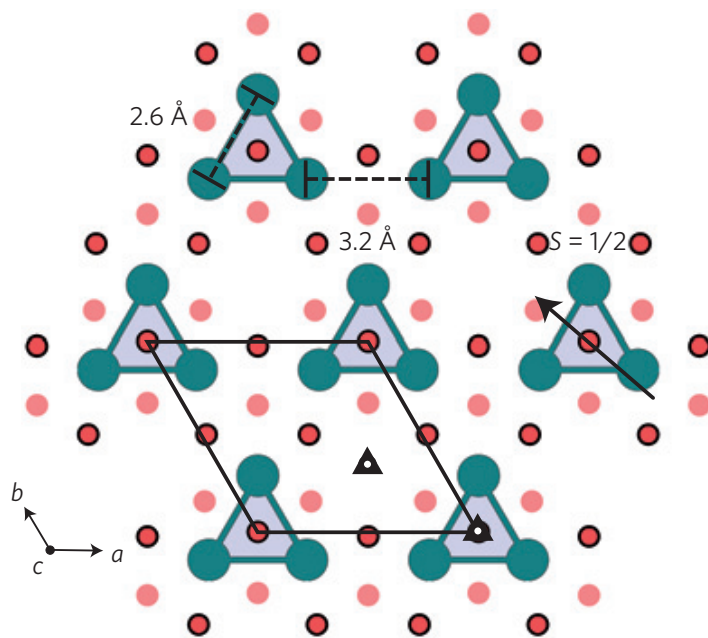
<sup>3</sup>*Department of Physics, Princeton University, Princeton, New Jersey 08540, USA*



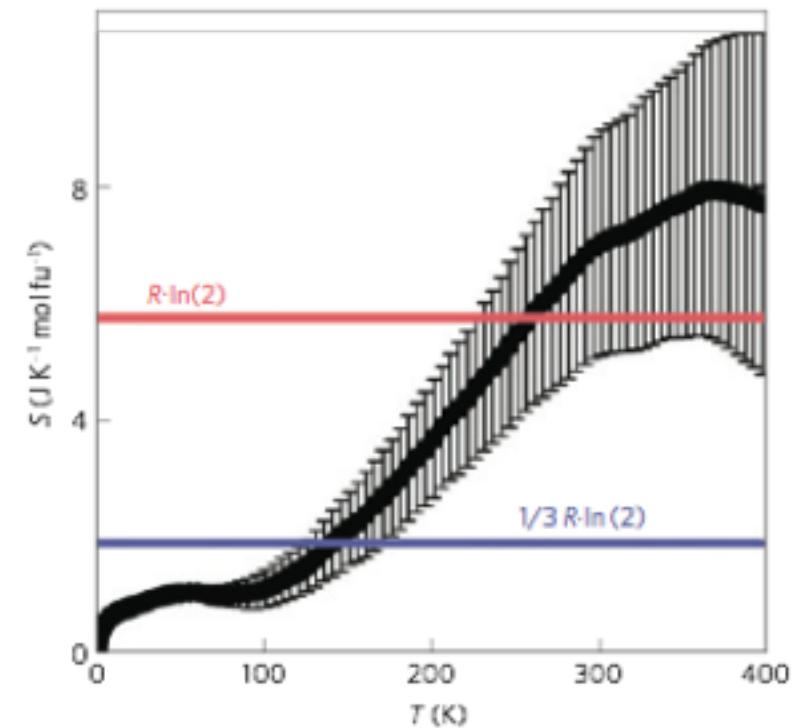
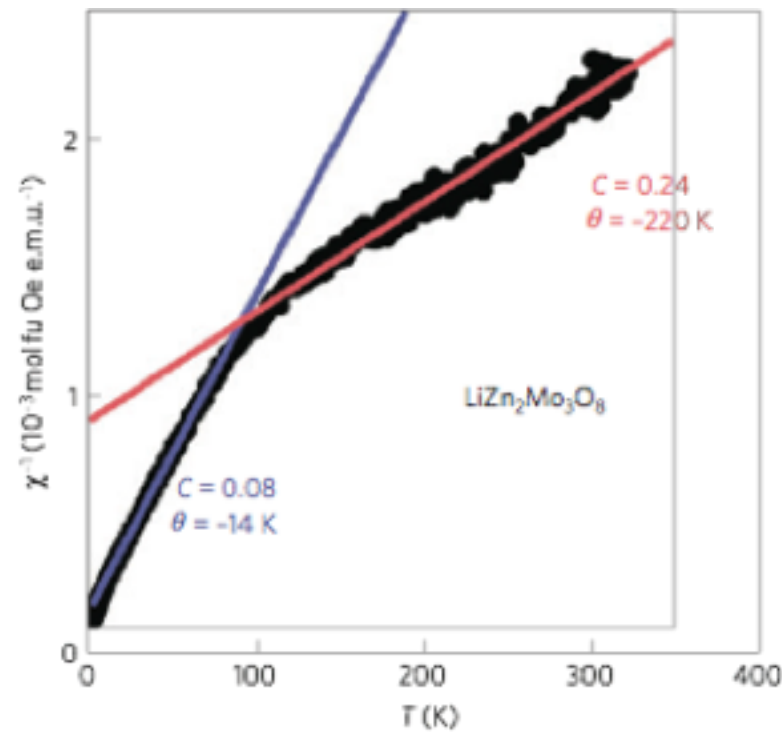
# Cluster localization in $\text{LiZn}_2\text{Mo}_3\text{O}_8$



T. McQueen



Nature Material 2012



- Why striking and difficult? Neither model works.
  1. Triangular lattice Heisenberg model
  2. Triangular lattice Hubbard model at 1/2 filling
- Further low-temperature experiments: NMR,  $\mu\text{SR}$ , neutron scattering, proposed as a spin liquid candidate.



# Emergent honeycomb lattice in $\text{LiZn}_2\text{Mo}_3\text{O}_8$

Rebecca Flint and Patrick A. Lee

*Department of Physics, Massachusetts Institute of Technology, Cambridge, Massachusetts 02139, U.S.A.*

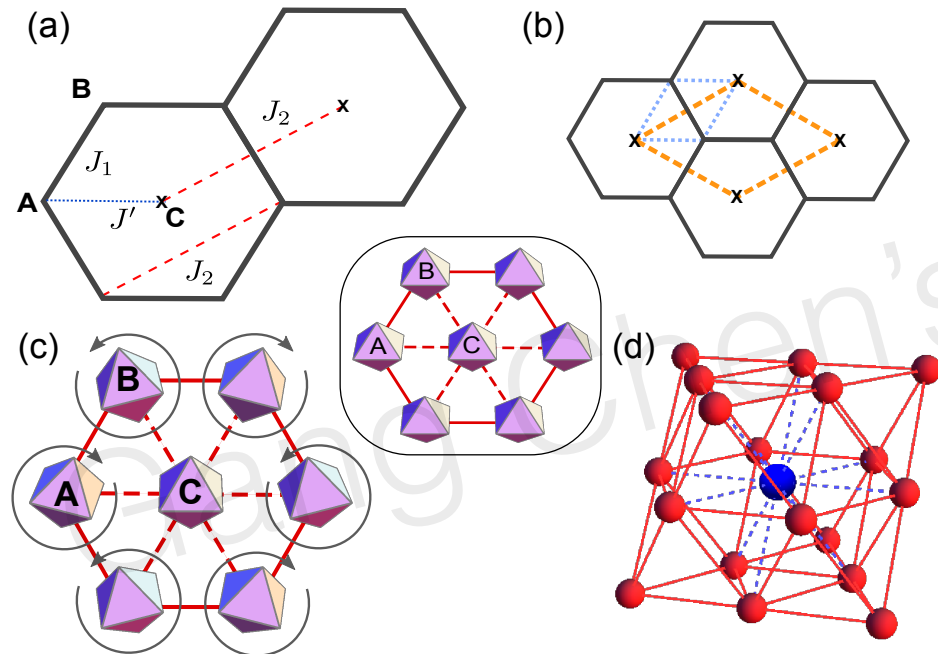
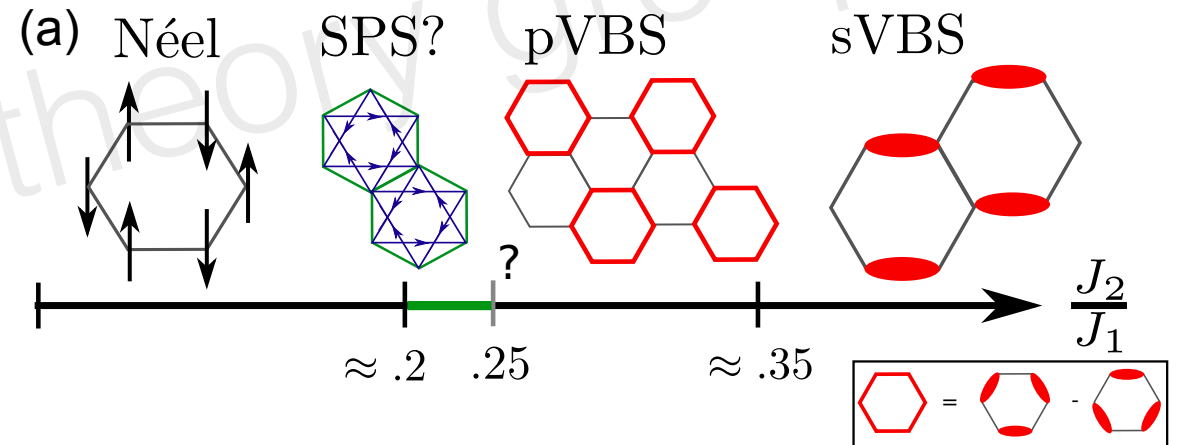
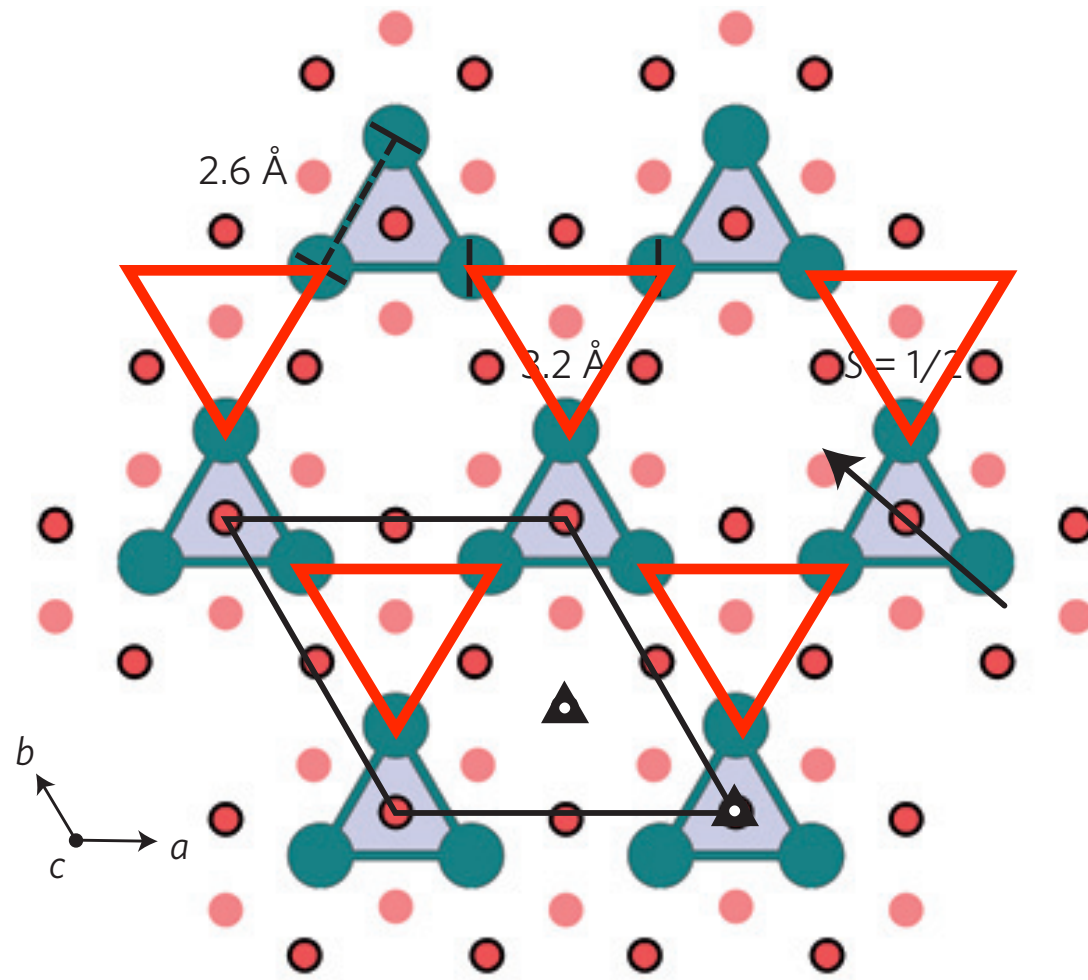


FIG. 1. (a)  $J_1 - J_2 - J'$  lattice, where  $J' = J_1$  describes the triangular lattice and  $J' = 0$  describes decoupled honeycomb ( $J_1 - J_2$ ) and triangular ( $J_2$ ) lattices. The A and B sublattices of the honeycomb lattice and the C sublattice of central spins are labeled. (b) Unit cells: blue dotted lines show the small initial unit cell, while orange dashed lines show the larger final unit cell. Both have trigonal symmetry - only the lattice vector changes. (c) These rotations convert the triangular lattice into the  $J_1 - J_2 - J'$  lattice: the A and B clusters rotate in opposite directions, while the C clusters do not rotate. Inset shows original configuration. (d) The basic unit of the depleted fcc lattice: strong bonds are shown as red (solid) lines, weak bonds as blue (dashed) lines. The central layer forms the emergent honeycomb lattice.

$$H = J_1 \sum_{\langle ij \rangle_{A,B}} \vec{S}_i \cdot \vec{S}_j + J_2 \sum_{\langle\langle ij \rangle\rangle_{A,B}} \vec{S}_i \cdot \vec{S}_j + J' \sum_{\langle ij \rangle_{\{(A,B),C\}}} \vec{S}_i \cdot \vec{S}_j.$$



A Claim: a single-band extended Hubbard model on an anisotropic Kagome lattice  
with **1/6 electron filling**.



$$\begin{aligned}
 H = & \sum_{\langle ij \rangle \in \text{u}} [-t_1 (c_{i\sigma}^\dagger c_{j\sigma} + h.c.) + V_1 n_i n_j] \\
 & + \sum_{\langle ij \rangle \in \text{d}} [-t_2 (c_{i\sigma}^\dagger c_{j\sigma} + h.c.) + V_2 n_i n_j] \\
 & + \sum_i \frac{U}{2} (n_i - \frac{1}{2})^2,
 \end{aligned}$$

3 spins behave as an effective  
spin-1/2 moments

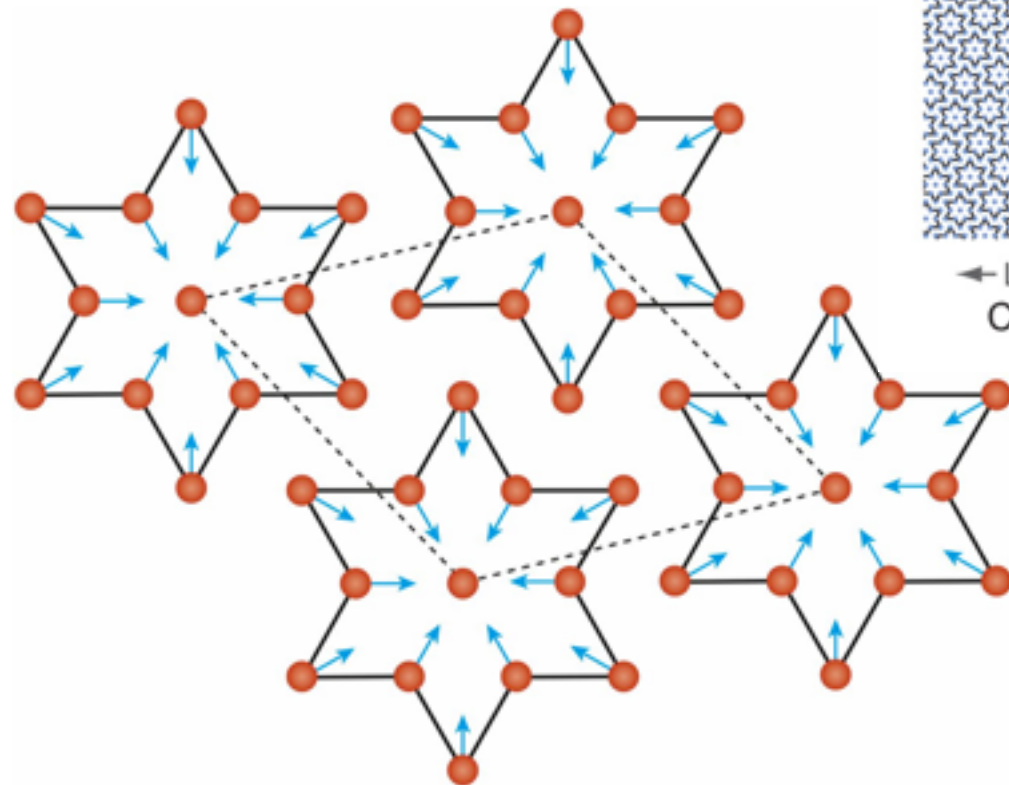
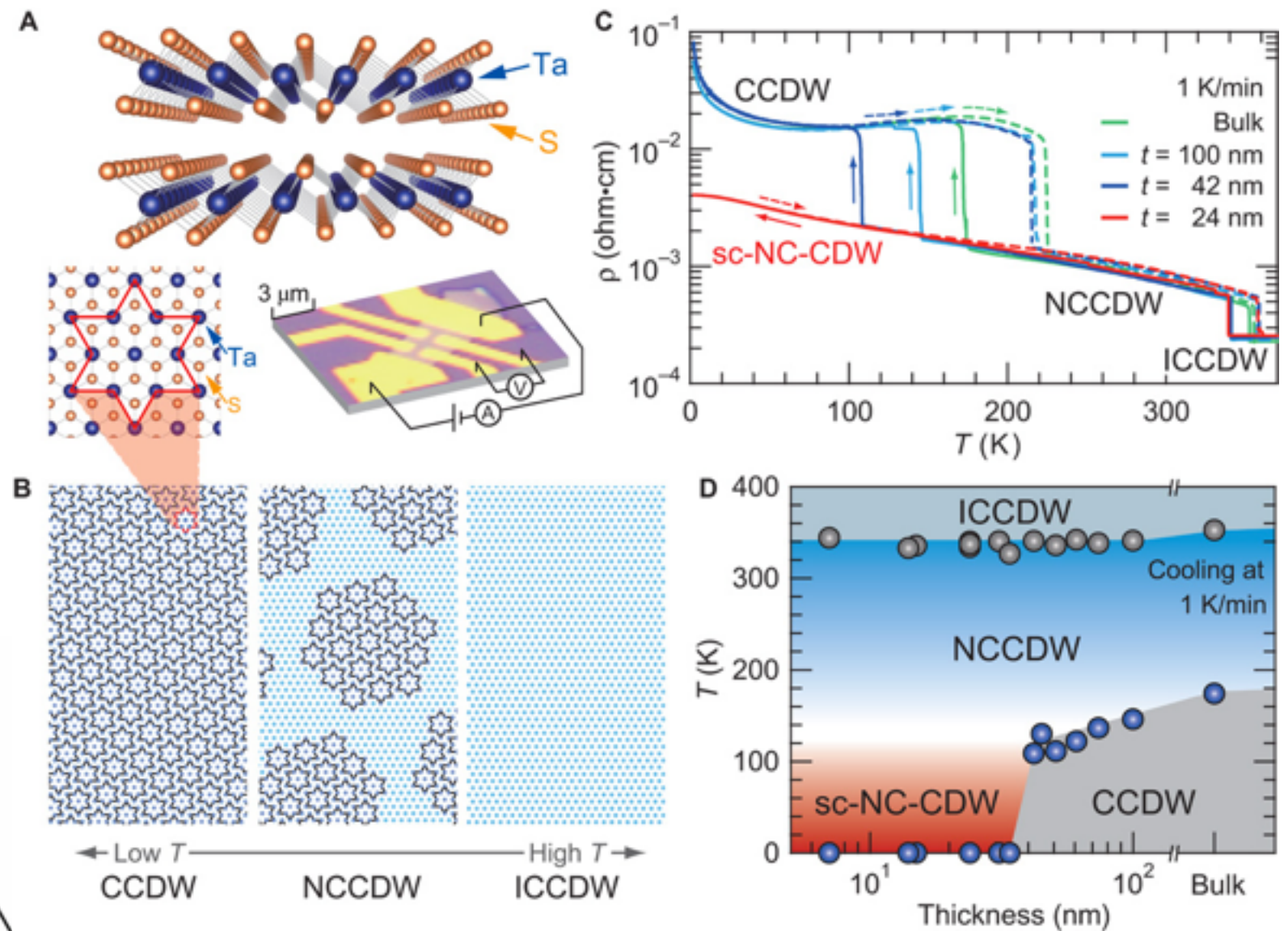
G Chen, HY Kee, YB Kim, 2015  
G Chen, PA Lee, 2018



# Cluster localization

1T-TaS<sub>2</sub>

PA Lee, KT Law



supertriangular lattice of David stars

# Spinon Fermi surface ?

## Spinon Fermi surface in a cluster Mott insulator model on a triangular lattice and possible application to 1T-TaS<sub>2</sub>

Wen-Yu He,<sup>1</sup> Xiao Yan Xu,<sup>1,\*</sup> Gang Chen,<sup>2,3</sup> K. T. Law,<sup>1</sup> and Patrick A. Lee<sup>4,†</sup>

$$\begin{aligned} \tilde{\mathcal{H}}_{\text{eff}} = & J \sum_{\langle i,j \rangle} \left( S_i^x S_j^x + S_i^y S_j^y + (1 + \gamma) S_i^z S_j^z \right) + K \sum_{\langle i,j,k,l \rangle} \left[ \left( S_i^x S_j^x + S_i^y S_j^y + (1 + \gamma) S_i^z S_j^z \right) \left( S_k^x S_l^x + S_k^y S_l^y + (1 + \gamma) S_k^z S_l^z \right) \right. \\ & \left. + \left( S_j^x S_k^x + S_j^y S_k^y + (1 + \gamma) S_j^z S_k^z \right) \left( S_i^x S_l^x + S_i^y S_l^y + (1 + \gamma) S_i^z S_l^z \right) - (S_i \cdot S_k) (S_j \cdot S_l) \right]. \end{aligned}$$

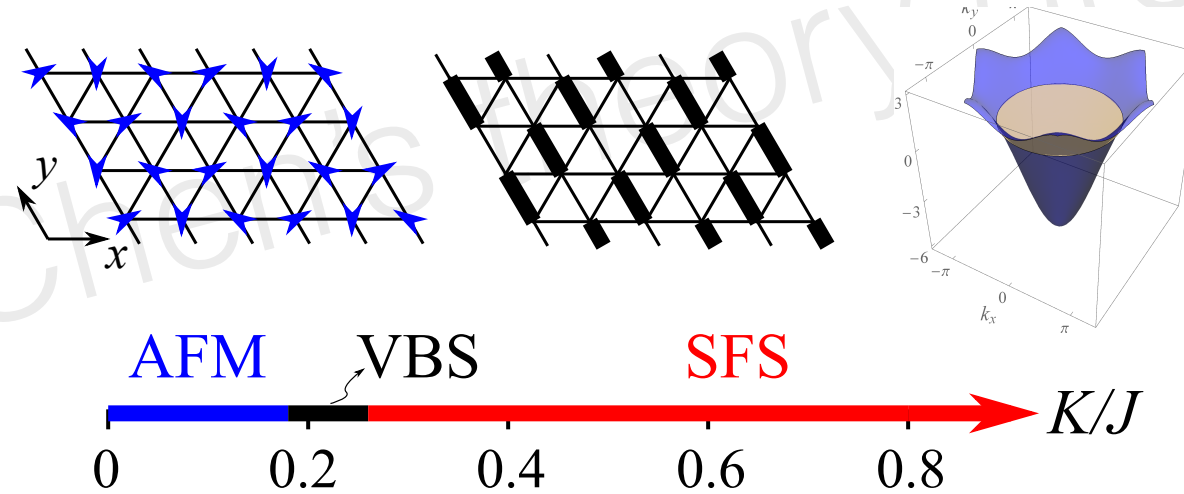
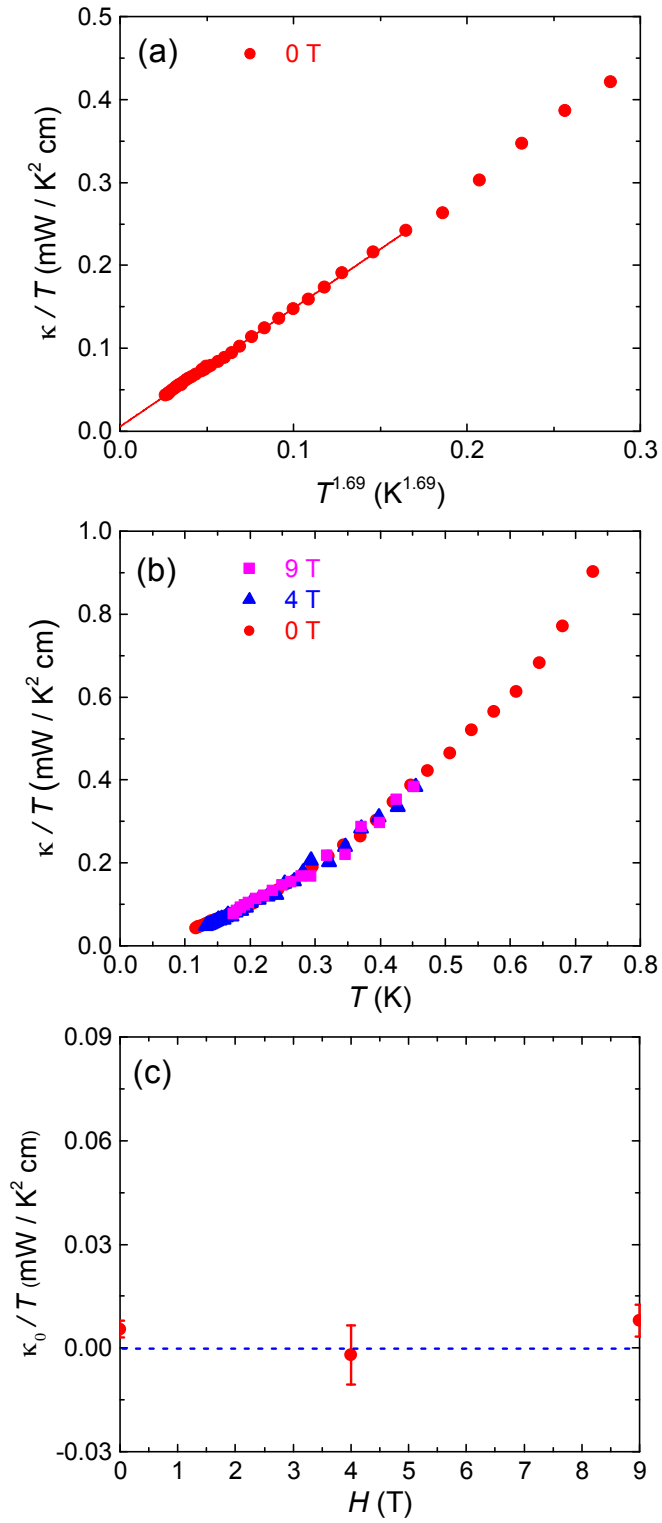


FIG. 1. Phase diagram for isotropic case ( $\gamma = 0$ ), while for small anisotropy case related to real materials 1T-TaS<sub>2</sub> the phase diagram is similar. It is mainly obtained from six wide systems and confirmed in eight wide systems. Here AFM denotes 120°-spin order; VBS denotes valence bond solid state (or call dimerized phase); SFS denotes a quantum spin liquid with a spinon Fermi surface.



Shiyan's data

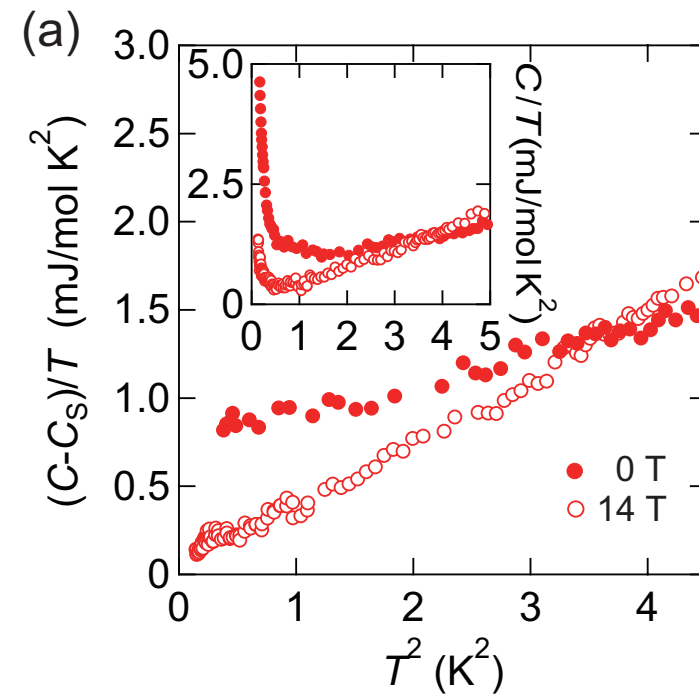
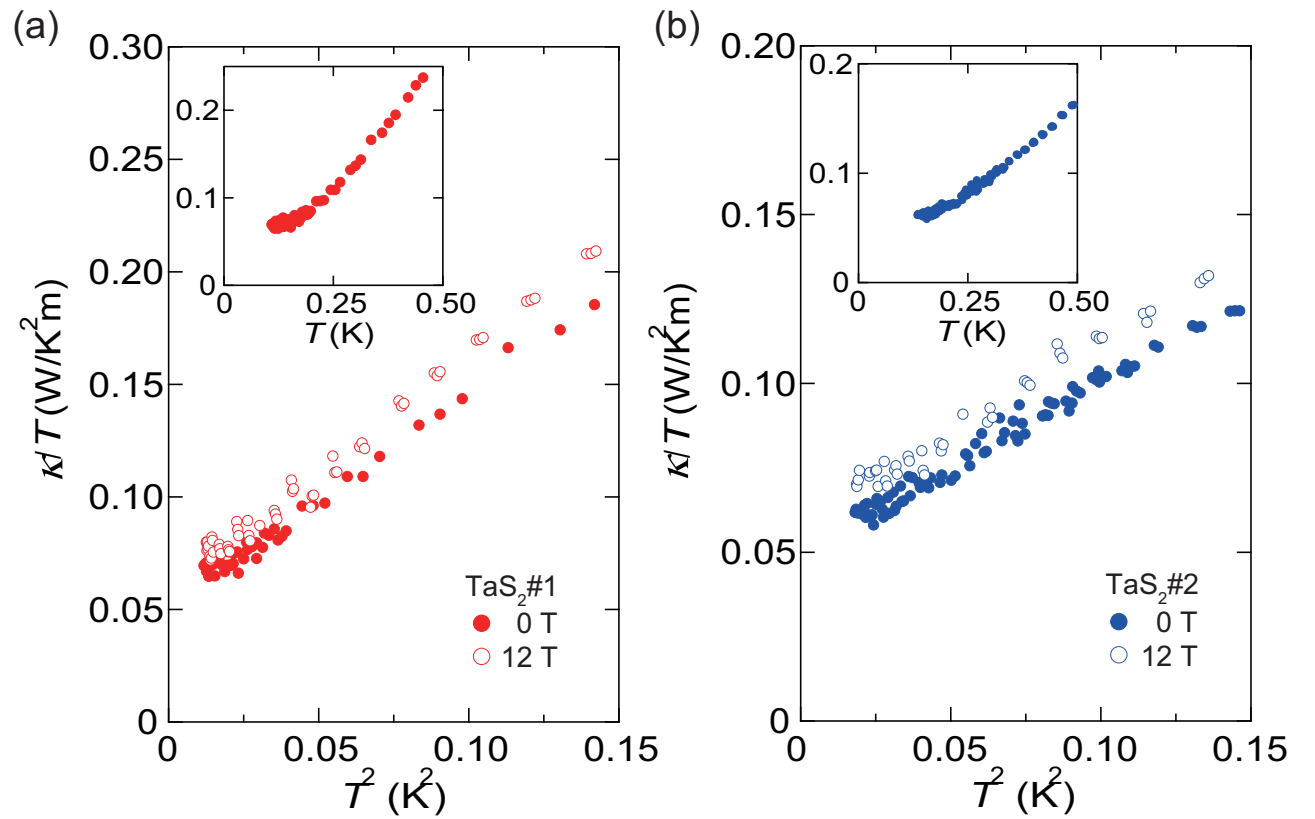


FIG. 2. (a) The inset shows  $C/T$  in zero field (filled red circles) and in magnetic field of  $\mu_0 H = 14$  T for  $\mathbf{H} \perp ab$  plane (open red circles) plotted as a function of  $T^2$ . The main panel shows the specific heat obtained after subtracting the Schottky contribution,  $(C - C_S)/T$ , plotted as a function of  $T^2$  in zero field (filled red circles) and at  $\mu_0 H = 14$  T (open



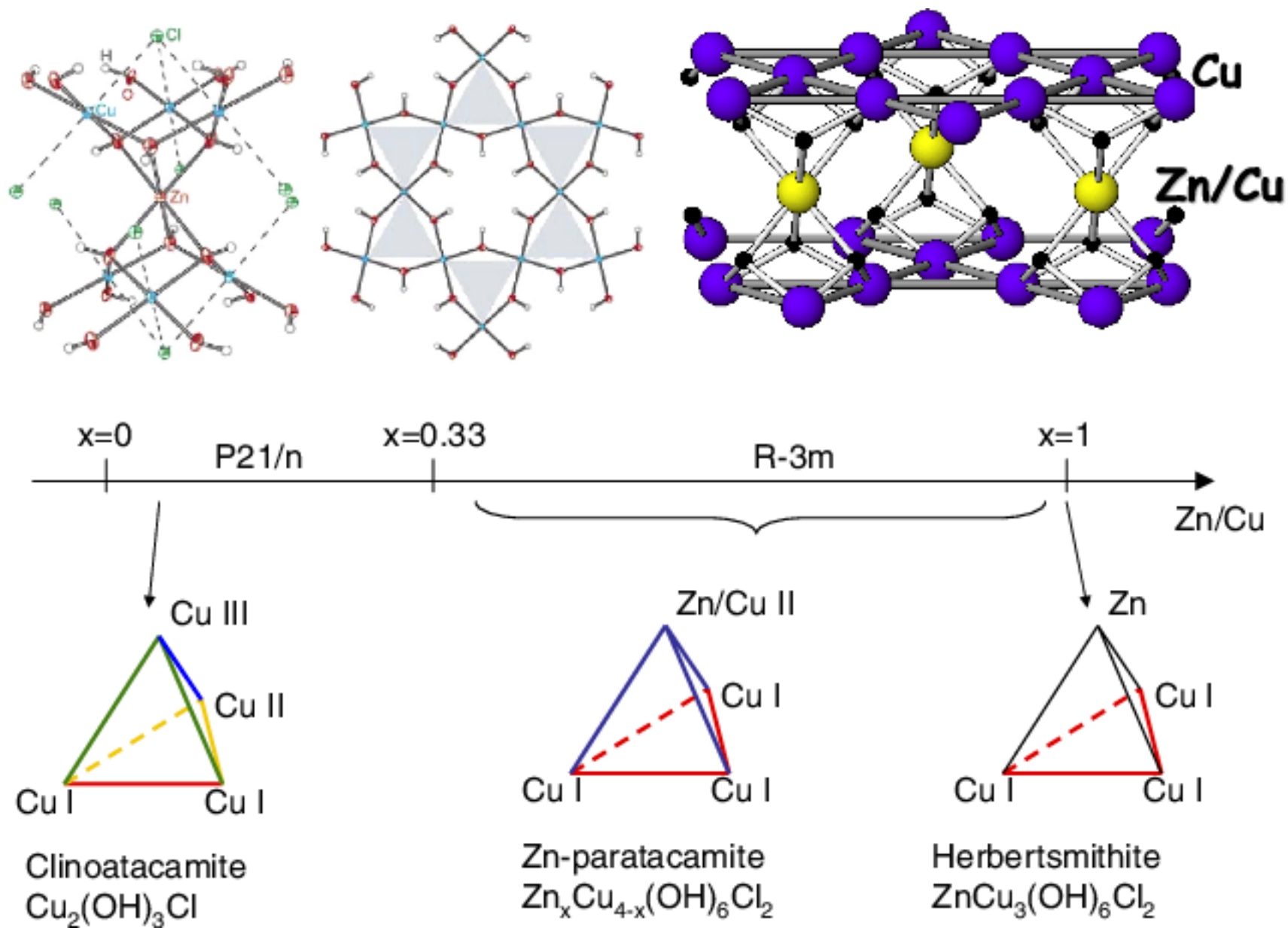
Matsuda

# Recent measurements

Unpublished STM data from Christopher Butler and Hanaguri, Japan on 1T-TaS<sub>2</sub>

Unpublished data on 1T-TaSe<sub>2</sub>, STM  
observe some extra supermodulation on top of the supercell structure

# Frustrated magnets: kagome



I assume Jiawei will talk about it

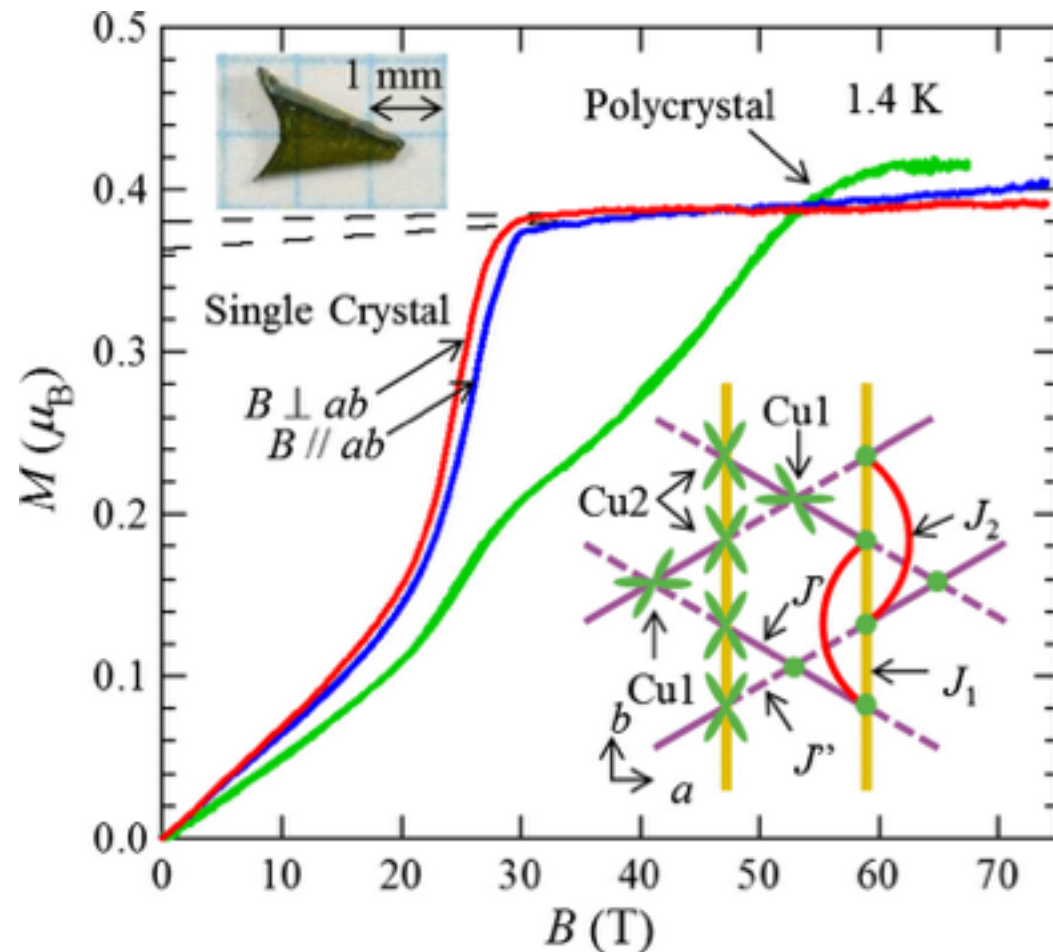
# Issues

1. “theory/numerics” on heisenberg model fluctuates between  $Z_2$  QSL and  $U(1)$  Dirac.
2. Expts by Young Lee points to  $Z_2$ , but some recent NMR may like fermi surface or Dirac.
3. Materials are not really Heisenberg, addition interactions comparable or larger than  $Z_2$  gaps (spinless gap). [Jiawei Mei, G Chen]

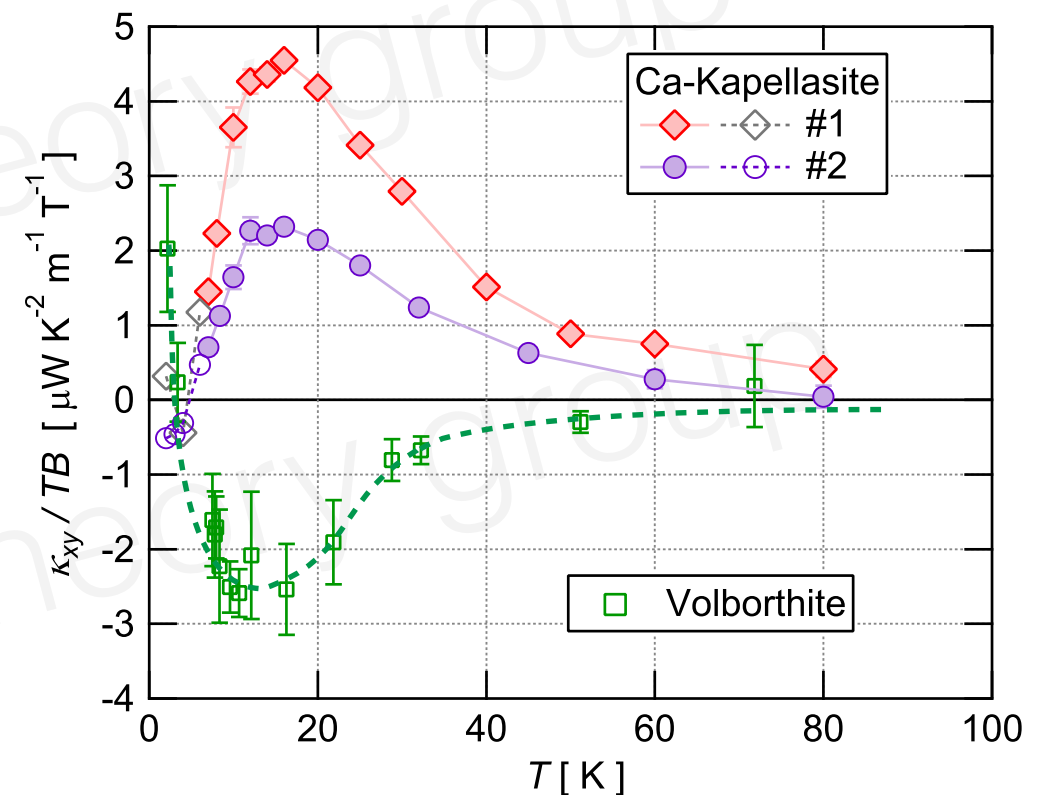


# Volborthite and Kapellasite

Large thermal Hall effect in spin-1/2 Kagome magnets



Z Hiroi's group



Minoru Yamashita's group

1. Why it is finite? All neutral excitations.
2. Non-monotonic.
3. Opposite signs in two materials.

# evolution in magnetic fields

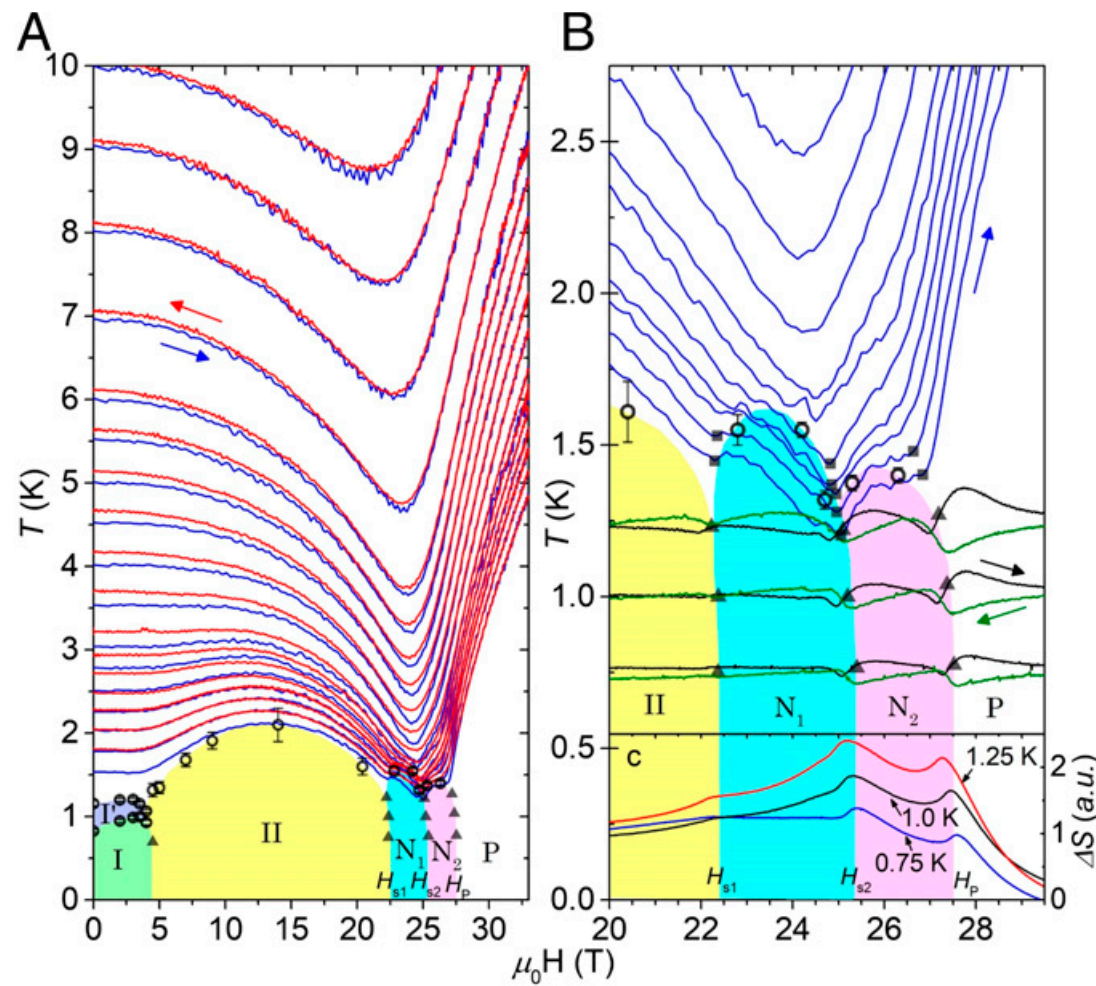
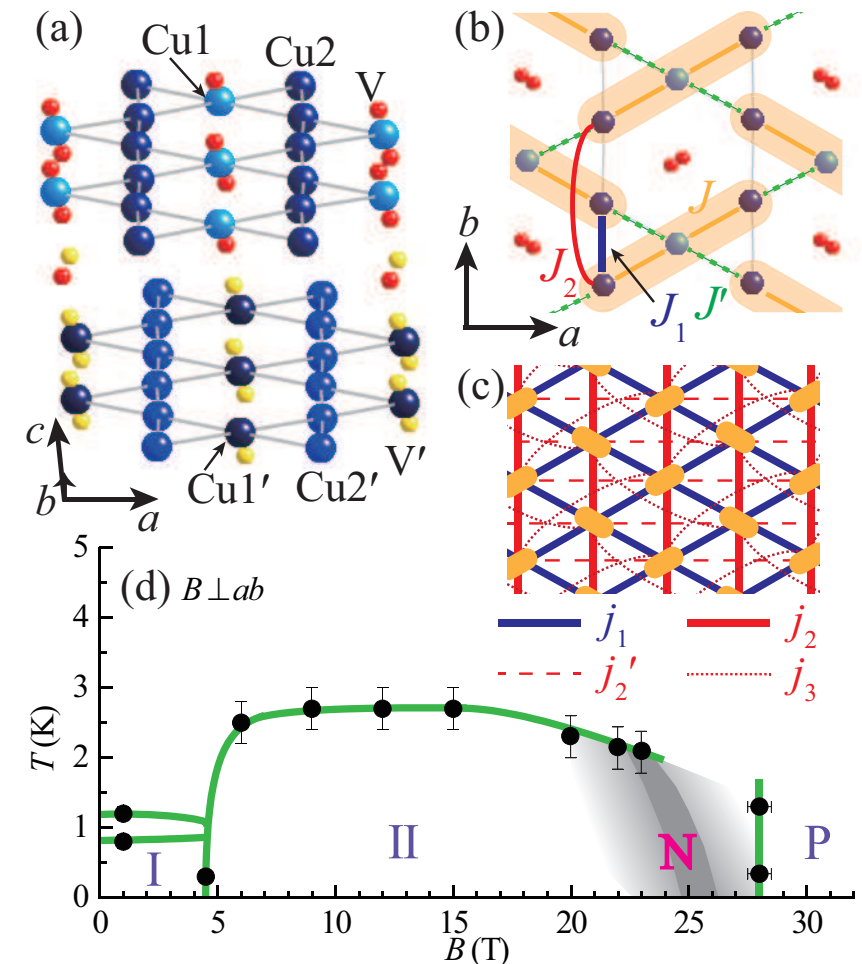


**Fig. 3.** Magnetocaloric effect and magnetic phase diagram of volborthite. (A) Experimental measurements of the MCE in volborthite, showing the evolution of temperature with changing magnetic field under (quasi-)adiabatic conditions (A-MCE). Results are shown for both rising (blue curves) and falling (red curves) magnetic field and reflect contours of constant entropy. The onset of the hidden-order phases,  $N_1$  and  $N_2$ , is associated with tight bunching curves and a dip in the entropy contour, corresponding to a change in sign of the MCE. Black triangles show phase boundaries at low temperature, extracted from complimentary measurements of MCE under isothermal conditions (I-MCE). The phase boundaries extracted from measurements of heat capacity,  $C(T)$ , are shown with open circles. (B) Detail of phases  $N_1$  and  $N_2$ , showing results for A-MCE measured in rising field (blue curves), I-MCE in rising field (black curves), and I-MCE in falling field (green curves). The black squares show the evolution of a corresponding feature in the A-MCE. Two distinct domes can be resolved at finite temperature, bounded by the critical fields  $H_{s1} = 22.5$  T,  $H_{s2} = 25.5$  T, and  $H_p = 27.5$  T. (C) Changes of entropy extracted from measurements of I-MCE at low temperature (*Methods*). The field boundaries of the SN phase,  $N_2$ , and presumed supersolid phase,  $N_1$ , are sharply distinguished by local anomalies in entropy.



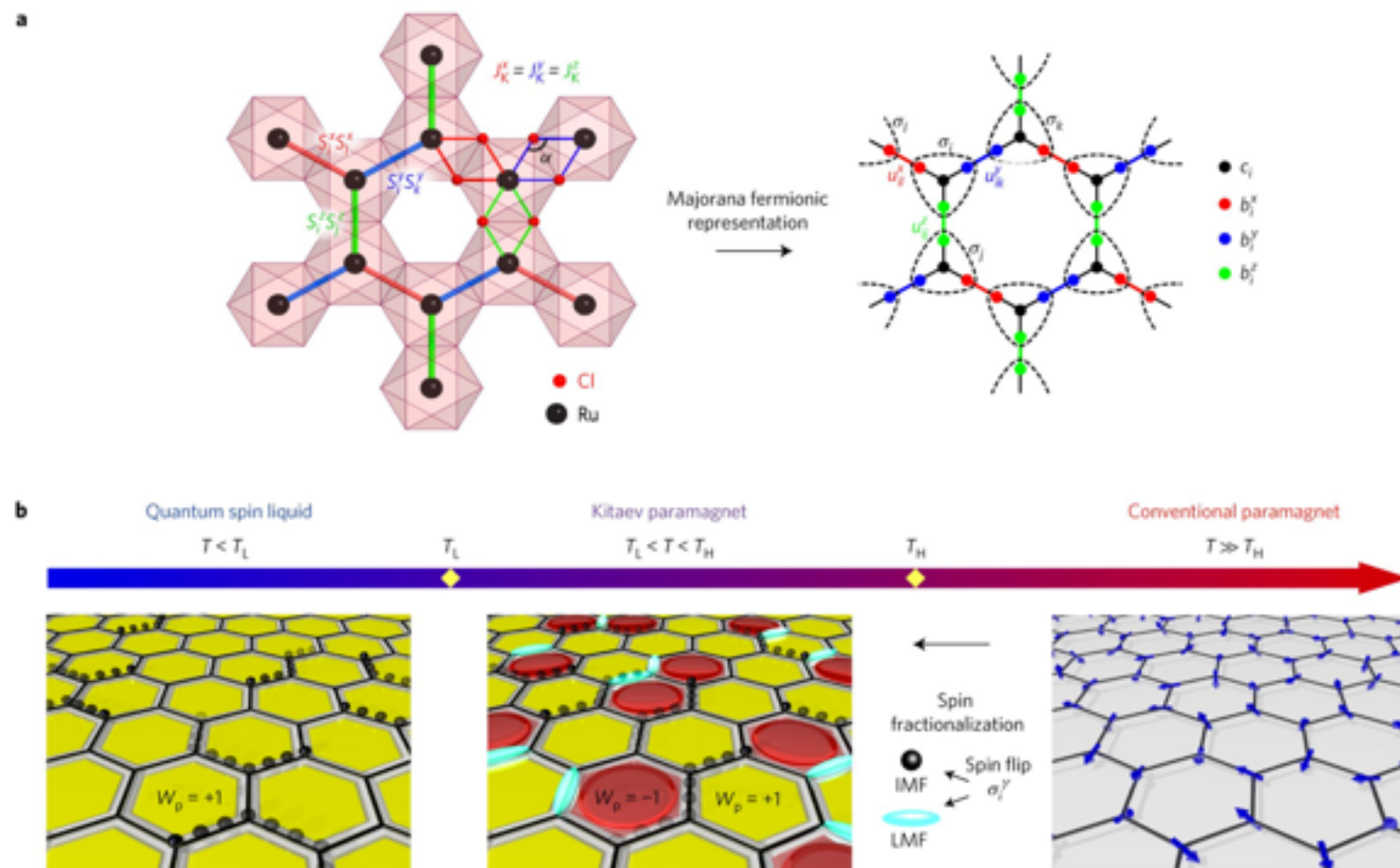
The interaction is anisotropic here, due to the distinct orbital content of the Cu ions.



# Frustrated magnets: honeycomb Kitaev materials (non heisenberg)

Na<sub>2</sub>IrO<sub>3</sub>, Li<sub>2</sub>IrO<sub>3</sub>, alpha-RuCl<sub>3</sub>, etc

**New examples:** OsCl<sub>3</sub>, Co-honeycomb, YbCl<sub>3</sub>



Let me talk about this on Wednesday

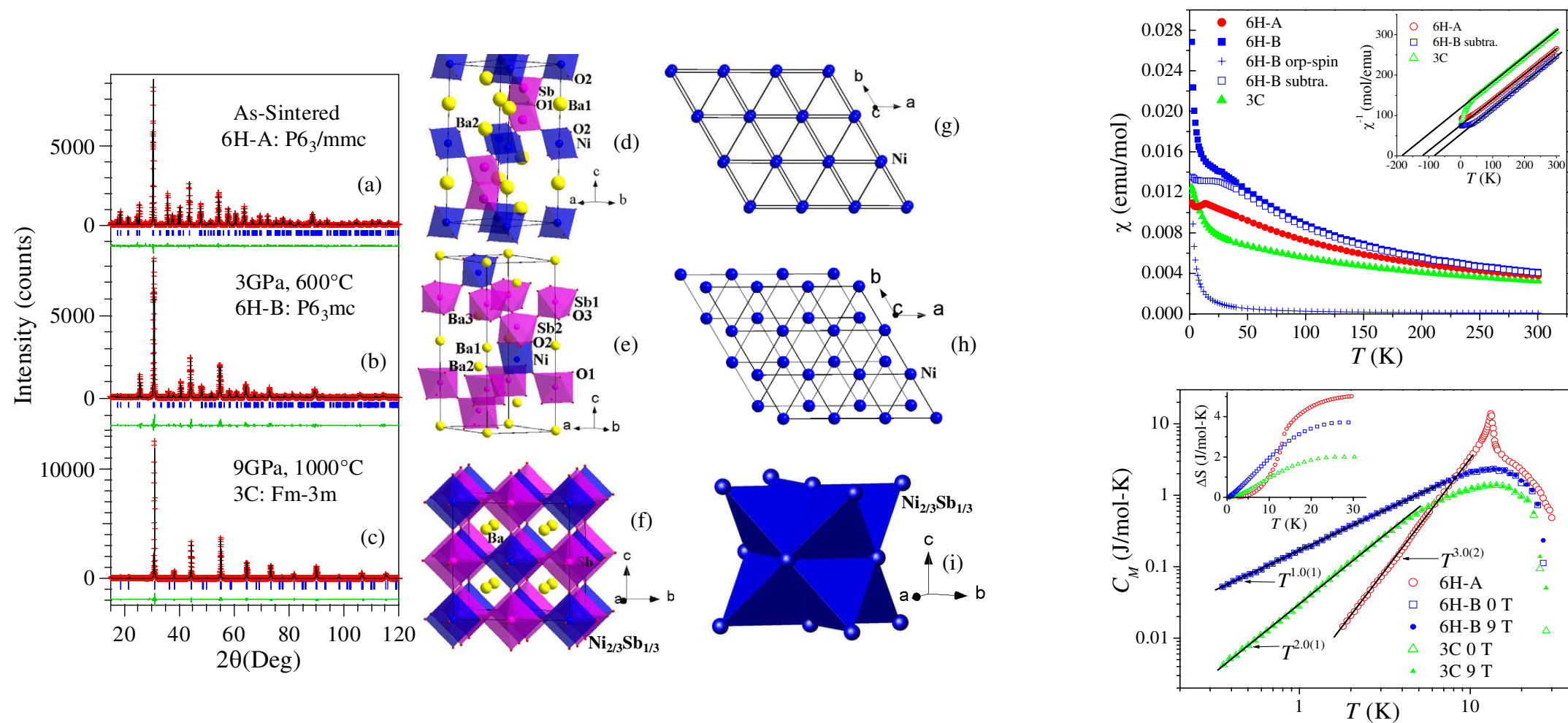
# Frustrated magnets: spin-1 magnets [可作为某个专题]

自旋-1 仍很quantum, 仍可以stabilize量子态。

## Ni-triangular magnets

High pressure sequence of  $\text{Ba}_3\text{NiSb}_2\text{O}_9$  structural phases: new  $S = 1$  quantum spin-liquids based on  $\text{Ni}^{2+}$

J. G. Cheng,<sup>1</sup> G. Li,<sup>2</sup> L. Balicas,<sup>2</sup> J. S. Zhou,<sup>1</sup> J. B. Goodenough,<sup>1</sup> Cenke Xu,<sup>3</sup> and H. D. Zhou<sup>2,\*</sup>



# 三个理论

## Spin Liquid Phases for Spin-1 systems on the Triangular lattice

Cenke Xu,<sup>1</sup> Fa Wang,<sup>2</sup> Yang Qi,<sup>3</sup> Leon Balents,<sup>1,4</sup> and Matthew P. A. Fisher<sup>1</sup>

construct a spin liquid state with quadratic band touching,  
not a model study

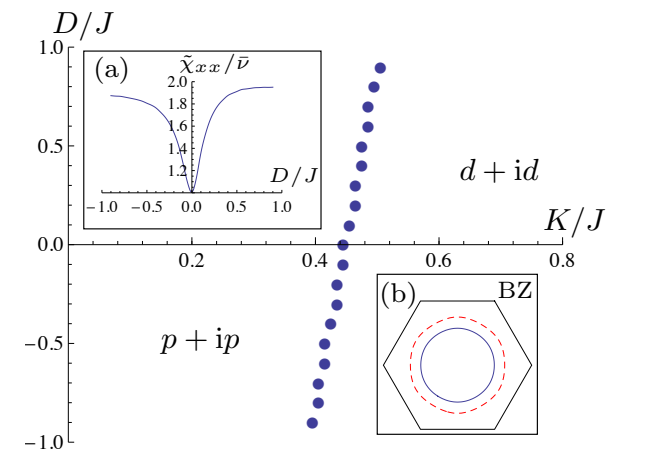
## Exotic $S = 1$ spin liquid state with fermionic excitations on triangular lattice

Maksym Serbyn, T. Senthil, and Patrick A. Lee

*Department of Physics, Massachusetts Institute of Technology, Cambridge, Massachusetts 02139*

(Dated: September 28, 2018)

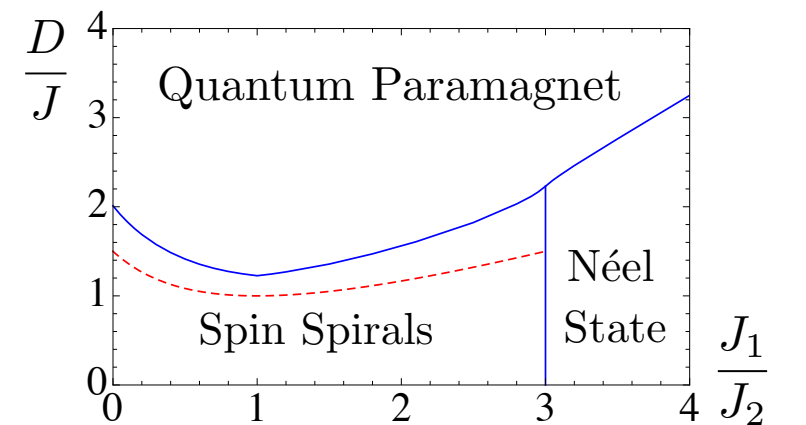
$$H = \sum_{\langle ij \rangle} [J \vec{S}_i \cdot \vec{S}_j + K (\vec{S}_i \cdot \vec{S}_j)^2] + D \sum_i (S_i^z)^2,$$



## Frustrated quantum critical theory of putative spin-liquid phenomenology in $6\text{H-B-Ba}_3\text{NiSb}_2\text{O}_9$

G. Chen, M. Hermele, and L. Radzihovsky

$$\mathcal{H}_{\text{ex}} = J_1 \sum_{\langle ij \rangle \in \text{AB}} \mathbf{S}_i \cdot \mathbf{S}_j + J_2 \sum_{\langle ij \rangle \in \text{AA and BB}} \mathbf{S}_i \cdot \mathbf{S}_j.$$



# Ni-diamond lattice: NiRh<sub>2</sub>O<sub>4</sub>

maybe SPT,  
maybe QSL

## APS March Meeting 2017

Monday–Friday, March 13–17, 2017; New Orleans, Louisiana

### Session B48: Frustrated Magnetism: Spinel, Pyrochlores, and Frustrated 3D Magnets I

11:15 AM–2:15 PM, Monday, March 13, 2017

Room: 395

Sponsoring Units: GMAG DMP

Chair: Martin Mourigal, Georgia Tech

### **Abstract: B48.00006 : $S = 1$ on a Diamond Lattice in NiRh<sub>2</sub>O<sub>4</sub>**

12:15 PM–12:27 PM

[Preview Abstract](#)

MathJax **On** | [Off](#)   ← Abstract →

#### **Authors:**

Juan Chamorro  
(Johns Hopkins University)

Tyrel McQueen  
(Johns Hopkins University)

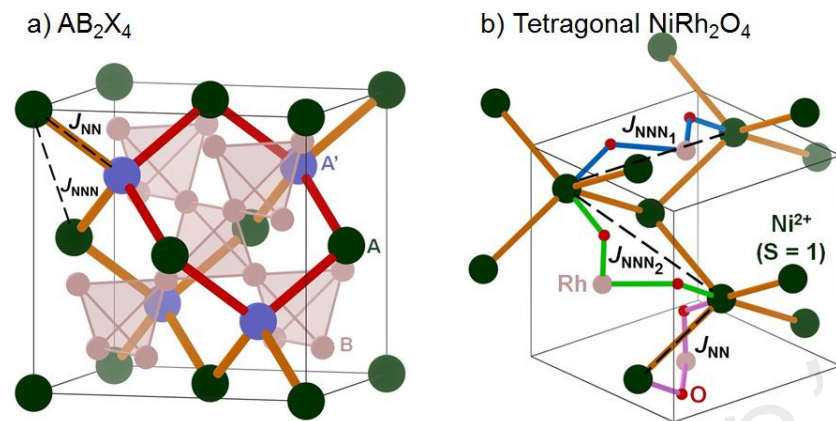
An  $S = 1$  system has the potential of rich physics, and has been the subject of intense theoretical work. Extensive work has been done on one-dimensional and two-dimensional  $S = 1$  systems, yet three dimensional systems remain elusive. Experimental realizations of three-dimensional  $S = 1$ , however, are limited, and no system to date has been found to genuinely harbor this. Recent theoretical work suggests that  $S = 1$  on a diamond lattice would enable a novel topological paramagnet state, generated by fluctuating Haldane chains within the structure, with topologically protected end states. Here we present data on NiRh<sub>2</sub>O<sub>4</sub>, a tetragonal spinel that has a structural phase transition from cubic to tetragonal at  $T = 380$  K. High resolution XRD shows it to have a tetragonally distorted spinel structure, with Ni<sup>2+</sup> ( $d^8$ ,  $S = 1$ ) on the tetrahedral, diamond sublattice site. Magnetic susceptibility and specific heat measurements show that it does not order magnetically down to  $T = 0.1$  K. Nearest neighbor interactions remain the same despite the cubic to tetragonal phase transition. Comparison to theoretical models indicate that this system might fulfill the requirements necessary to have both highly entangled and topological behaviors.



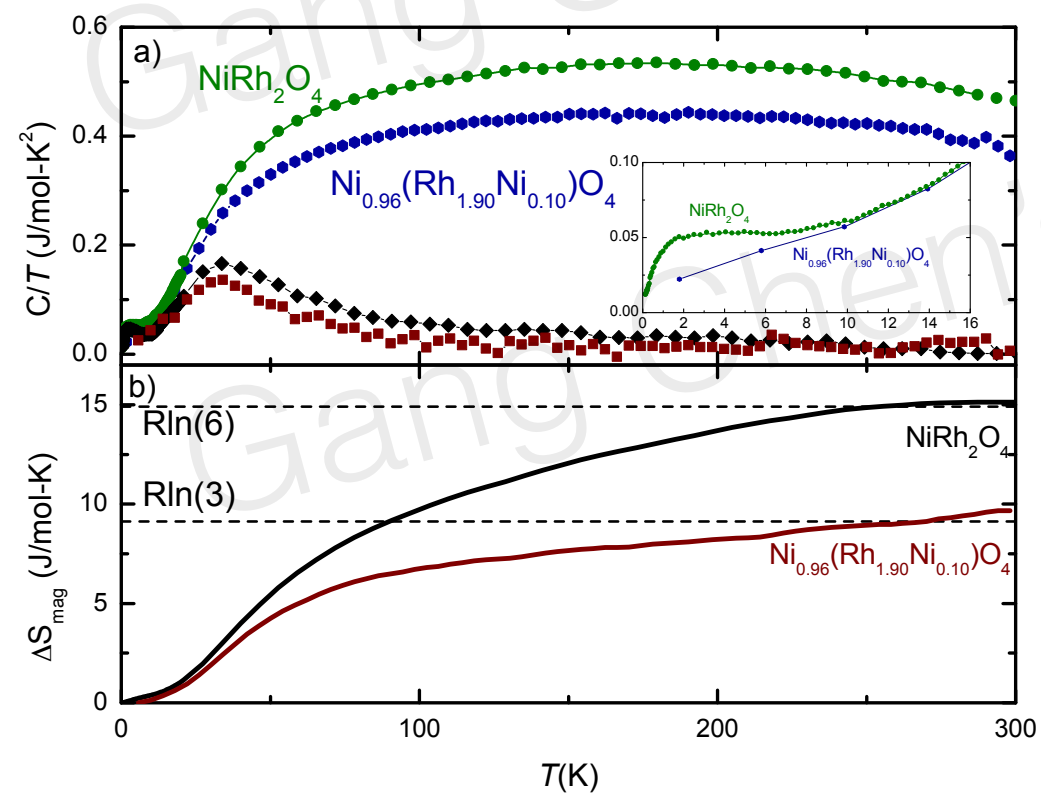
T. McQueen



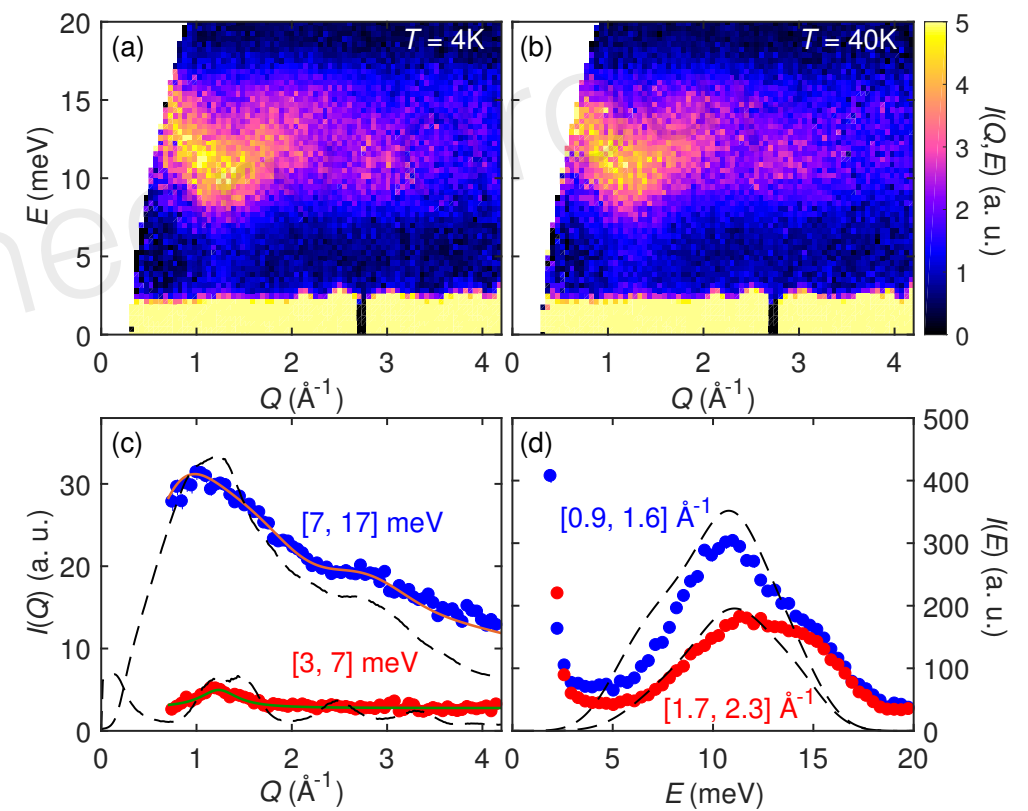
# Ni-diamond lattice: NiRh<sub>2</sub>O<sub>4</sub>



T. McQueen



orbital active



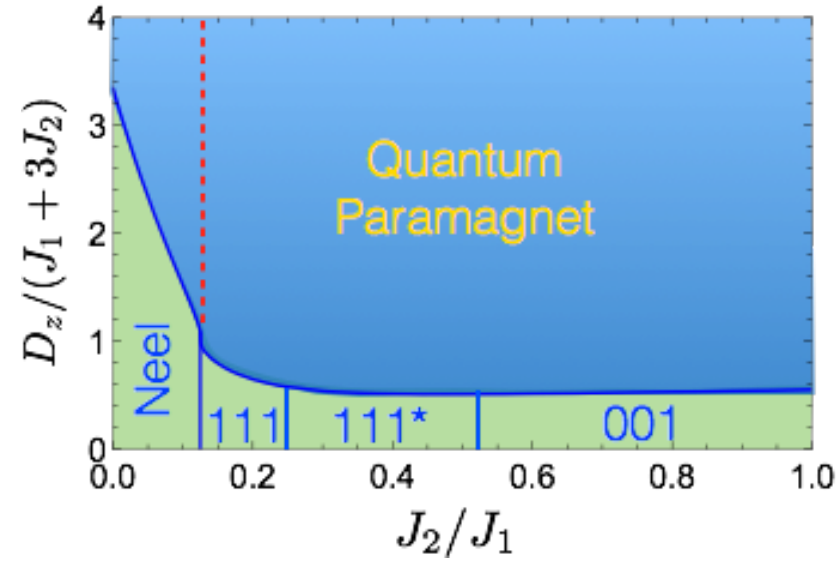
inelastic neutron

## Quantum Paramagnet and Frustrated Quantum Criticality in a Spin-One Diamond Lattice Antiferromagnet

Gang Chen<sup>1,2\*</sup>

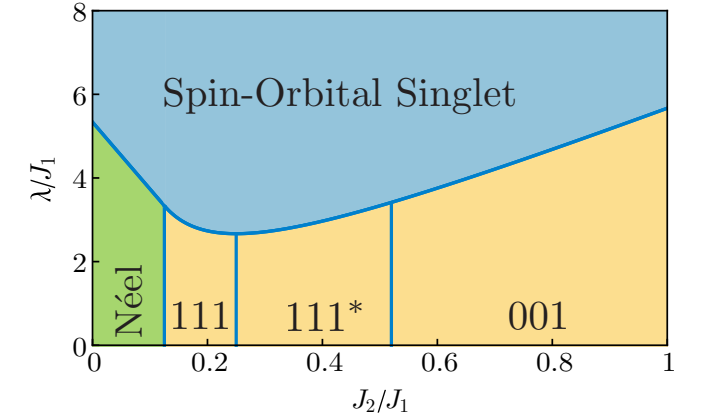
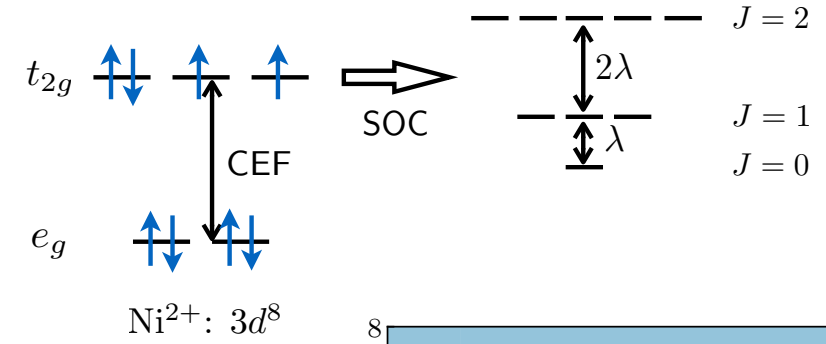
<sup>1</sup>State Key Laboratory of Surface Physics, Department of Physics,

$$H = J_1 \sum_{\langle \mathbf{r}\mathbf{r}' \rangle} \mathbf{S}_{\mathbf{r}} \cdot \mathbf{S}_{\mathbf{r}'} + J_2 \sum_{\langle\langle \mathbf{r}\mathbf{r}' \rangle\rangle} \mathbf{S}_{\mathbf{r}} \cdot \mathbf{S}_{\mathbf{r}'} + D_z \sum_{\mathbf{r}} (S_{\mathbf{r}}^z)^2, \quad (1)$$



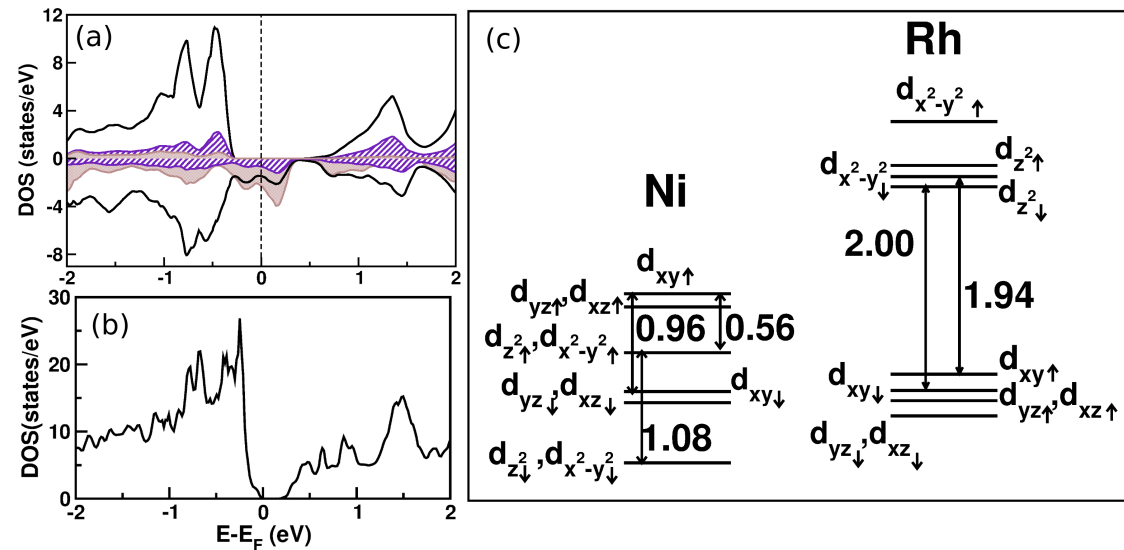
## Spin-orbital entanglement in $d^8$ Mott insulators: Possible excitonic magnetism in diamond lattice antiferromagnets

Fei-Ye Li and Gang Chen<sup>\*</sup>



## The Curious Case of $\text{NiRh}_2\text{O}_4$ : A Spin-Orbit Entangled Diamond Lattice Paramagnet

Shreya Das,<sup>1</sup> Dhani Nafday,<sup>2</sup> Tanusri Saha-Dasgupta,<sup>1,2</sup> and Arun Paramakanti<sup>3,\*</sup>

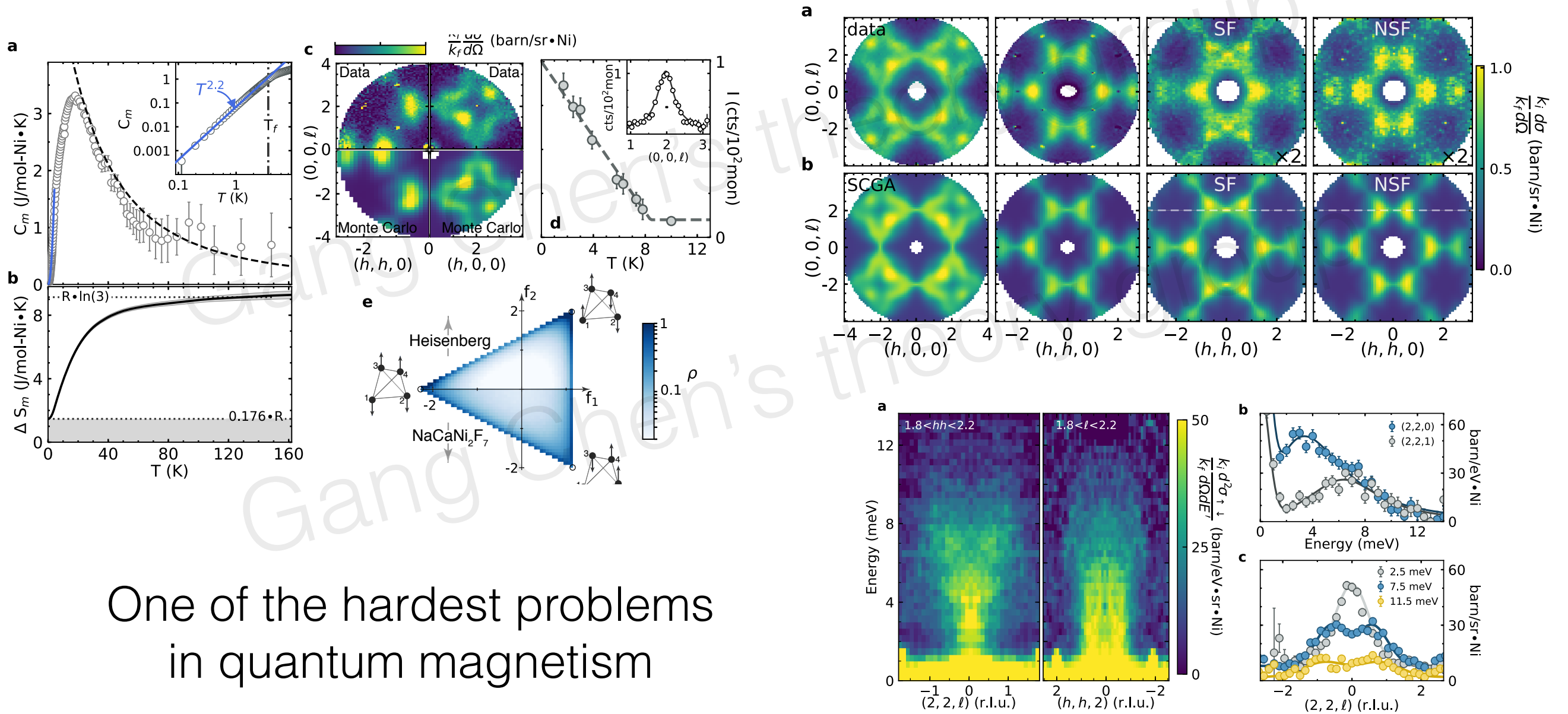


# Ni-pyrochlore magnet

## NaCaNi<sub>2</sub>F<sub>7</sub>

# Continuum of quantum fluctuations in a three-dimensional $S=1$ Heisenberg magnet

K. W. Plumb,<sup>1</sup> Hitesh J. Changlani,<sup>1</sup> A. Scheie,<sup>1</sup> Shu Zhang,<sup>1</sup> J. W. Krizan,<sup>2</sup> J. A. Rodriguez-Rivera,<sup>3,4</sup> Yiming Qiu,<sup>3</sup> B. Winn,<sup>5</sup> R. J. Cava,<sup>2</sup> and C. L. Broholm<sup>1,3,6</sup>

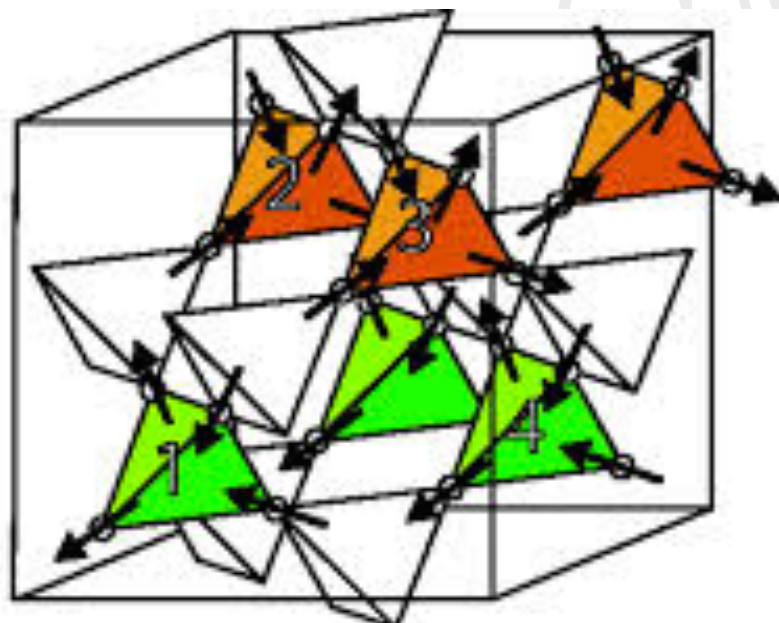


One of the hardest problems  
in quantum magnetism

Figure 4: Magnetic excitations in NaCaNi<sub>2</sub>F<sub>7</sub>. a, Energy-momentum cuts through the

# Frustrated magnets: pyrochlore spin ice

1. rare-earth pyrochlores:  $\text{Ho}_2\text{Ti}_2\text{O}_7$ ,  $\text{Dy}_2\text{Ti}_2\text{O}_7$ ,  $\text{Ho}_2\text{Sn}_2\text{O}_7$ ,  $\text{Dy}_2\text{Sn}_2\text{O}_7$ ,  $\text{Er}_2\text{Ti}_2\text{O}_7$ ,  $\text{Yb}_2\text{Ti}_2\text{O}_7$ ,  $\text{Tb}_2\text{Ti}_2\text{O}_7$ ,  $\text{Er}_2\text{Sn}_2\text{O}_7$ ,  $\text{Tb}_2\text{Sn}_2\text{O}_7$ ,  $\text{Pr}_2\text{Sn}_2\text{O}_7$ ,  $\text{Nd}_2\text{Sn}_2\text{O}_7$ ,  $\text{Gd}_2\text{Sn}_2\text{O}_7$ , .....
2. rare-earth B-site spinel:  $\text{CdEr}_2\text{S}_4$ ,  $\text{CdEr}_2\text{Se}_4$ ,  $\text{CdYb}_2\text{S}_4$ ,  $\text{CdYb}_2\text{Se}_4$ ,  $\text{MgYb}_2\text{S}_4$ ,  $\text{MgYb}_2\text{S}_4$ ,  $\text{MnYb}_2\text{S}_4$ ,  $\text{MnYb}_2\text{Se}_4$ ,  $\text{FeYb}_2\text{S}_4$ ,  $\text{CdTm}_2\text{S}_4$ ,  $\text{CdHo}_2\text{S}_4$ ,  $\text{FeLu}_2\text{S}_4$ ,  $\text{MnLu}_2\text{S}_4$ ,  $\text{MnLu}_2\text{Se}_4$ , ....

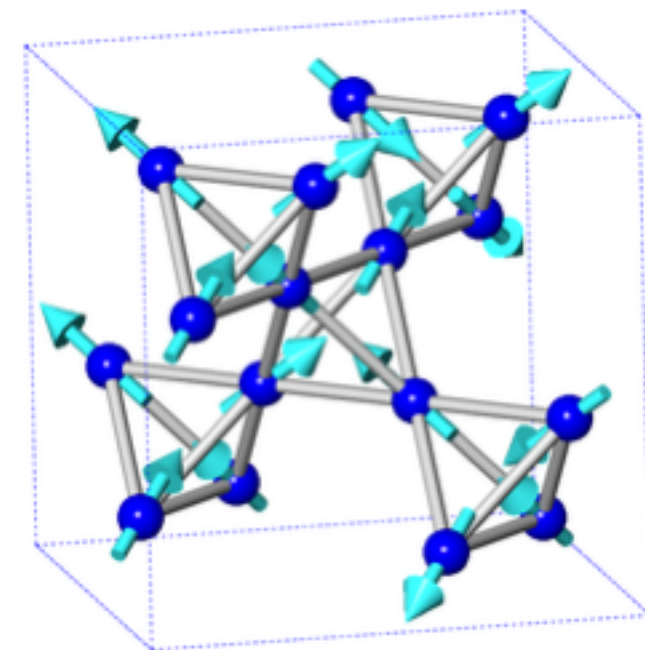
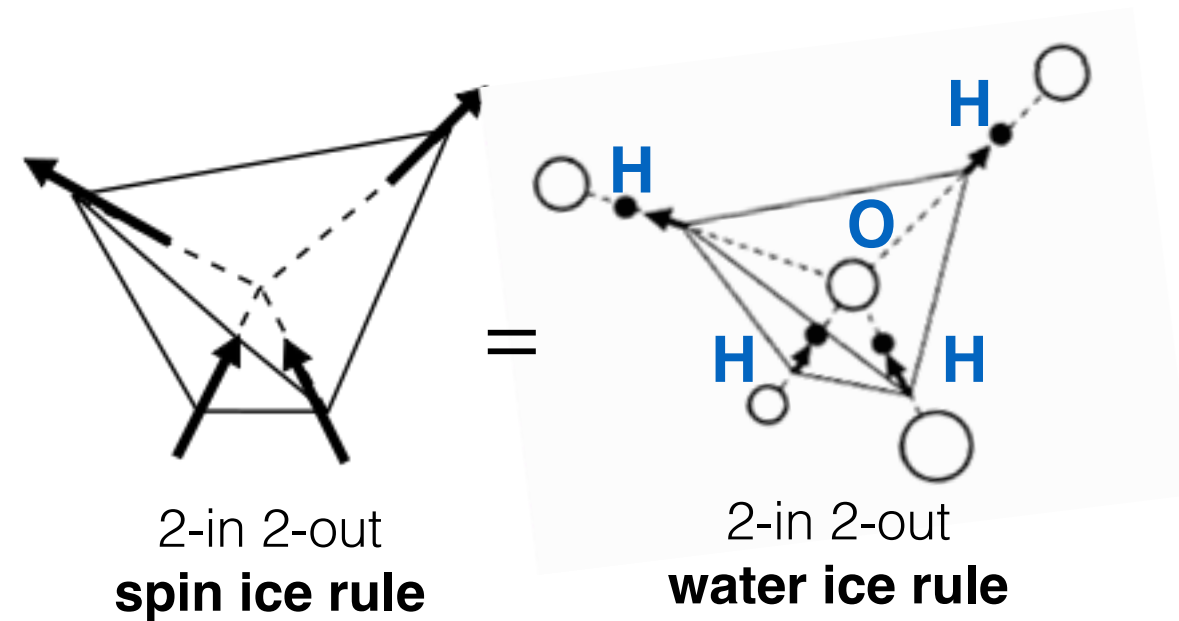
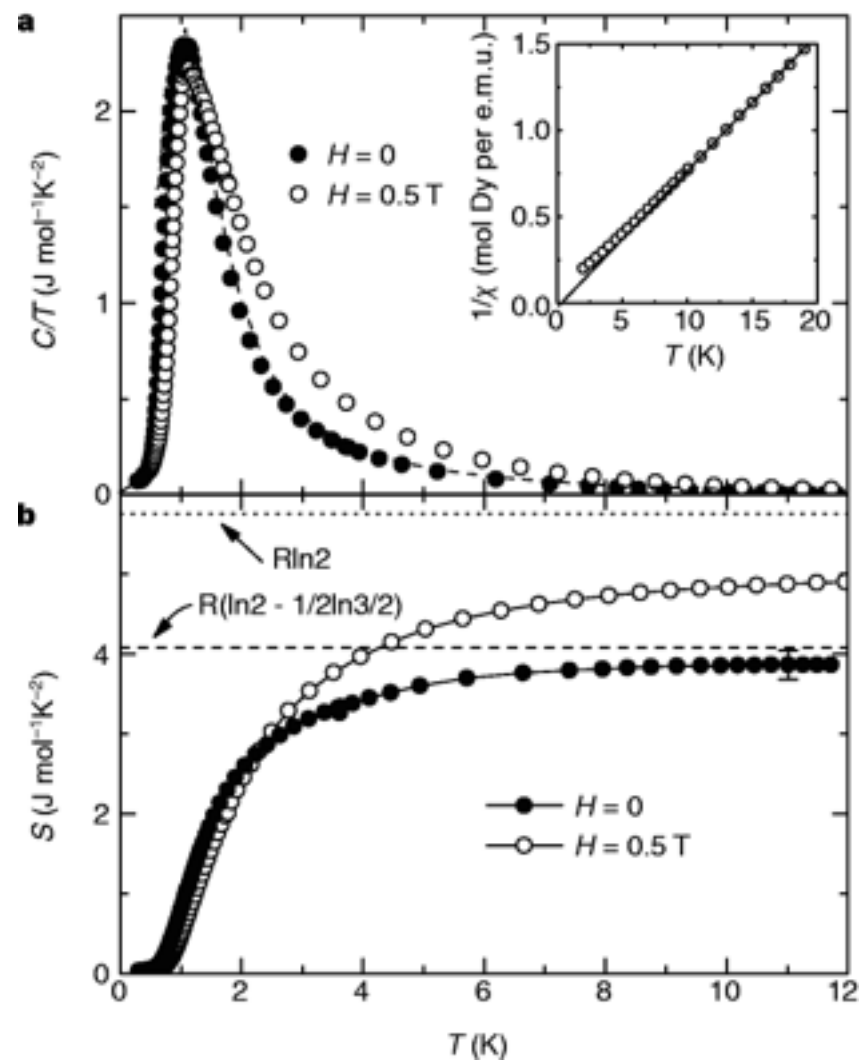


crystal field doublet  $\rightarrow$  effective spin-1/2



# Spin ice

## $\text{Dy}_2\text{Ti}_2\text{O}_7$



Pauling entropy in spin ice,  
Ramirez, etc, Science 1999

# Lattice gauge theory for U(1) spin liquid

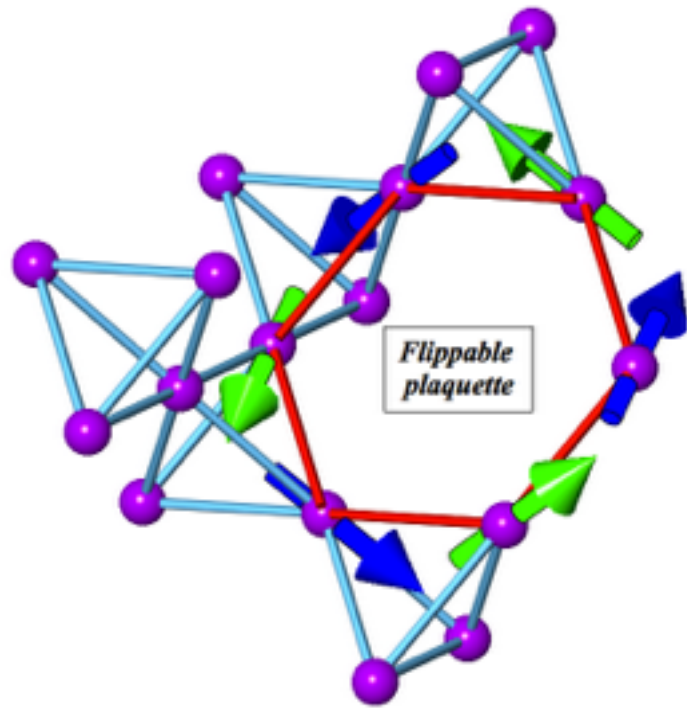


Figure from Michel Gingras

Lattice gauge theory  
on the diamond lattice

inserting spinon matter (Savary Balents 2012)

$$\mathcal{H}_{\text{XXZ}} = \sum_{\langle ij \rangle} J_{zz} S_i^z S_j^z - J_{\perp} (S_i^+ S_j^- + S_i^- S_j^+),$$

3rd order degenerate perturbation  
(Hermele, Fisher, Balents 2004)



$$\mathcal{H}_{\text{eff}} = -\frac{12J_{\perp}^3}{J_{zz}^2} \sum_{\hexagon_p} (S_i^+ S_j^- S_k^+ S_l^- S_m^+ S_n^- + h.c.),$$



$$K = 24J_{\perp}^3 / J_{zz}^2$$

$$\begin{aligned} E_{\mathbf{r}\mathbf{r}'} &\simeq S_{\mathbf{r}\mathbf{r}'}^z \\ e^{iA_{\mathbf{r}\mathbf{r}'}} &\simeq S_{\mathbf{r}\mathbf{r}'}^{\pm} \end{aligned}$$

$$\mathcal{H}_{\text{LGT}} = -K \sum_{\hexagon_d} \cos(\text{curl } A) + U \sum_{\mathbf{r}\mathbf{r}'} (E_{\mathbf{r}\mathbf{r}'} - \frac{\eta_{\mathbf{r}}}{2})^2$$

$$H = \sum_{\mathbf{r} \in \text{I, II}} \frac{J_{zz}}{2} Q_{\mathbf{r}}^2 - J_{\pm} \left\{ \sum_{\mathbf{r} \in \text{I}} \sum_{\mu, \nu \neq \mu} \Phi_{\mathbf{r}+\mathbf{e}_{\mu}}^{\dagger} \Phi_{\mathbf{r}+\mathbf{e}_{\nu}} S_{\mathbf{r}, \mathbf{r}+\mathbf{e}_{\mu}}^{-} S_{\mathbf{r}, \mathbf{r}+\mathbf{e}_{\nu}}^{+} + \sum_{\mathbf{r} \in \text{II}} \sum_{\mu, \nu \neq \mu} \Phi_{\mathbf{r}-\mathbf{e}_{\mu}}^{\dagger} \Phi_{\mathbf{r}-\mathbf{e}_{\nu}} S_{\mathbf{r}, \mathbf{r}-\mathbf{e}_{\mu}}^{+} S_{\mathbf{r}, \mathbf{r}-\mathbf{e}_{\nu}}^{-} \right\}$$

# One could think more realistically, ...

- Kramers' doublet

$$H = \sum_{\langle ij \rangle} \{ J_{zz} \mathbf{S}_i^z \mathbf{S}_j^z - J_{\pm} (\mathbf{S}_i^+ \mathbf{S}_j^- + \mathbf{S}_i^- \mathbf{S}_j^+) \\ + J_{\pm\pm} (\gamma_{ij} \mathbf{S}_i^+ \mathbf{S}_j^+ + \gamma_{ij}^* \mathbf{S}_i^- \mathbf{S}_j^-) \\ + J_{z\pm} [\mathbf{S}_i^z (\zeta_{ij} \mathbf{S}_j^+ + \zeta_{ij}^* \mathbf{S}_j^-) + i \leftrightarrow j] \},$$

S. H. Curnoe, PRB (2008).

Savary, **Balents**, PRL 2012

- Non-Kramers' doublet

$$H = \sum_{\langle ij \rangle} \{ J_{zz} \mathbf{S}_i^z \mathbf{S}_j^z - J_{\pm} (\mathbf{S}_i^+ \mathbf{S}_j^- + \mathbf{S}_i^- \mathbf{S}_j^+) \\ + J_{\pm\pm} (\gamma_{ij} \mathbf{S}_i^+ \mathbf{S}_j^+ + \gamma_{ij}^* \mathbf{S}_i^- \mathbf{S}_j^-) \}$$

S. Onoda, etc, 2009

SB Lee, Onoda, **Balents**, 2012

- Dipole-octupole doublet

$$H = \sum_{\langle ij \rangle} J_x S_i^x S_j^x + J_y S_i^y S_j^y + J_z S_i^z S_j^z \\ + J_{xz} (S_i^x S_j^z + S_i^z S_j^x).$$

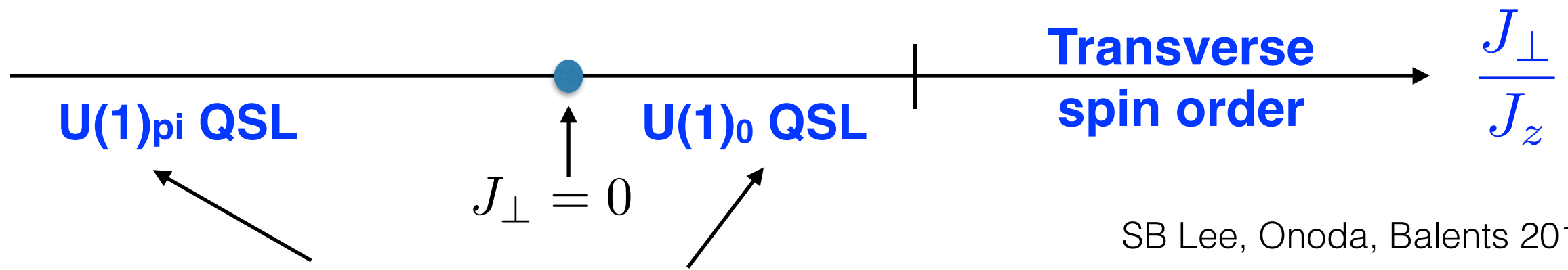
Y-P Huang, **GC**, M Hermele, PRL 2014

Y-D LI, **GC**, PRB 2017

Nd<sub>2</sub>Ir<sub>2</sub>O<sub>7</sub>, Nd<sub>2</sub>Sn<sub>2</sub>O<sub>7</sub>, Nd<sub>2</sub>Zr<sub>2</sub>O<sub>7</sub>, Ce<sub>2</sub>Sn<sub>2</sub>O<sub>7</sub>

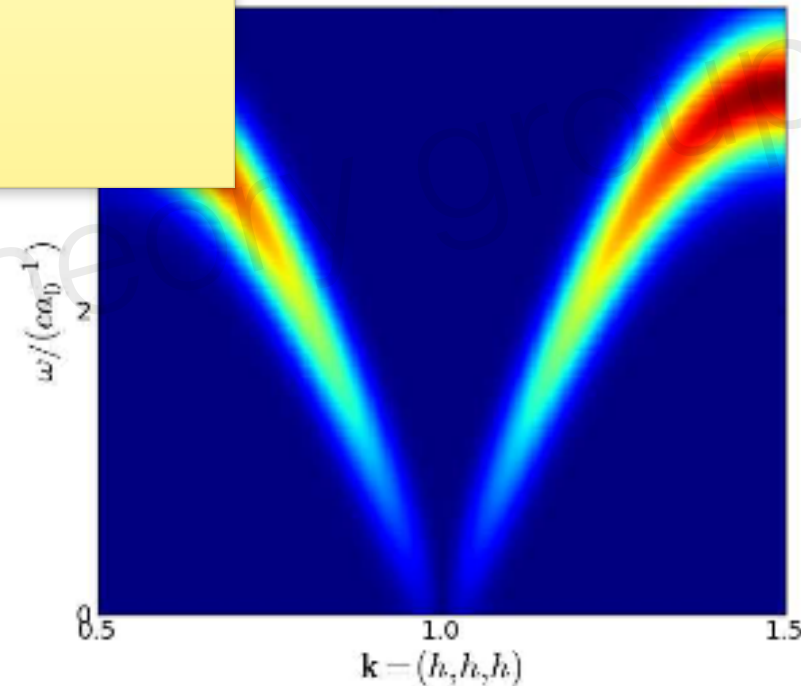
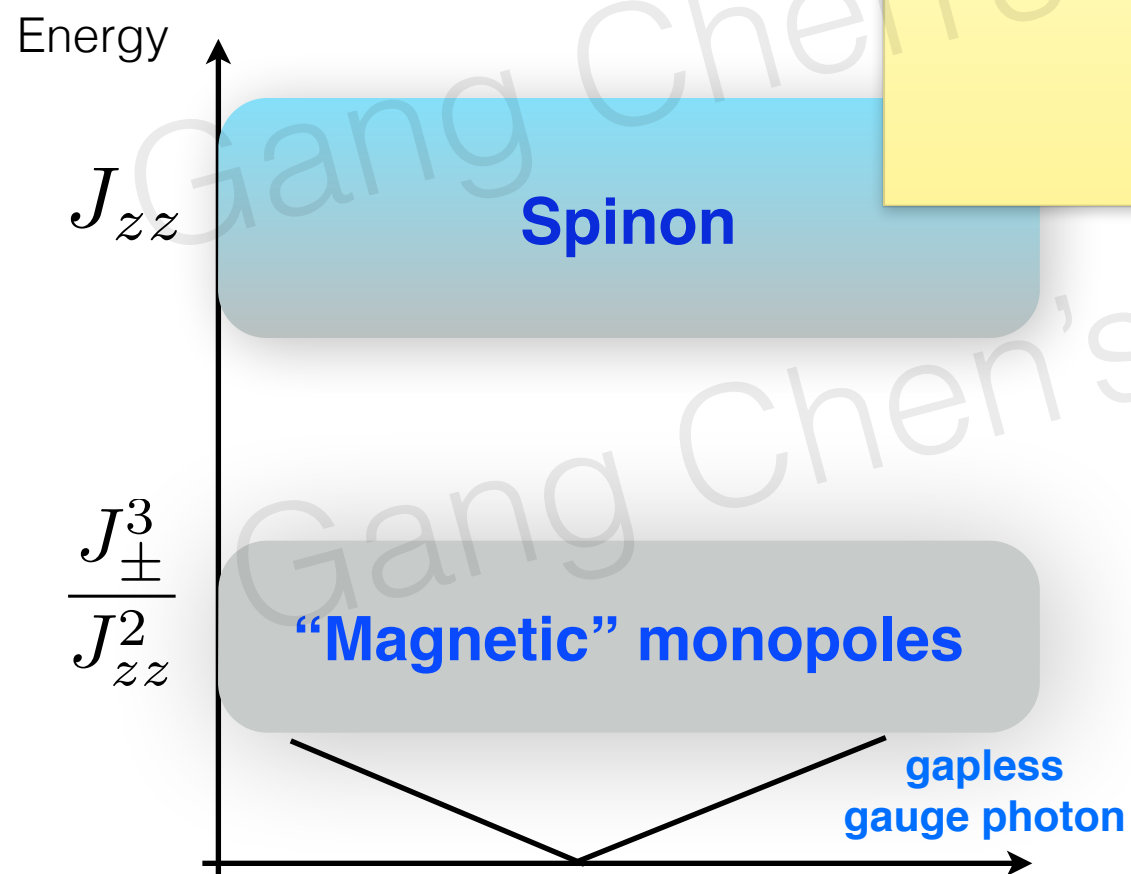
no sign problem for QMC on any lattice.

It supports nontrivial phases



Related by unitary transformation (Hermele, Fisher, Balents 2004)

Besides the quantitative differences, are there sharp distinctions between the U(1)<sub>π</sub> QSL on the left and the U(1)<sub>0</sub> QSL on the right?

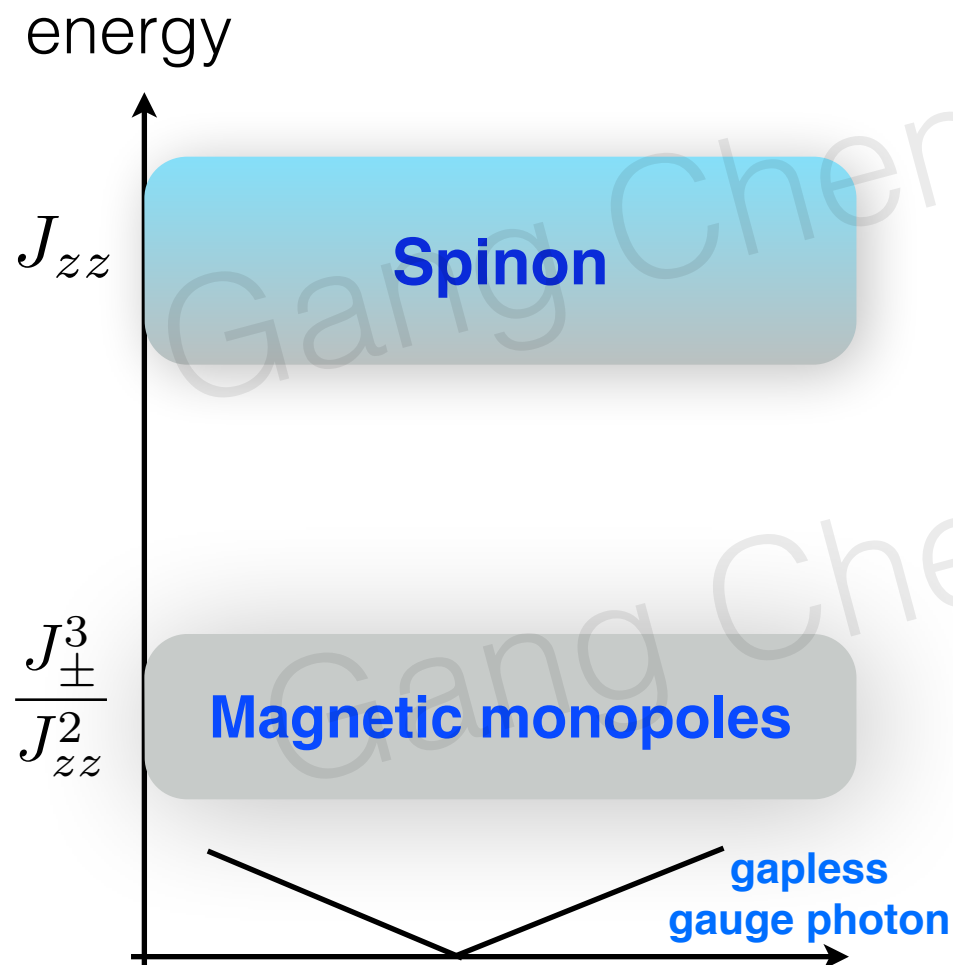


$$I(\omega) \sim \omega$$

Nic Shannon, et al 2012, Savary, Balents, 2012

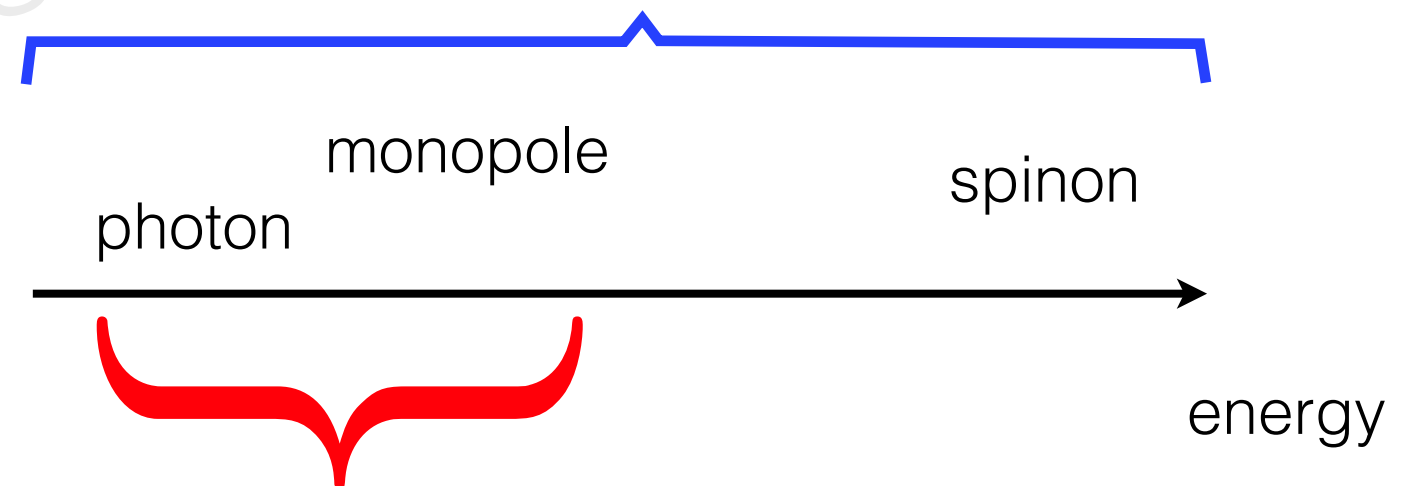
low energy scale suppressed intensity

Suggestion 1: combine thermal transport with inelastic neutron



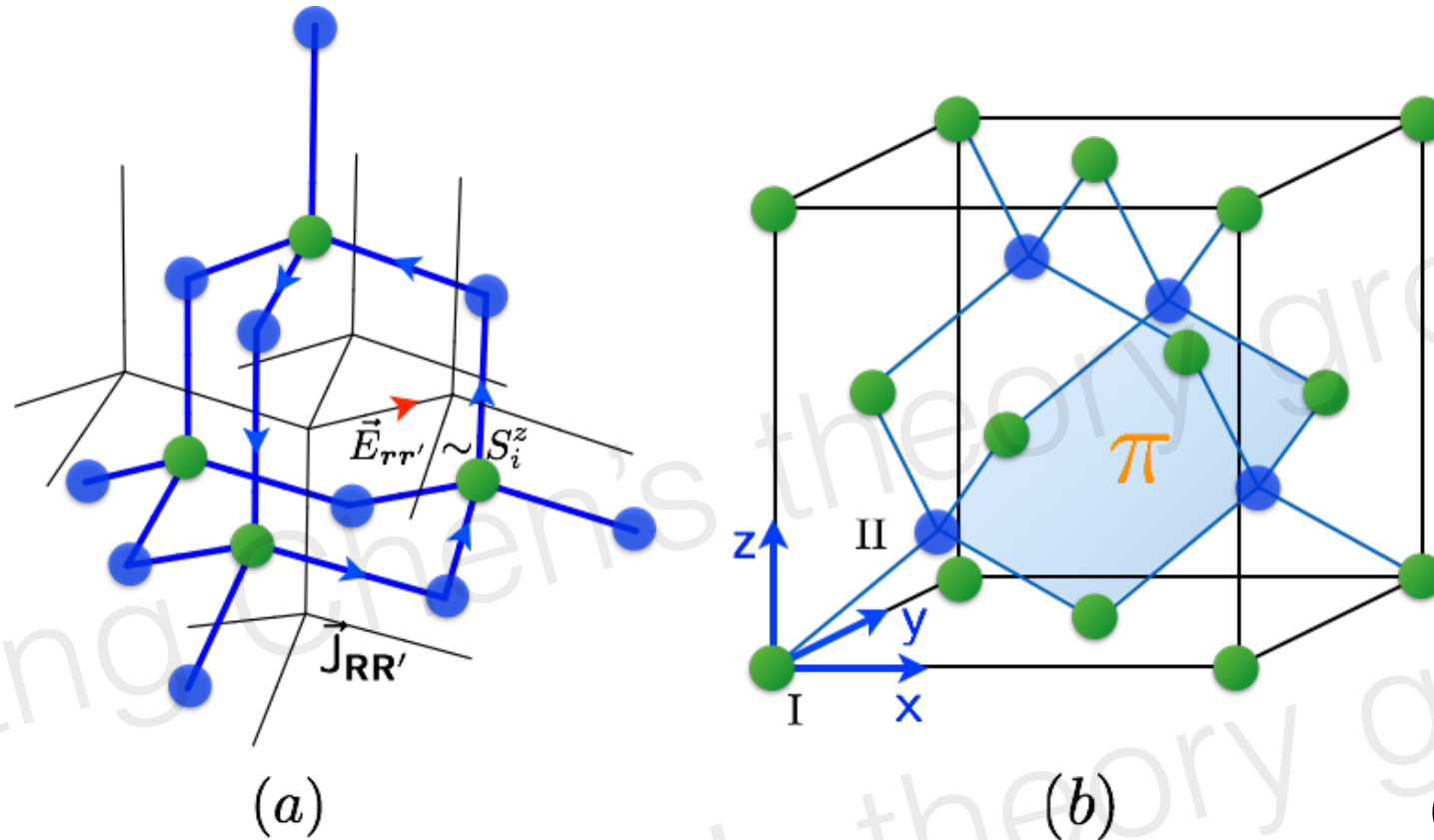
For **non-Kramers doublets** such as Pr ion in  $\text{Pr}_2\text{Zr}_2\text{O}_7$  and Tb ion in  $\text{Tb}_2\text{Ti}_2\text{O}_7$

**Visible in thermal transport**



**Visible in inelastic neutron scattering**

## Suggestion 2: effect of the external magnetic field



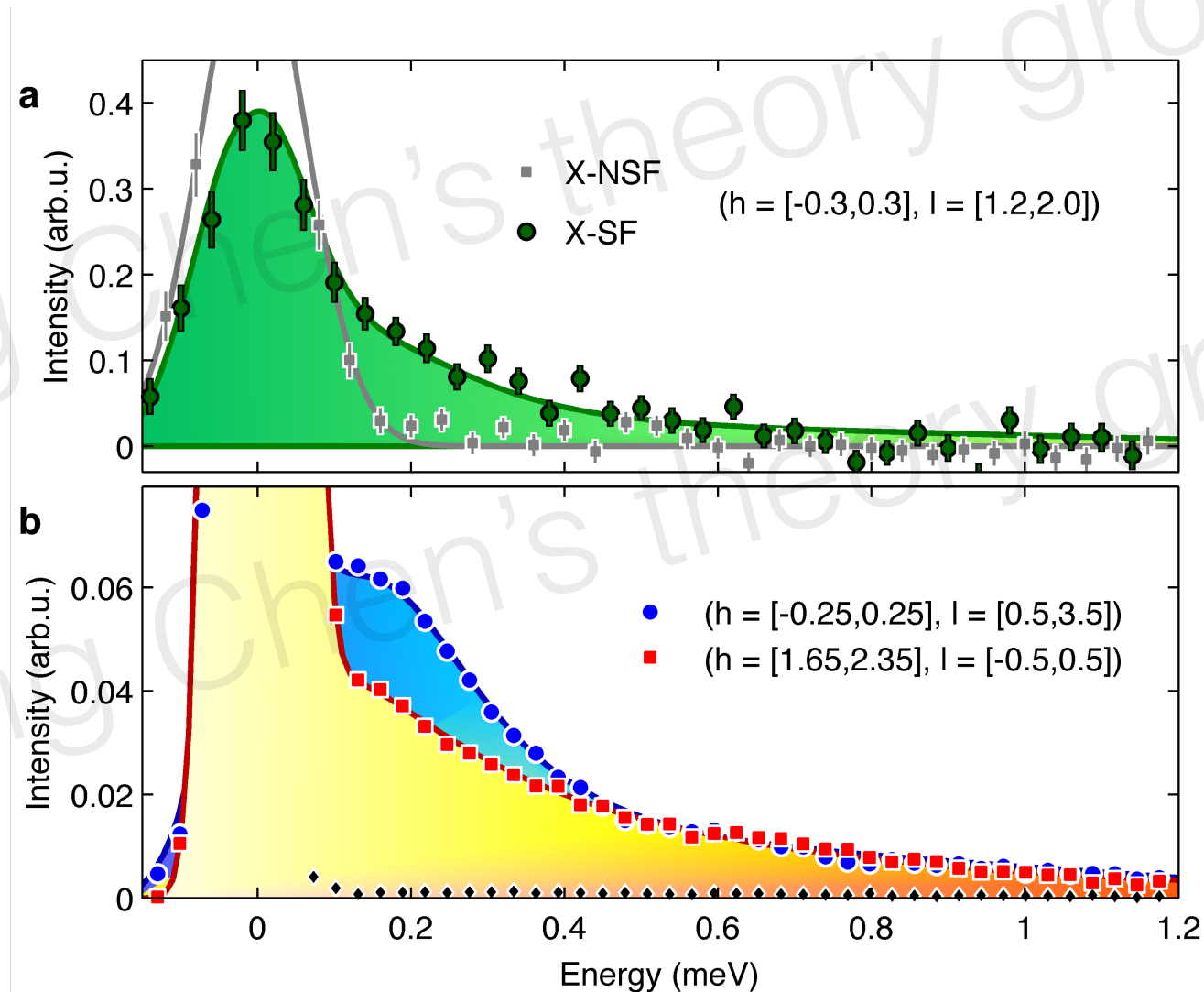
G Chen, PRB 2017

$$H_{Zeeman} = \vec{B} \cdot \sum_i S_i^z \hat{z}_i$$

The weak magnetic field polarizes  $S_z$  slightly, and thus modifies the background electric field distribution. This further modulates monopole band structure, creating “**Hofstadter**” monopole band, which may be detectable in inelastic neutron.

Thermal Hall effect: theory by XT Zhang, G Chen, etc,  
expts by P Ong, Science 2013

In fact, continuum has been observed in  $\text{Pr}_2\text{Hf}_2\text{O}_7$   
( R. Sibille, et al, arXiv 1706.03604). Nature Physics



This is a non-Kramers doublet version of pyrochlore  $U(1)$  spin liquid candidate.



# Candidate Quantum Spin Liquid in the $\text{Ce}^{3+}$ Pyrochlore Stannate $\text{Ce}_2\text{Sn}_2\text{O}_7$

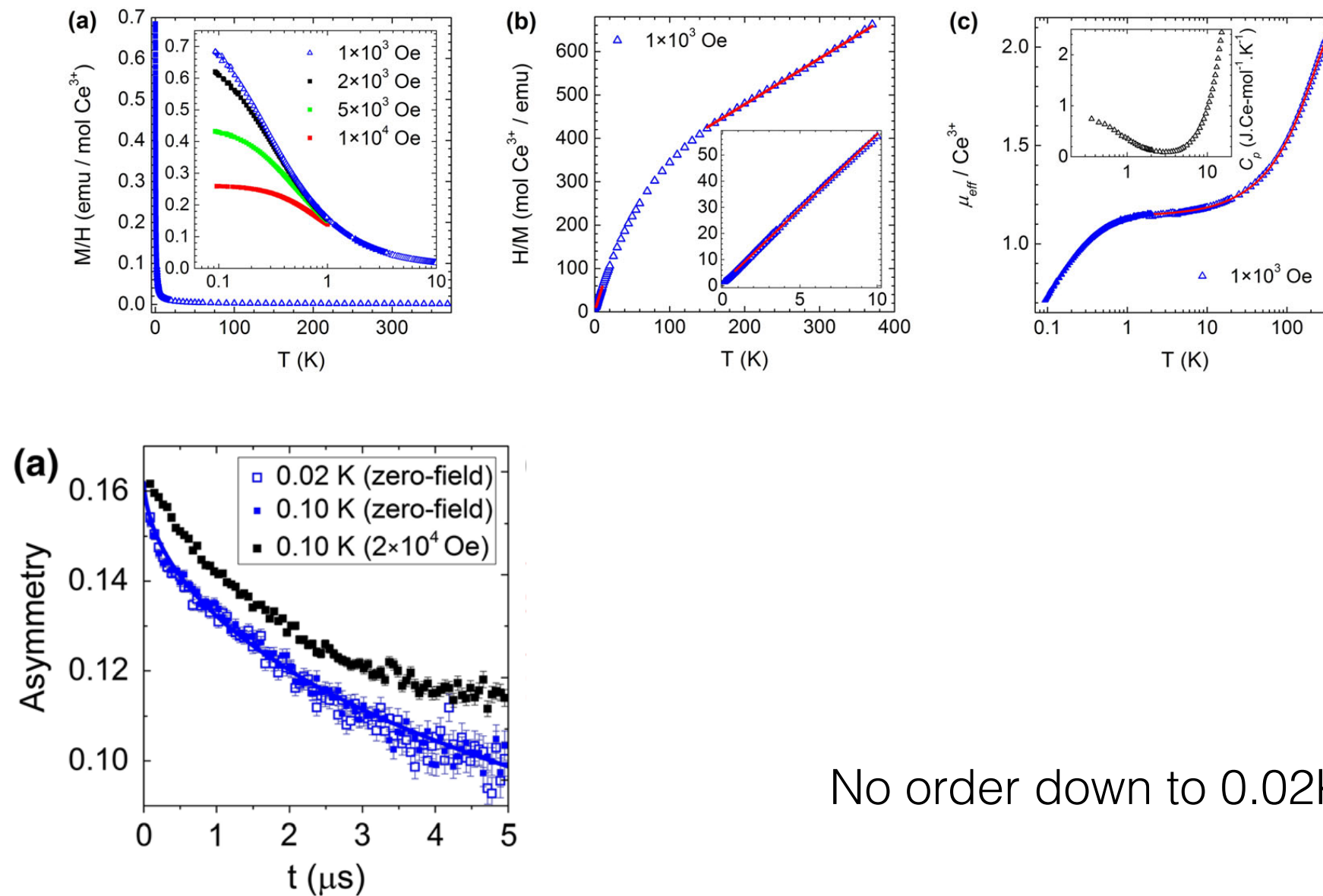
Romain Sibille,<sup>1,\*</sup> Elsa Lhotel,<sup>2</sup> Vladimir Pomjakushin,<sup>3</sup> Chris Baines,<sup>4</sup> Tom Fennell,<sup>3,†</sup> and Michel Kenzelmann<sup>1</sup>

<sup>1</sup>Laboratory for Scientific Developments and Novel Materials, Paul Scherrer Institut, 5232 Villigen PSI, Switzerland

<sup>2</sup>Institut Néel, CNRS, and Université Joseph Fourier, BP 166, 38042 Grenoble Cedex 9, France

<sup>3</sup>Laboratory for Neutron Scattering and Imaging, Paul Scherrer Institut, 5232 Villigen PSI, Switzerland

<sup>4</sup>Laboratory for Muon Spin Spectroscopy, Paul Scherrer Institut, 5232 Villigen PSI, Switzerland



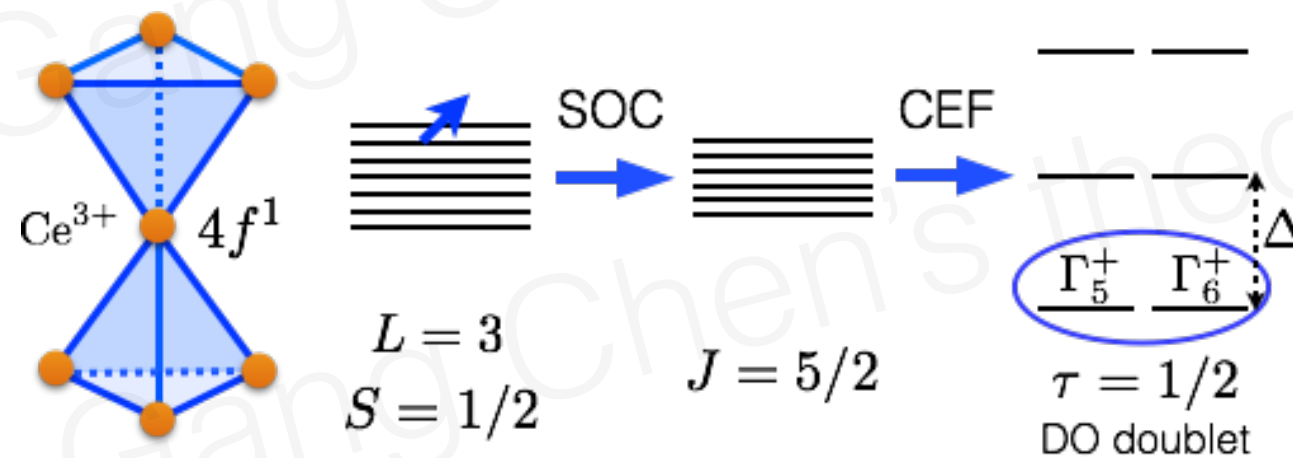
No order down to 0.02K !



# Candidate Quantum Spin Liquid in the $\text{Ce}^{3+}$ Pyrochlore Stannate $\text{Ce}_2\text{Sn}_2\text{O}_7$

Romain Sibille,<sup>1,\*</sup> Elsa Lhotel,<sup>2</sup> Vladimir Pomjakushin,<sup>3</sup> Chris Baines,<sup>4</sup> Tom Fennell,<sup>3,†</sup> and Michel Kenzelmann<sup>1</sup>

$4f^1$  ion in  $D_{3d}$  local symmetry to the susceptibility was realized between  $T = 1.8$  and 370 K, and the resulting calculation of the single ion magnetic moment is shown in Fig. 2(c). The wave functions of the ground state Kramers doublet correspond to a linear combination of  $m_J = \pm 3/2$  states. The fitted coefficients result in energy levels at  $50 \pm$



Yao-Dong Li, [GC](#),  
arXiv2016, PRB 2017

This doublet is **dipole-octupole doublet**

Huang, [GC](#), Hermele,

PRL, 112, 167203 (2014), arXiv Nov 2013

Yao-Dong Li, [GC](#),

PRB Rapid Comm 2017

Yao-Dong Li, XQ Wang, [GC](#), PRB Rapid Comm 2016

all the theor  
sentence.

# Ce<sub>2</sub>Zr<sub>2</sub>O<sub>7</sub>: a non-spin-ice pyrochlore U(1) spin liquid

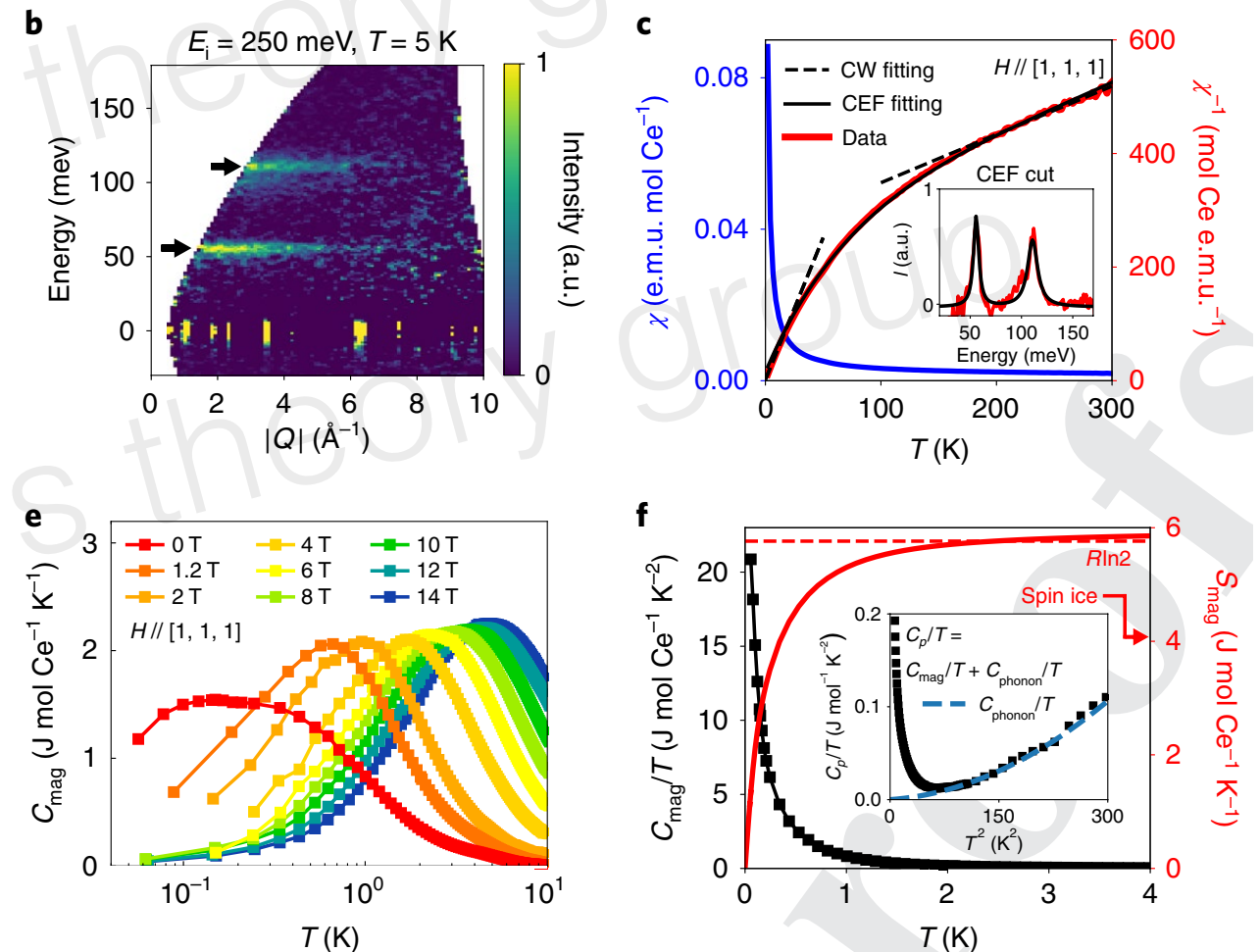
## Experimental signatures of a three-dimensional quantum spin liquid in effective spin-1/2 Ce<sub>2</sub>Zr<sub>2</sub>O<sub>7</sub> pyrochlore

Bin Gao<sup>1,11</sup>, Tong Chen<sup>1,11</sup>, David W. Tam<sup>1</sup>, Chien-Lung Huang<sup>1</sup>, Kalyan Sasmal<sup>2</sup>, Devashibhai T. Adroja<sup>3</sup>, Feng Ye<sup>4</sup>, Huibo Cao<sup>4</sup>, Gabriele Sala<sup>4</sup>, Matthew B. Stone<sup>4</sup>, Christopher Baines<sup>5</sup>, Joel A. T. Barker<sup>5</sup>, Haoyu Hu<sup>1</sup>, Jae-Ho Chung<sup>1,6</sup>, Xianghan Xu<sup>7</sup>, Sang-Wook Cheong<sup>7</sup>, Manivannan Nallaiyan<sup>8</sup>, Stefano Spagna<sup>8</sup>, M. Brian Maple<sup>2</sup>, Andriy H. Nevidomskyy<sup>1</sup>, Emilia Morosan<sup>1</sup>, Gang Chen<sup>1,9,10</sup> and Pengcheng Dai<sup>1\*</sup>

Nature Physics, 2019

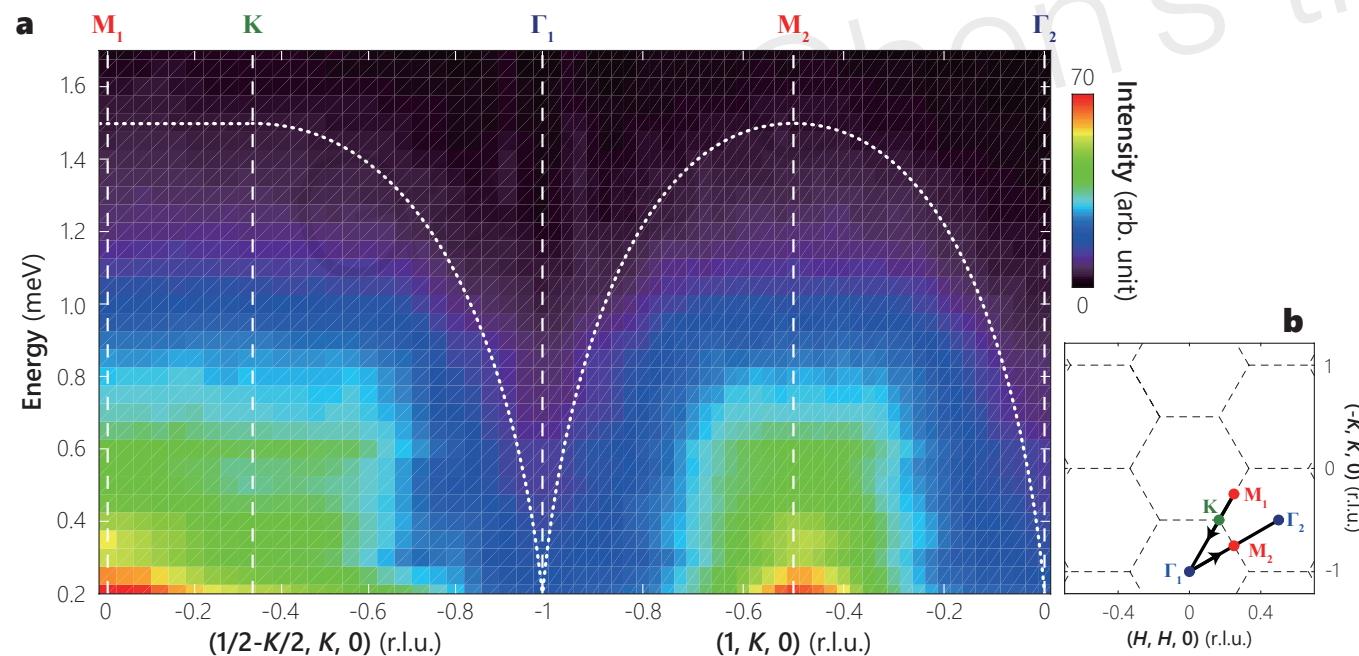
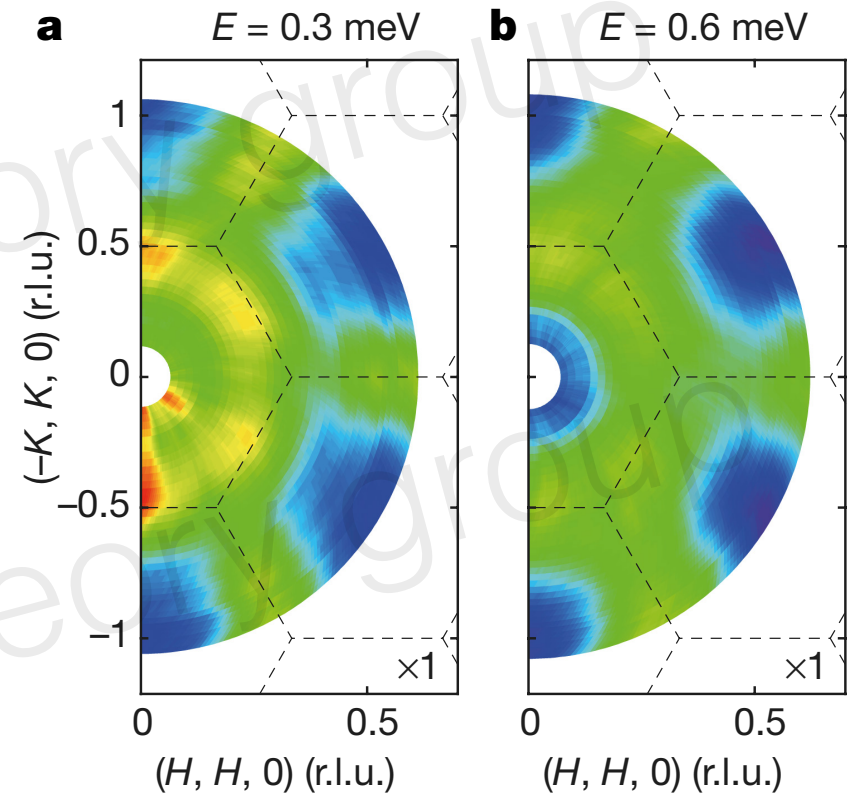
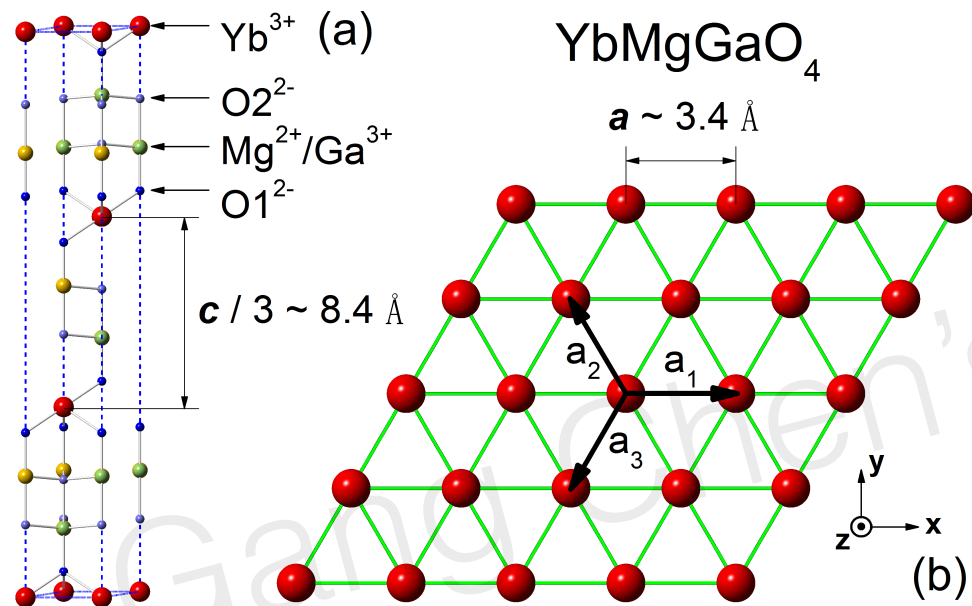
also Gaulin's group, PRL 2019

nature of fermion sign problem



Our suggestion [**YD Li & GC, 1902.07075**]: this material is in U1B phase?

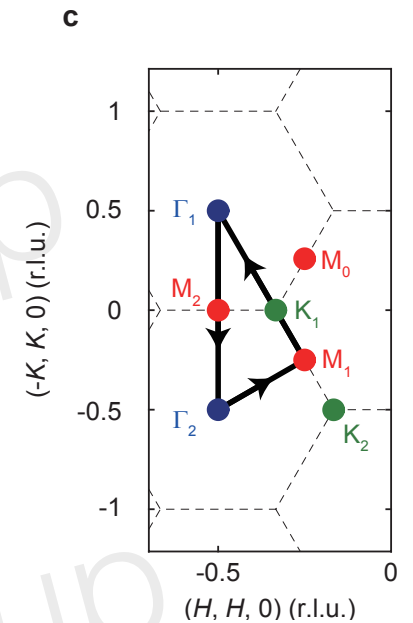
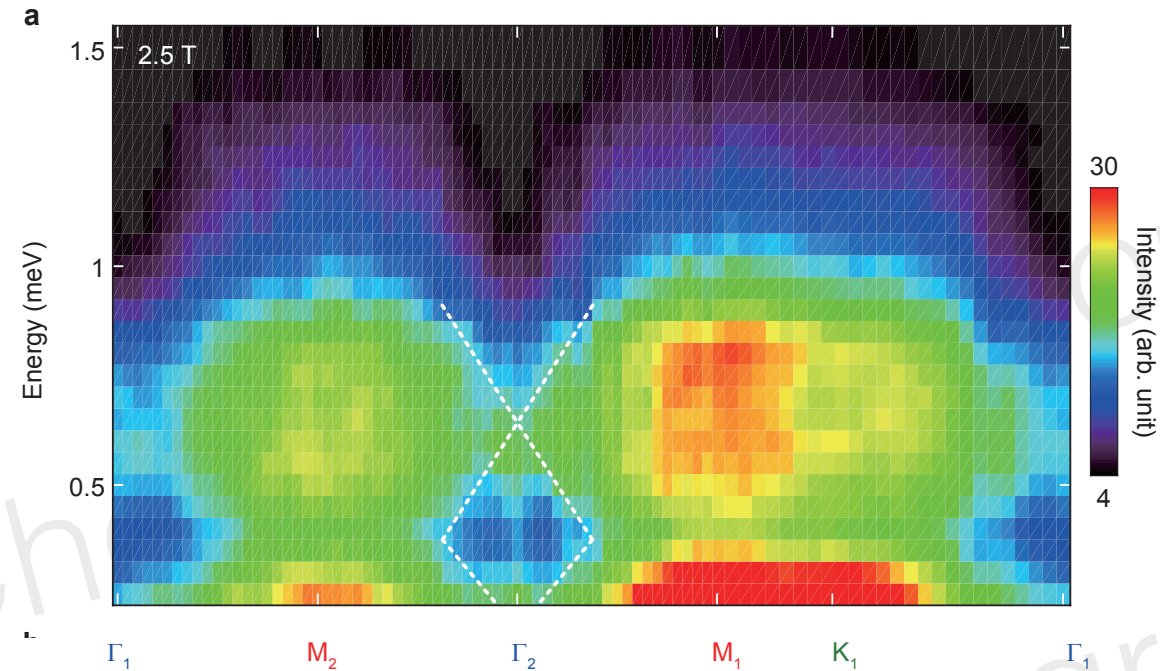
# Rare-earth triangular lattice magnets: spin liquid



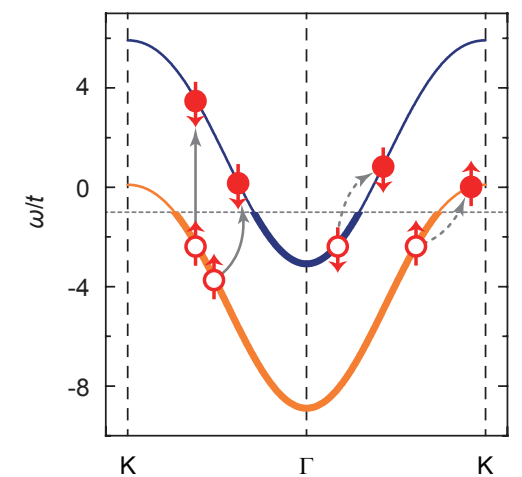
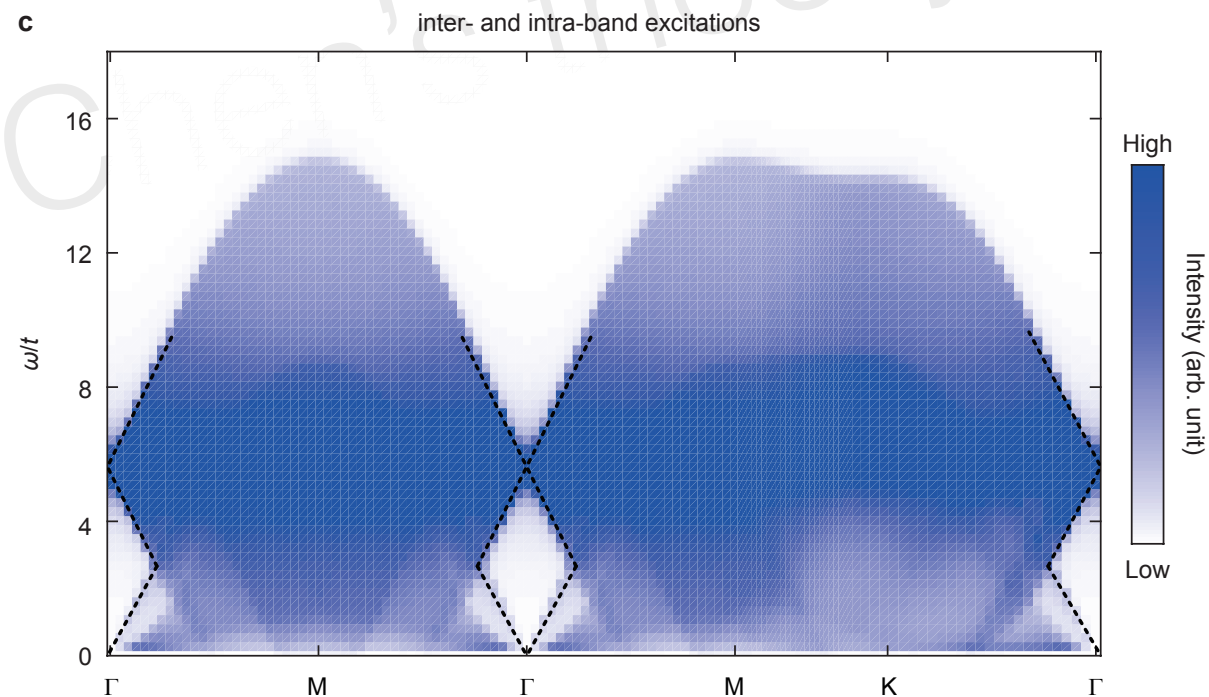
Yuesheng Li, Qingming Zhang,  
Jun Zhao, Yao Shen, Yaodong Li, G Chen

# Excitation continuum in weakly magnetized YbMgGaO4

Experiment:  
Y Shen, YD Li, ..., GC\*, J Zhao\*  
arXiv: 1708.06655  
Nat Comm



Theoretical results for  
the experimental parameter





# Use new materials to support materials

Compound	Magnetic ion	Space group	Local moment	$\Theta_{\text{CW}}$ (K)	Magnetic transition	Frustration para. $f$	Refs.
YbMgGaO <sub>4</sub>	Yb <sup>3+</sup> (4 <i>f</i> <sup>13</sup> )	R $\bar{3}$ m	Kramers doublet	−4	PM down to 60 mK	$f > 66$	[4]
CeCd <sub>3</sub> P <sub>3</sub>	Ce <sup>3+</sup> (4 <i>f</i> <sup>1</sup> )	P6 <sub>3</sub> / <i>mmc</i>	Kramers doublet	−60	PM down to 0.48 K	$f > 200$	[5]
CeZn <sub>3</sub> P <sub>3</sub>	Ce <sup>3+</sup> (4 <i>f</i> <sup>1</sup> )	P6 <sub>3</sub> / <i>mmc</i>	Kramers doublet	−6.6	AFM order at 0.8 K	$f = 8.2$	[7]
CeZn <sub>3</sub> As <sub>3</sub>	Ce <sup>3+</sup> (4 <i>f</i> <sup>1</sup> )	P6 <sub>3</sub> / <i>mmc</i>	Kramers doublet	−62	Unknown	Unknown	[8]
PrZn <sub>3</sub> As <sub>3</sub>	Pr <sup>3+</sup> (4 <i>f</i> <sup>2</sup> )	P6 <sub>3</sub> / <i>mmc</i>	Non-Kramers doublet	−18	Unknown	Unknown	[8]
NdZn <sub>3</sub> As <sub>3</sub>	Nd <sup>3+</sup> (4 <i>f</i> <sup>3</sup> )	P6 <sub>3</sub> / <i>mmc</i>	Kramers doublet	−11	Unknown	Unknown	[8]

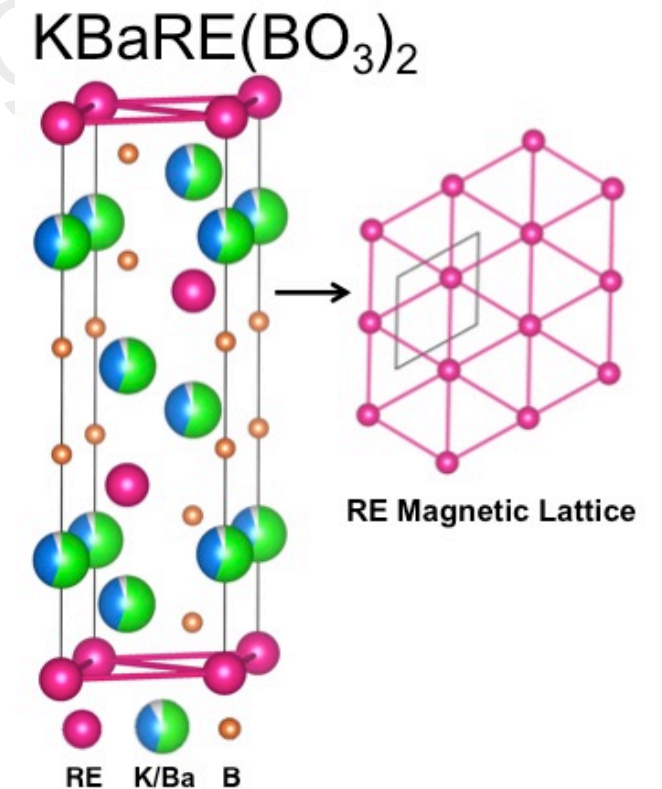
YD Li, XQ Wang, GC\*, PRB 94, 035107 (2016)

Magnetism in the KBaRE(BO<sub>3</sub>)<sub>2</sub> (RE=Sm, Eu, Gd, Tb, Dy, Ho, Er, Tm, Yb, Lu) series: materials with a triangular rare earth lattice

M. B. Sanders, F. A. Cevallos, R. J. Cava  
Department of Chemistry, Princeton University, Princeton, New Jersey 08544

many ternary chalcogenides NaRES<sub>2</sub>, NaRESe<sub>2</sub>, KRES<sub>2</sub>, KRESe<sub>2</sub>, KRETe<sub>2</sub>, RbRES<sub>2</sub>, RbRESe<sub>2</sub>, RbRETe<sub>2</sub>, CsRES<sub>2</sub>, CsRESe<sub>2</sub>, etc.)

**A recent fashion !**



# Spin-orbit entanglement: e.g. Ba<sub>2</sub>YMoO<sub>6</sub>

PRL **104**, 177202 (2010)

PHYSICAL REVIEW LETTERS

week ending  
30 APRIL 2010

## Valence Bond Glass on an fcc Lattice in the Double Perovskite Ba<sub>2</sub>YMoO<sub>6</sub>

M. A. de Vries,<sup>1,2,\*</sup> A. C. McLaughlin,<sup>3</sup> and J.-W. G. Bos<sup>4,5</sup>

<sup>1</sup>*School of Physics and Astronomy, E. C. Stoner Laboratory, University of Leeds, Leeds, LS2 9JT, United Kingdom*

<sup>2</sup>*School of Physics & Astronomy, University of St-Andrews, the North Haugh, KY16 9SS, United Kingdom*

<sup>3</sup>*Department of Chemistry, University of Aberdeen, Meston Walk, Aberdeen AB24 3UE, United Kingdom*

<sup>4</sup>*School of Chemistry, University of Edinburgh, King's Buildings, Mayfield Road, Edinburgh EH9 3JZ, United Kingdom*

<sup>5</sup>*Department of Chemistry - EPS, Heriot-Watt University, Edinburgh, EH14 4AS, United Kingdom*

(Received 10 November 2009; revised manuscript received 6 April 2010; published 27 April 2010)

We report on the unconventional magnetism in the cubic *B*-site ordered double perovskite Ba<sub>2</sub>YMoO<sub>6</sub>, using ac and dc magnetic susceptibility, heat capacity and muon spin rotation. No magnetic order is observed down to 2 K while the Weiss temperature is  $\sim -160$  K. This is ascribed to the geometric frustration in the lattice of edge-sharing tetrahedra with orbitally degenerate Mo<sup>5+</sup>  $s = 1/2$  spins. Our experimental results point to a gradual freezing of the spins into a disordered pattern of spin singlets, quenching the orbital degeneracy while leaving the global cubic symmetry unaffected, and providing a rare example of a valence bond glass.

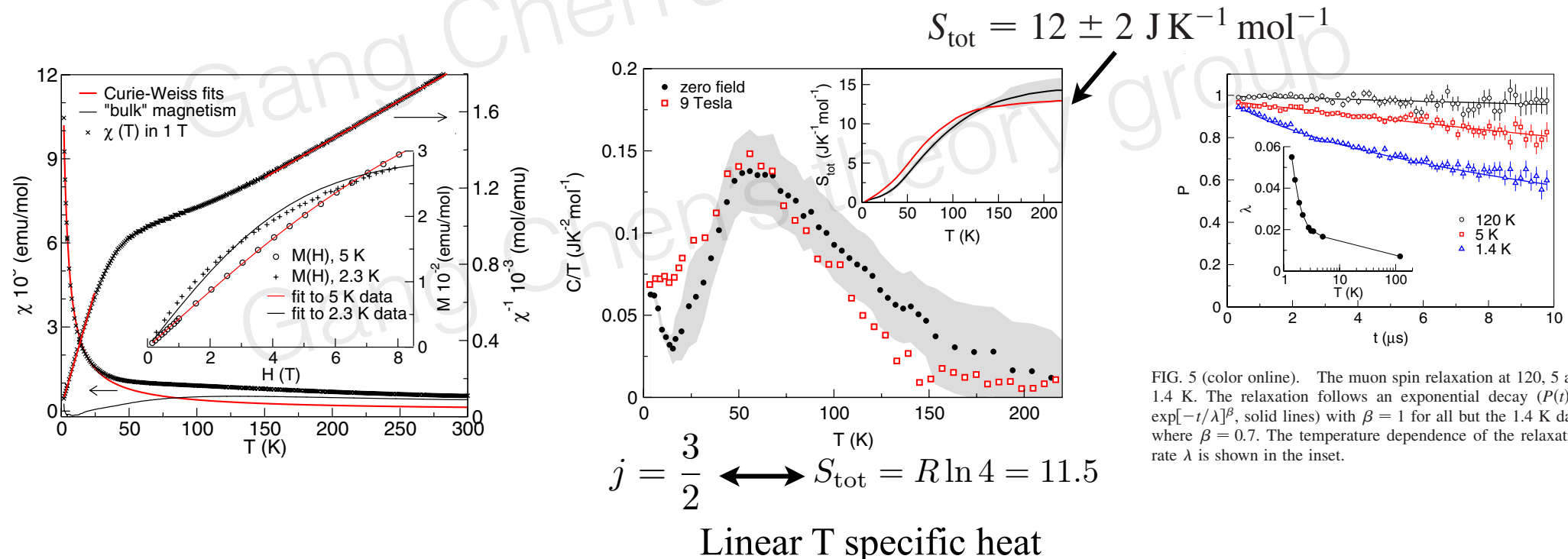


FIG. 5 (color online). The muon spin relaxation at 120, 5 and 1.4 K. The relaxation follows an exponential decay ( $P(t) = \exp[-t/\lambda]^\beta$ , solid lines) with  $\beta = 1$  for all but the 1.4 K data, where  $\beta = 0.7$ . The temperature dependence of the relaxation rate  $\lambda$  is shown in the inset.



# Triplet and in-gap magnetic states in the ground state of the quantum frustrated fcc antiferromagnet $\text{Ba}_2\text{YMoO}_6$

J. P. Carlo,<sup>1,2,\*</sup> J. P. Clancy,<sup>1</sup> T. Aharen,<sup>3</sup> Z. Yamani,<sup>2</sup> J. P. C. Ruff,<sup>1</sup> J. J. Wagman,<sup>1</sup> G. J. Van Gastel,<sup>1</sup> H. M. L. Noad,<sup>1</sup> G. E. Granroth,<sup>4</sup> J. E. Greedan,<sup>3,5</sup> H. A. Dabkowska,<sup>5</sup> and B. D. Gaulin<sup>1,5,6</sup>

<sup>1</sup>Department of Physics and Astronomy, McMaster University, Hamilton, Ontario L8S 4M1, Canada

<sup>2</sup>Canadian Neutron Beam Centre, National Research Council, Chalk River, Ontario K0J 1J0, Canada

<sup>3</sup>Department of Chemistry, McMaster University, Hamilton, Ontario L8S 4M1, Canada

<sup>4</sup>Neutron Scattering Sciences Division, Oak Ridge National Laboratory, Oak Ridge, TN, USA

<sup>5</sup>Brockhouse Institute for Materials Research, McMaster University, Hamilton, Ontario L8S 4M1, Canada

<sup>6</sup>Canadian Institute for Advanced Research, Toronto, Ontario M5G 1Z8, Canada

(Received 20 May 2011; revised manuscript received 16 August 2011; published 19 September 2011)

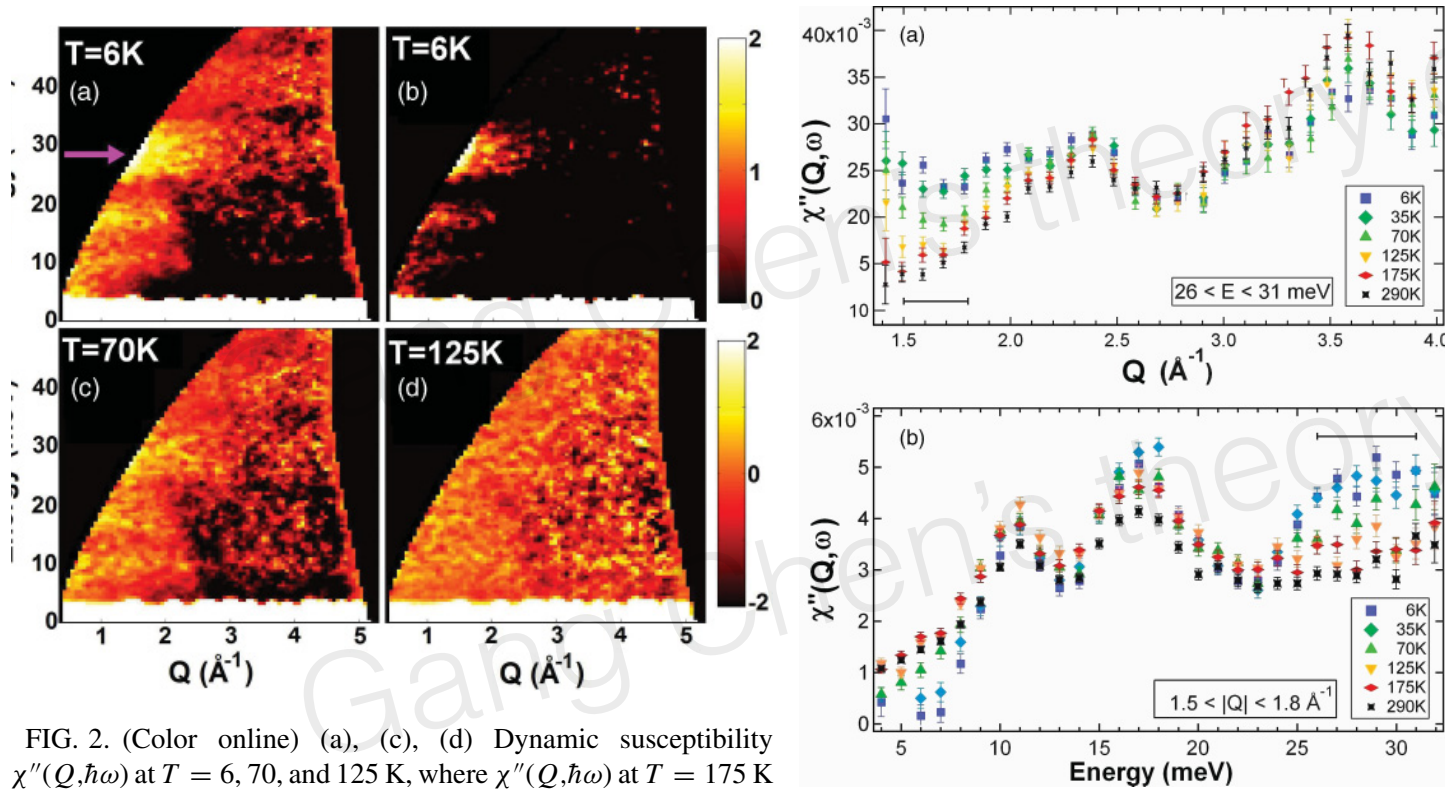


FIG. 2. (Color online) (a), (c), (d) Dynamic susceptibility  $\chi''(Q, \hbar\omega)$  at  $T = 6, 70$ , and  $125$  K, where  $\chi''(Q, \hbar\omega)$  at  $T = 175$  K is been subtracted from each to isolate the magnetic scattering, described in the text. (b) shows  $\Delta\chi''(Q, \hbar\omega)$  at  $T = 6$  K with  $= 175$  K subtracted, but with the plotted intensity scale restricted to  $>0$  only, thus highlighting where  $\chi''(Q, \hbar\omega)$  at  $6$  K exceeds that at  $175$  K. The lower intensity scale refers to (a), (c), and (d), and the upper refers to (b).

FIG. 3. (Color online) (a)  $\chi''(Q, \hbar\omega)$  plotted versus  $Q$  for six temperatures, integrated in energy between  $26$  and  $31$  meV. (b)  $\chi''(Q, \hbar\omega)$  plotted versus energy for six temperatures, integrated in  $Q$  over the range  $1.5 \text{ \AA}^{-1} < Q < 1.8 \text{ \AA}^{-1}$ . The scattering centered on  $\sim 28$  meV exists only at low  $Q < 2.5 \text{ \AA}^{-1}$  and at low  $T < 125$  K, and is therefore magnetic in origin and consistent with a weakly dispersive spin-triplet excitation.

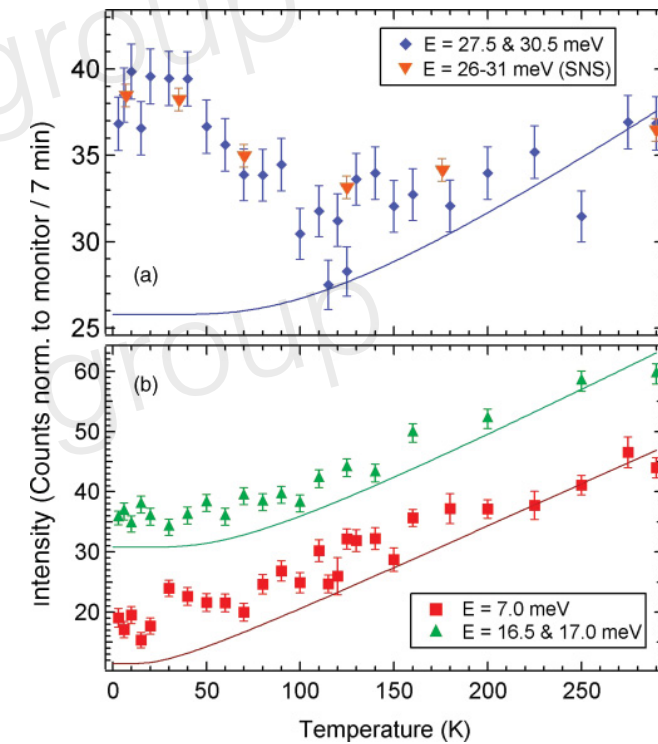
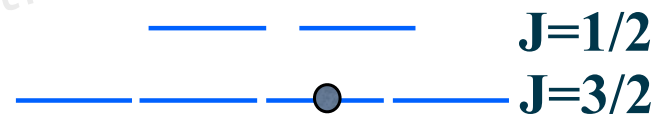
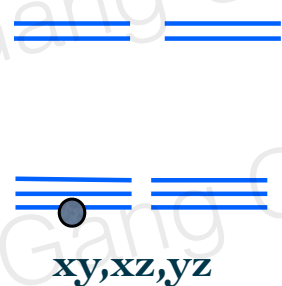
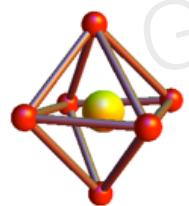


FIG. 4. (Color online) (a) Temperature dependence of the background-subtracted scattering intensity at  $Q = 1.7 \text{ \AA}^{-1}$  at the average of  $27.5$  and  $30.5$  meV, collected with the C5 triple-axis spectrometer, showing a characteristic fall-off of the triplet intensity toward zero at  $\sim 125$  K; normalized SEQUOIA (SNS) data at  $26$ – $31$  meV is included for reference. (b) Temperature dependence of the background-subtracted intensity at  $7$  meV and a  $16.5$ – $17$  meV energy transfer. The solid lines represent fits of the  $T > 200$  K data to the thermal occupancy factor. Excess low-temperature scattering is attributed to either (a) the triplet excitation, or (b) magnetic states within the gap.

$Re^{6+}, Os^{7+}, Mo^{5+}$



$$M = \mathcal{P}_{\frac{3}{2}}[2S + (-l)]\mathcal{P}_{\frac{3}{2}} = 0!!$$

$\lambda \sim 1481K$  in  $Mo^{5+}$

$M \sim 1.3 - 1.4\mu_B$

for  $Ba_2YMoO_6$

$M \sim 0.6 - 0.7\mu_B$

for  $Ba_2CaReO_6, Ba_2LiOsO_6, Ba_2CaOsO_6$

# Periodic Table of the Elements

1																	2						
H																	He						
3	4																	5	6	7	8	9	10
Li	Be																	B	C	N	O	F	Ne
11	12																	13	14	15	16	17	18
Na	Mg																	Al	Si	P	S	Cl	Ar
19	20	21	22	23	24	25	26	27	28	29	30	31	32	33	34	35	36						
K	Ca	Sc	Ti	V	Cr	Mn	Fe	Co	Ni	Cu	Zn	Ga	Ge	As	Se	Br	Kr						
37	38	39	40	41	42	43	44	45	46	47	48	49	50	51	52	53	54						
Rb	Sr	Y	Zr	Nb	Mo	Tc	Ru	Rh	Pd	Ag	Cd	In	Sn	Sb	Te	I	Xe						
55	56	57	72	73	74	75	76	77	78	79	80	81	82	83	84	85	86						
Cs	Ba	*La	Hf	Ta	W	Re	Os	Ir	Pt	Au	Hg	Tl	Pb	Bi	Po	At	Rn						
87	88	89	104	105	106	107	108	109	110	111	112	113											
Fr	Ra	+Ac	Rf	Ha	Sg	Ns	Hs	Mt	110	111	112	113											

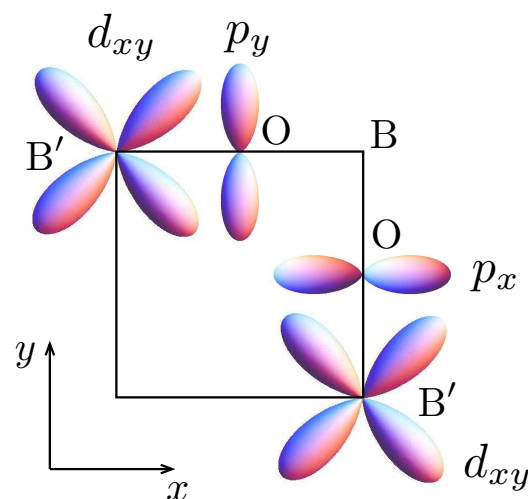
\* Lanthanide Series

+ Actinide Series

58	59	60	61	62	63	64	65	66	67	68	69	70	71
Ce	Pr	Nd	Pm	Sm	Eu	Gd	Tb	Dy	Ho	Er	Tm	Yb	Lu
90	91	92	93	94	95	96	97	98	99	100	101	102	103
Th	Pa	U	Np	Pu	Am	Cm	Bk	Cf	Es	Fm	Md	No	Lr

Chen, Balents, Rodrigo, PRB 2010

## Exchange interaction and singlets



$$H_{XY} = J(\mathbf{S}_{i,xy} \cdot \mathbf{S}_{j,xy} - \gamma n_{i,xy} n_{j,xy}) - \lambda \mathbf{l}_i \cdot \mathbf{S}_i - \lambda \mathbf{l}_j \cdot \mathbf{S}_j$$

$$\mathbf{S}_{i,xy} \equiv \mathbf{S}_i n_{i,xy}$$

Singlets

$$J \gg \lambda \quad \frac{1}{\sqrt{2}}(|S_i^z = \frac{1}{2}, xy\rangle |S_j^z = -\frac{1}{2}, xy\rangle - |S_i^z = -\frac{1}{2}, xy\rangle |S_j^z = \frac{1}{2}, xy\rangle)$$

$$J \ll \lambda \quad \frac{1}{\sqrt{2}}(|j^z = \frac{1}{2}\rangle_i |j^z = -\frac{1}{2}\rangle_j - |j^z = -\frac{1}{2}\rangle_i |j^z = \frac{1}{2}\rangle_j)$$

# Na<sub>4</sub>Ir<sub>3</sub>O<sub>8</sub> hyperkagome AFMagnet

Frozen state and spin liquid physics in Na<sub>4</sub>Ir<sub>3</sub>O<sub>8</sub>: an NMR study

A.C. Shockley,<sup>1,\*</sup> F. Bert,<sup>1</sup> J-C. Orain,<sup>1</sup> Y. Okamoto,<sup>2</sup> and P. Mendels<sup>1</sup>

Spin-Liquid State in the  $S = 1/2$  Hyperkagome Antiferromagnet Na<sub>4</sub>Ir<sub>3</sub>O<sub>8</sub>

Yoshihiko Okamoto<sup>1,\*</sup>, Minoru Nohara<sup>2</sup>, Hiroko Aruga-Katori<sup>1</sup>, and Hidenori Takagi<sup>1,2</sup>

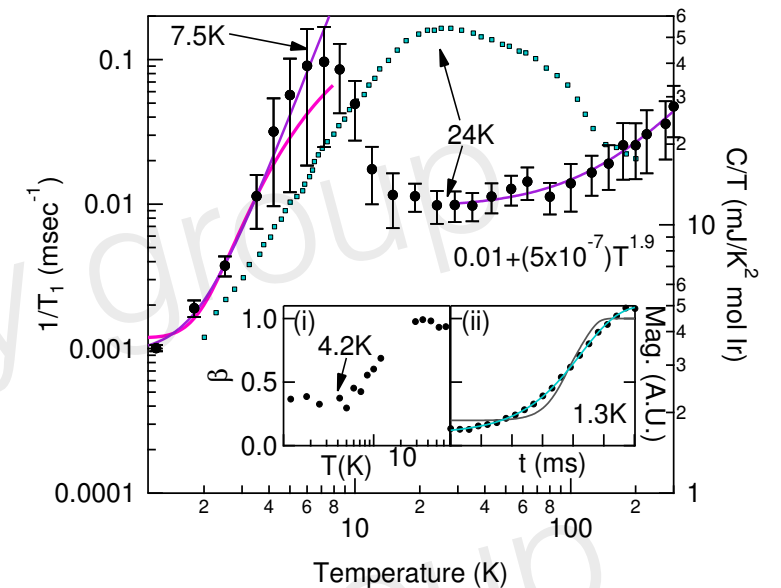
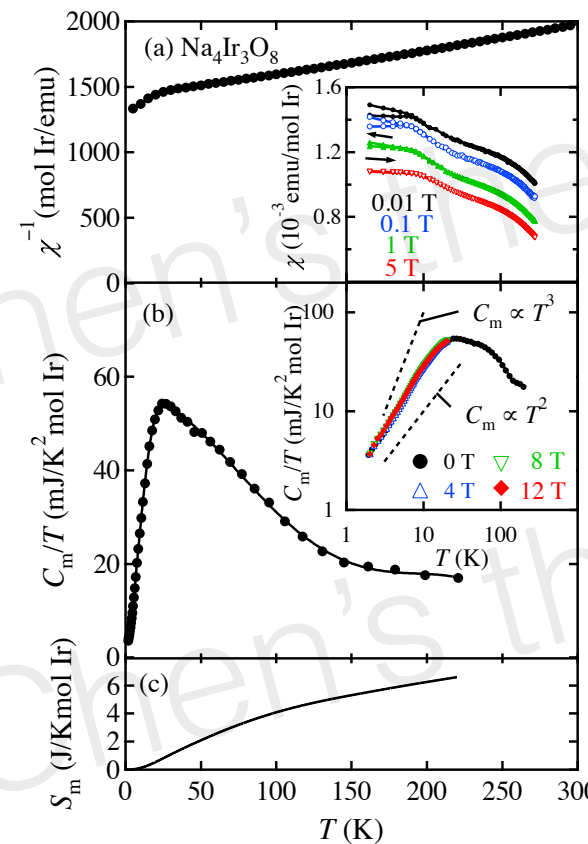
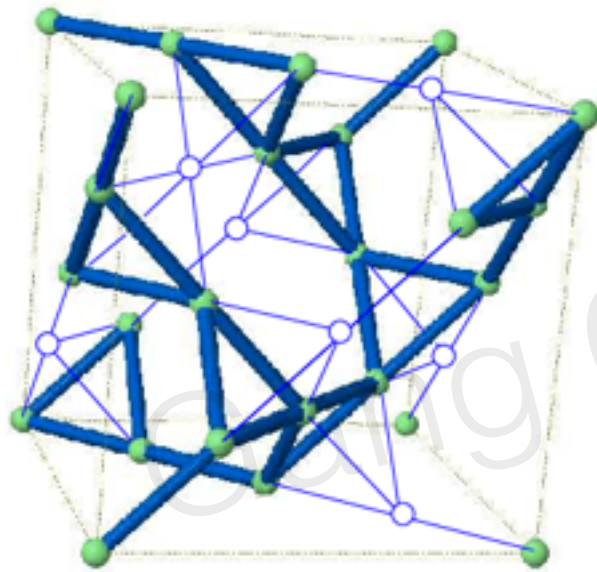


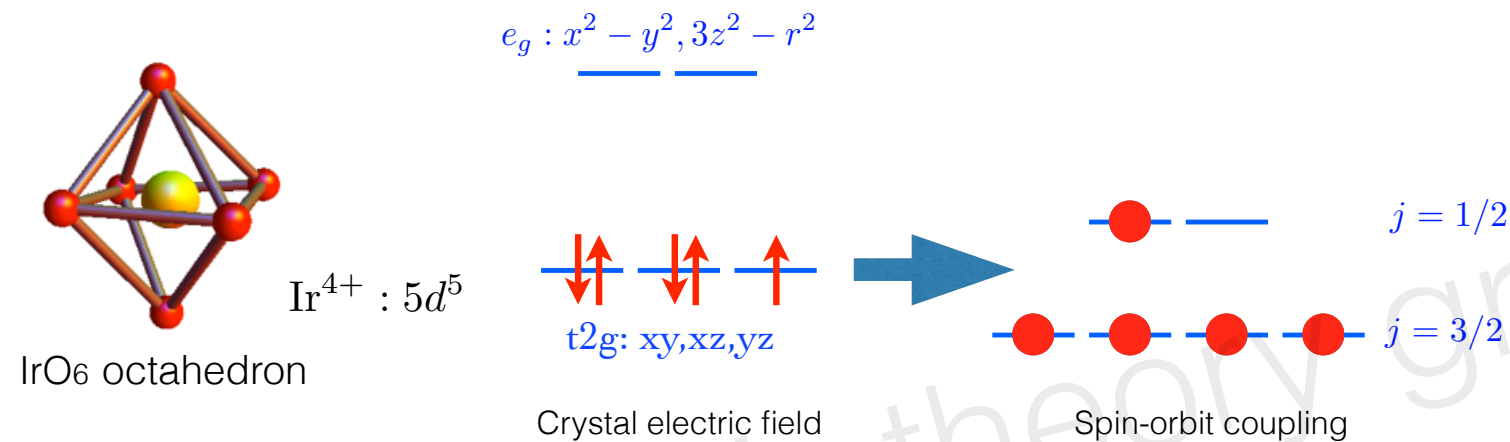
FIG. 4.  $^{23}\text{Tl}^{-1}$  (left axis, black circles) and  $C/T$  from [14] (right axis, blue squares) as a function of temperature. The purple lines are fits. Inset: (i) The stretch exponent,  $\beta$ , as described in the text as a function of temperature. (ii) The relaxation curve (solid circles) at 1.3 K fit with a stretched exponent (blue line,  $\beta = 0.4$ ) and exponential fit (grey line,  $\beta = 1$ ).

(i) A fermionic approach naturally leading to a spinon Fermi surface. The maximum of  $C/T$ , far too high for a spin glass freezing [43], could be the landmark of a crossover from a  $U(1)$  spin liquid to a  $\mathbb{Z}_2$  one with a paired spinon state and line nodes in the gap below 20 K [18]. The mixing with triplet states induced by SOC or Dzyaloshinskii-Moriya interactions could explain why the susceptibility keeps its Pauli-like behavior. Yet, our  $1/T_1$  data, if intrinsic, contradicts the existence of a gap as it does not decrease, below the maximum of the specific heat. Furthermore, for a Dirac  $U(1)$  spin liquid, one expects  $1/T_1 \sim T^\eta$  where  $\eta$  is related to the shape of the correlation function and remains unknown [44]. This is not what is observed here since  $T_1$  is dominated by a constant term for  $T > 20$  K.

very large  
Wilson Ratio !



# theories



$$\langle \{t_{2g}\} | \mathbf{L} | \{t_{2g}\} \rangle = -1, \quad H_{soc} = -\lambda \mathbf{L} \cdot \mathbf{S}, \quad \mathbf{j} = \mathbf{L} + \mathbf{S}$$

It is interesting to look at how the magnetic moment  $M = L + 2S = -1 + 2S$  varies.

Yi Zhou, Fuchun Zhang, PA Lee

G Chen, Balents

G Chen, YB Kim

perature independent at temperatures below  $\sim T_c$ . The transition at 20 K is then interpreted as a transition between a  $U(1)$  spin liquid to a  $Z_2$  spin liquid where spinons are paired at low temperature. This theory also predicts the appearance of superconductivity if the Na<sub>4</sub>Ir<sub>3</sub>O<sub>8</sub> system can be doped.

spin-orbit coupling of Ir,  
anisotropic superexchange  
 $J=1/2$

proximate to Mott transition  
spinon-Fermi surface  $U(1)$  QSL

Orbital degree of freedom:  
e.g. Fe-based diamond magnet,  $\text{LaTiO}_3$ ,  $\text{LiNiO}_2$ ,  $\text{NaNiO}_2$

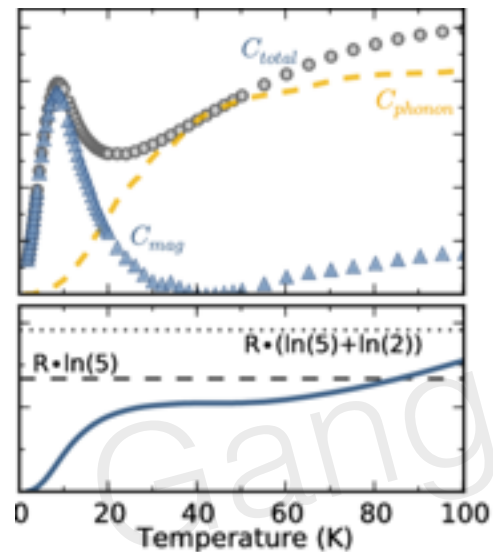
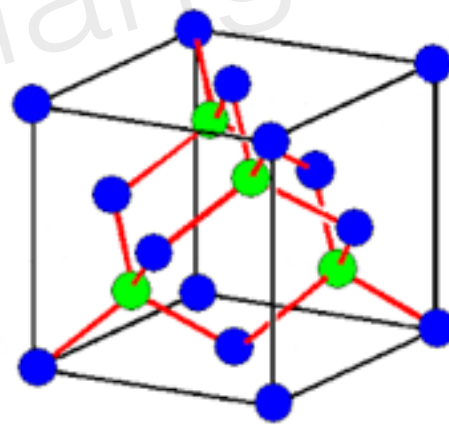
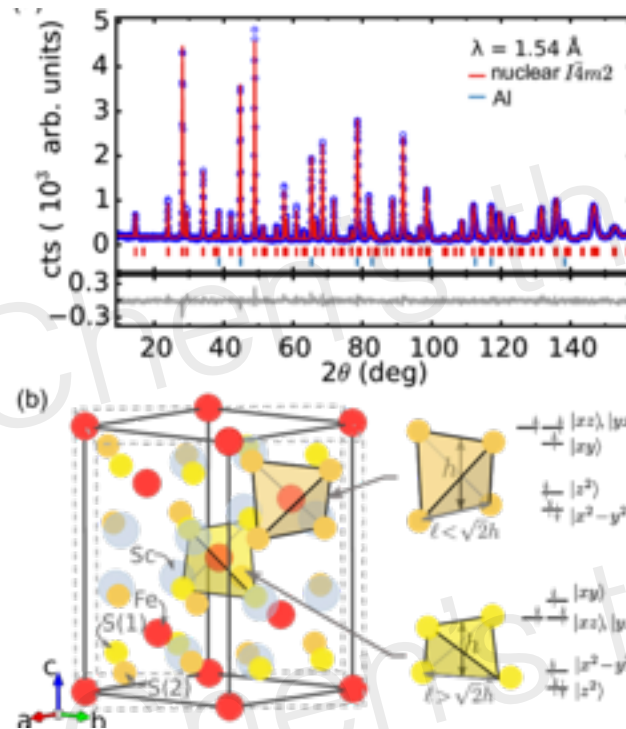
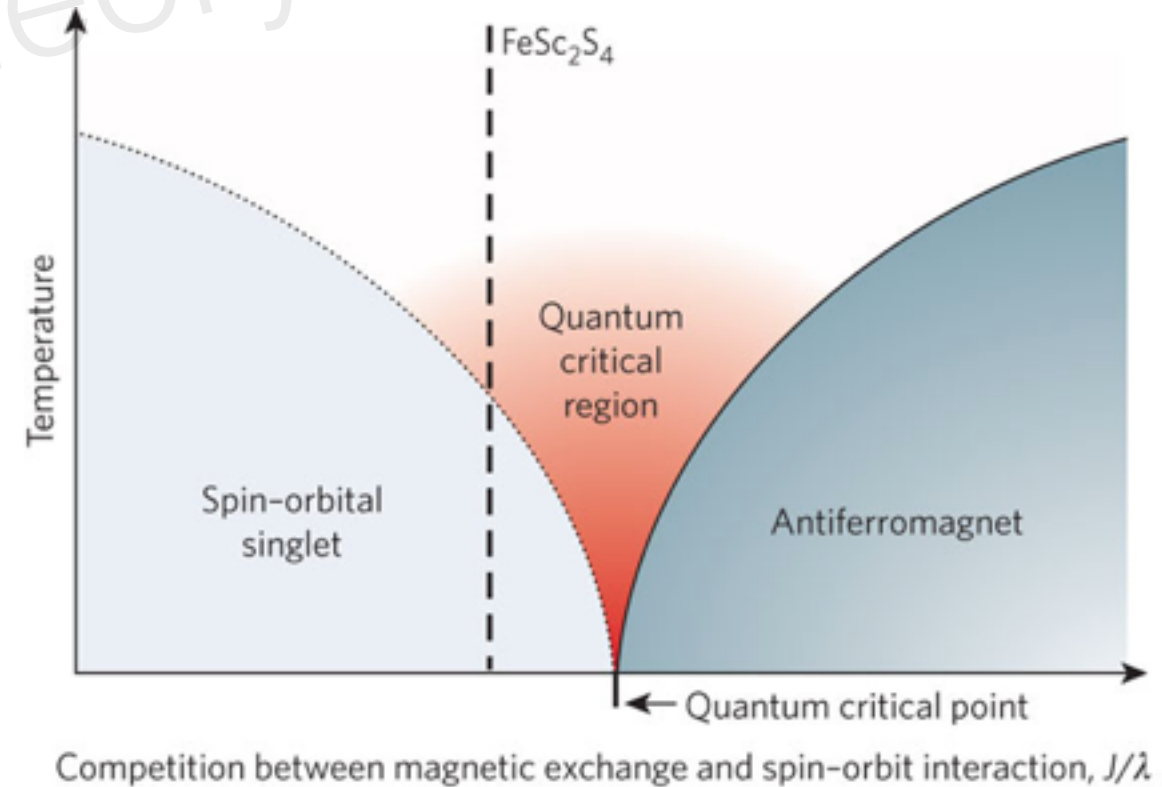


Figure 1: Specific heat for powder samples of  $\text{FeSc}_2\text{S}_4$  used in (a) Total specific heat (grey circles) and estimated contribution (blue triangles). Dashed yellow line is estimated phonon contribution. (b) Estimated magnetic entropy.



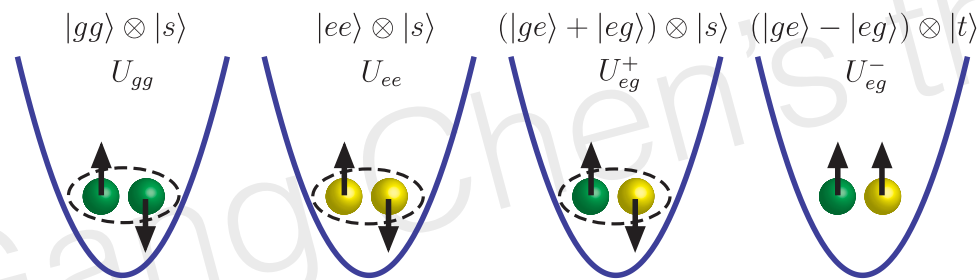
G Chen, Balents, Schnyer,



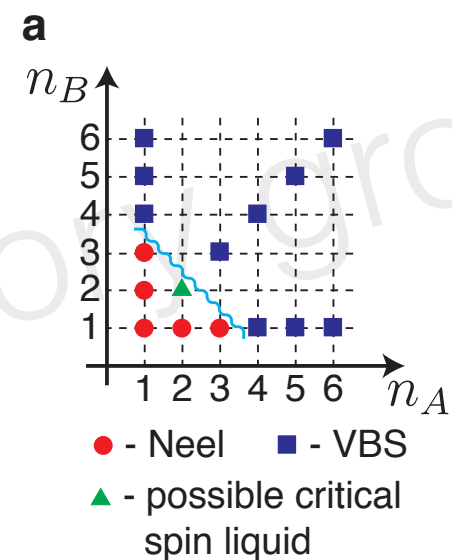
# SU(N) “magnets”: more generally, large-symmetry-group magnets

## Two-orbital SU(N) magnetism with ultracold alkaline-earth atoms

A. V. Gorshkov<sup>1\*</sup>, M. Hermele<sup>2</sup>, V. Gurarie<sup>2</sup>, C. Xu<sup>1</sup>, P. S. Julienne<sup>3</sup>,  
J. Ye<sup>4</sup>, P. Zoller<sup>5</sup>, E. Demler<sup>1,6</sup>, M. D. Lukin<sup>1,6</sup>, and A. M. Rey<sup>4</sup>



$$\begin{aligned}
 H = & \sum_{\alpha m} \int d^3 \mathbf{r} \Psi_{\alpha m}^\dagger(\mathbf{r}) \left( -\frac{\hbar^2}{2M} \nabla^2 + V_\alpha(\mathbf{r}) \right) \Psi_{\alpha m}(\mathbf{r}) \quad (1) \\
 & + \hbar \omega_0 \int d^3 \mathbf{r} (\rho_e(\mathbf{r}) - \rho_g(\mathbf{r})) + \frac{g_{eg}^+ + g_{eg}^-}{2} \int d^3 \mathbf{r} \rho_e(\mathbf{r}) \rho_g(\mathbf{r}) \\
 & + \sum_{\alpha, m < m'} g_{\alpha\alpha} \int d^3 \mathbf{r} \rho_{\alpha m}(\mathbf{r}) \rho_{\alpha m'}(\mathbf{r}) \\
 & + \frac{g_{eg}^+ - g_{eg}^-}{2} \sum_{mm'} \int d^3 \mathbf{r} \Psi_{gm}^\dagger(\mathbf{r}) \Psi_{em'}^\dagger(\mathbf{r}) \Psi_{gm'}(\mathbf{r}) \Psi_{em}(\mathbf{r}).
 \end{aligned}$$





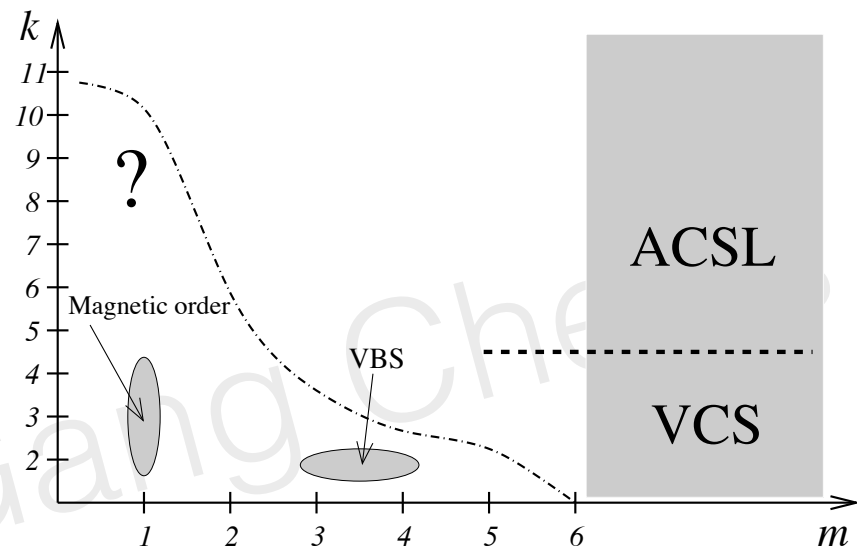
# Mott Insulators of Ultracold Fermionic Alkaline Earth Atoms: Underconstrained Magnetism and Chiral Spin Liquid

Michael Hermele,<sup>1</sup> Victor Gurarie,<sup>1</sup> and Ana Maria Rey<sup>1,2</sup>

<sup>1</sup>*Department of Physics, University of Colorado, Boulder, Colorado 80309, USA*

<sup>2</sup>*JILA, University of Colorado and NIST, Boulder, Colorado, 80309, USA*

(Dated: October 7, 2018)



$$\mathcal{H} = J \sum_{\langle \mathbf{r} \mathbf{r}' \rangle} S_{\alpha\beta}(\mathbf{r}) S_{\beta\alpha}(\mathbf{r}'), \quad S_{\alpha\beta}(\mathbf{r}) = f_{\mathbf{r}\alpha}^\dagger f_{\mathbf{r}\beta},$$

more delocalized in local Hilbert space  
even with a large local Hilbert space

## Dimer description of the SU(4) antiferromagnet on the triangular lattice

Anna Keselman<sup>1\*,2</sup>, Lucile Savary<sup>3,1</sup>, Leon Balents<sup>1,4</sup>

## Emergent Fermi surface in a triangular-lattice SU(4) quantum antiferromagnet

Anna Keselman,<sup>1</sup> Bela Bauer,<sup>2</sup> Cenke Xu,<sup>3</sup> and Chao-Ming Jian<sup>2</sup>

May be relevant to twisted bilayer graphene

# Summary

This field is quite rich.

There is no general guiding principle.